Design, Fabrication, and Testing of Assistive Mobility Solutions for Health Care Facilities

by

Maltiti Braimah

A thesis

presented to the University of Waterloo

in fulfillment of the

thesis requirement for the degree of

Master of Applied Science

in

Mechanical and Mechatronics Engineering

Waterloo, Ontario, Canada, 2024

© Maltiti Braimah 2024

Author's Declaration

I hereby declare that I am the sole author of this thesis. This is a true copy of the thesis, including any required final revisions, as accepted by my examiners.

I understand that my thesis may be made electronically available to the public.

Abstract

The movement of people, medication, and equipment in health care is a crucial part of the workflow, however, it is also an area that causes significant physical strain to the workers. This thesis proposes a design which is used to retrofit existing medical beds and carts with motorized modules that reduce the amount of force required for a worker to move equipment within hospitals and long-term care homes. The unique design makes use of mechatronic design principals to offer reliable and effective solutions to mobility problems in health care environments.

Though available motorized beds and carts exist, they tend to be expensive as they are integrated in the bed and cart designs, thus requiring new equipment to be purchased. This is not always possible as it requires a large initial investment, while also introducing a foreign piece of equipment that workers must learn to use. The designed solution solves this by considering the existing design of medical equipment and adding technology to its frame to vastly reduce the costs. Adding onto the established medical designs allows for the electromechanical assembly to be the focus of the retrofit, coupling its additional functionality to familiar equipment.

In this thesis, modules for improving beds and carts are designed, fabricated, and tested. The mechatronic design of the bed establishes a set of components and parameters that are successful in allowing for locomotion in indoor environments without the need for significant muscle exertion. The thesis scope details the mechanical design and electric and pneumatic component selection of the bed for a platform created to allow for manual, assistive, and autonomous controls.

Using the experience and observations made while designing the bed platform, a more general assistive cart design is created. The cart offers a streamlined module that offers longitudinal torque assistance and can be paired with a wider range of medical equipment. An assistive handle allows for a seamless control experience on the assistive cart, wherein the assistive torque provided by the motorized module can be scaled by sensing the force exerted on the handle. This is observed to reduce the force needed to push a cart, and significantly decreases the effort needed to maneuver a heavy cart. The cart is also proven to be effective in its intended environment through limited prototype use in Grand River Hospital. An alternative cart is also designed, which can couple and detach from carts. This solution allows for a large fleet of similar carts to be powered using one product, rather than requiring a module for each cart.

Acknowledgements

I would like to thank each of the members of the Mechatronic Vehicle Systems Lab that helped make the mobility project a possibility. Professor Khajepour was an irreplaceable supervisor and was crucial in helping set short and long-term project goals and encouraging me to perform my best. Each of the lab's technicians served an important role in helping assess the feasibility of original designs, as well as overseeing the manufacturing process. Due to this work from Jeff, Michael, and Aaron, I was able to achieve streamline research and literature review processes to achieve the best possible solutions. Additionally, I would like to thank my fellow graduate students that supported me throughout my time at Waterloo, and provided important information on their areas of specialty. From these fellow students, I would like to thank Frank Yang, who developed much of the controls required for my work to come to fruition.

Finally, I would like to thank my father, mother and sister for support throughout the various phases of study throughout my life. You have made it possible to achieve the things that I can.

Table of Contents

Author's Declaration ii

Abstract iii

Acknowledgements iv

List of Figures vii

List of Tables xi

List of Abbreviations xii

List of Symbols xiii

CHAPTER 1 INTRODUCTION 1

1.1 Objectives 1

1.2 Motivation 1

1.3 Outline of Chapters 2

CHAPTER 2 LITERATURE REVIEW 4

2.1 Existing Beds, Stretchers, other Transportation in Health Care Facilities 4

2.2 Existing Semi-Autonomous robot platforms 10

2.3 Existing Motorized carts 13

2.4 Prerequisite Assistive Bed Prototypes 16

CHAPTER 3 DESIGN AND ANALYSIS OF AN ASSISTIVE HOSPITAL BED PLATFORM 19

3.1 Motivation for an Assistive Hospital Bed 19

3.2 Goals for Assistive Bed Design 20

3.3 Technical Requirements for Assistive Bed Design 21

3.4 Assistive Bed Calculations 22

3.4.1 Driving Torque Requirements 22

3.4.2 Steering Torque Requirements 26

3.4.3 Pneumatic Calculations 30

3.4.4 Bearing Calculations 33

3.4.5 Other Design Elements 38

CHAPTER 4 DESIGN AND ANALYSIS OF ASSISTIVE CART AND CART HAULER 44
4.1 Design of Assistive Cart 44
4.1.1 Design Goals and Motivations 44
4.1.2 Required Parameters 48
4.1.3 Required Torque 49
4.1.4 Pneumatic Requirements 53
4.1.5 Assistive Handle 55
4.1.6 Other User Interface and Safety Features 63
4.1.7 Complete Assistive Cart Assembly 66
4.2 Design of a Cart Hauler 68
4.2.1 Motivation for Cart Hauler 68
4.2.2 Dynamics of Lifting with Cart Hauler 69
4.2.3 Complete Cart Hauler Design 71
CHAPTER 5 PROTOTYPING AND TEST RESULTS 74
5.1 Prototyping of the Assistive Bed Design 74
5.1.1 Fabrication and Assembly of the Assistive Bed 75
5.1.2 Assistive Bed Operation 77
5.1.3 Assistive Bed Test Results 78
5.2 Prototyping of the Assistive Cart 83
5.2.1 Fabrication and Assembly of the Assistive Cart 83
5.2.2 Assistive Cart Operation 94
5.2.3 Assistive Cart Test Results 95
5.2.4 Cart Hauler Fabrication 103
CHAPTER 6 CONCLUSIONS AND FUTURE RECCOMENDATIONS 105
6.1 Conclusion 105
6.2 Future Advancements 106
References 109

List of Figures

Figure 2.1: (a) Vitalflex Home Hospital Bed [4]. (b) Invacare Carroll CS Series CS7 Bed with Hi-Lo Lockout Package [5]. (c) VersaTech 1100 ULB Rotec Ultra Low Bed [6]. 5
Figure 2.2: Controls and positions of HillROM century series hospital beds [7]. 6
Figure 2.3: Flexbed design, used to transport neurosurgery patients autonomously from one location to a destination [8]. 8
Figure 2.4: SESTO Robotic bed mover [9]. 9
Figure 2.5: (a) Ultrasonic sensor for person following [11], (b) semi-autonomous golf caddie robot [12], and (c) autonomous person-specific following robot [13]. 12
Figure 2.6: MPC 2741 motorized platform truck [14]. 13
Figure 2.7: Overland Electric powered 44” chassis [16]. 14
Figure 2.8: Overland Electric Powered Appliance Hand Truck [17]. 15
Figure 2.9: First MVS drive wheel prototype [18]. 16
Figure 2.10: Second MVS drive wheel prototype [18]. 17
Figure 3.1: Longitudinal forces acting upon assistive bed on a slope. 23
Figure 3.2: Forces acting on assistive bed wheels, directly after coming in contact with a bump. 24
Figure 3.3: Previous drive assembly featuring in-wheel motor [18]. 26
Figure 3.4: Computer-aided design (CAD) model of ZLTECH ZLLG80ASM800 motor and its polyurethane tire. 27
Figure 3.5: Compressed wheel and patch diameter. 28
Figure 3.6: Diagram depicting steering moment required to overcome force of friction. 29
Figure 3.7: Z4BLD60-24GNL2-30S-MB brushless DC motor. 30
Figure 3.8: New pump and air valve selected for use in the assistive bed. 31
Figure 3.9: 25 mm and 40 mm air cylinders from XCPC. 33
Figure 3.10: Diagram showing rough locations used for calculating thrust and radial bearing specifications. 34
Figure 3.11: CAD model depicting location of bearings. 35
Figure 3.12: Distance from center of wheel to radial bearing location on CAD model. 37
Figure 3.13: Fractured 3D printed wheel case. 38
Figure 3.14: CAD Model of main drive assembly, featuring in-wheel motor, air cylinders, and steering motor. 39
Figure 3.15: Wheel fork with 1070 N from the in-wheel motor exerted. 40

Figure 3.16: Wheel fork with 60 Nm of torque from the steering motor exerted. 40
Figure 3.17: Front view of the assistive bed module CAD model. 42
Figure 3.18: Rear view of the assistive bed module CAD model. 42
Figure 3.19: CAD model of non-steering bed module. 43
Figure 4.1: Various carts observed at Schlegal Villages Retirement Home and Schlegal-UW Research Institute for Aging. 45
Figure 4.2: Various carts observed at Grand River Hospital 46
Figure 4.3: Vintage Encore Series Treatment Cart from Cancard [41]. 47
Figure 4.4: Free body diagram depicting the force balance for calculating the required torque for the cart's climbing of a 1:10 incline. 49
Figure 4.5: Forces acting on wheels when in contact with an obstacle. 51
Figure 4.6: ZLLG65ASM500 motor. 52
Figure 4.7: Air cylinder equilibrium free-body diagram. 54
Figure 4.8: Assistive handle hollow circular bar and strain gauge locations. 56
Figure 4.9: Stress and strain results of assistive handle under expected loads. 59
Figure 4.10: Reduction of endurance limits caused by various surface finishes [44]. 60
Figure 4.11: Free body diagram of bending cantilever representing the assistive handle. 61
Figure 4.12: The stress and strain for a handle is also designed with the bed dimensions in mind. It is, however, simpler to attach the stain gauges directly to the frame of the bed to avoid outfitting the bed with new parts. 63
Figure 4.13: CAD model of the assistive cart's screen assembly 64
Figure 4.14: Manufactured screen assembly 65
Figure 4.15: Cart infrared sensors, as viewed from front of cart. 66
Figure 4.16: Cart main component assembly 67
Figure 4.17: Hot food delivery cart and surgical equipment case cart at Grand River Hospital. These carts share a platform 69
Figure 4.18: Free body diagram depicting forces of dolly lifting. 70
Figure 4.19: Renders of complete cart hauler design. 72
Figure 4.20: Render of cart hauler design, showing internal component placement. 72
Figure 4.21: Stress analysis of cart hauler under expected load. 73
Figure 4.22: Rotating locking bar. 73
Figure 5.1: (a) previous bed module and (b) new bed module designs. The profile of the new module is slightly larger at 805 x 325 x 210 mm when compared to the previous prototype's 805 x 315 x 190 mm. 74

Figure 5.2: Updated bed module prototype featuring new core system components and additional technology shared with assistive cart. 76
Figure 5.3 Assistive bed after the updated components are installed. As stated, the larger battery and steering motor prevent the usage of its lid. 77
Figure 5.4: Four main assistive bed steering modes. (a) Linear motion, where both wheels are aligned longitudinally with the bed, (b) mixed linear and steering motion, where the wheels are not in line with the bed, (c) crab motion, where the wheels are aligned transversally with the bed in the same direction, and (d) spinning motion, where the wheels are aligned transversally with the bed in opposite directions. 78
Figure 5.5: Speed of the assistive bed motors during linear travel forward and backward. 79
Figure 5.6 Steering angles of the assistive bed motors during linear travel forward and backward. 79
Figure 5.7 Speed of the assistive bed motors during crab motion. 80
Figure 5.8: Steering angles of the assistive bed motors during crab motion. 80
Figure 5.9: Speed of the assistive bed motors during spinning motion. 81
Figure 5.10: Steering angle of the assistive bed motors during spinning motion. 81
Figure 5.11: Speed of the assistive bed motors during mixed motion. 82
Figure 5.12: Steering of the assistive bed motors during mixed motion. 82
Figure 5.13: CAD model of the assistive cart and frame for a medication cart. 83
Figure 5.14: Bent sheet metal parts used for module frame, as received from external supplier. 85
Figure 5.15: Welded cart frame. 86
Figure 5.16: (a) Powder coated drive plate and fork and (b) painted drive plate. 87
Figure 5.17: 3D Printed Strain gauge cover. The part on the right can be observed to be slightly darker than its right counterpart. 88
Figure 5.18: Initial 3D printed rear screen assembly component. 89
Figure 5.19: 3D printed screen components after redesign, printed successfully. 90
Figure 5.20: Assembled electromechanical system. 91
Figure 5.21: Completed assistive cart assembly 92
Figure 5.22: Completed assistive cart with sample cabinets. 92
Figure 5.23: Stainless steel cart featuring revised design. 93
Figure 5.24: Assistive Cart with a total mass of 205 kg. 96
Figure 5.25: Speed of assistive cart, pushing. 97
Figure 5.26: Speed of assistive cart, pulling. 97
Figure 5.27: Handle and motor forces applied during driving. 98
Figure 5.28: Speed of assistive cart driving on concrete for a single acceleration and brake. 98

Figure 5.29: Manual and assistive forces applied during driving on concrete for a single acceleration and brake..... 99
Figure 5.30: RPM speed feedback on a carpeted floor. 100
Figure 5.31: Fully manual pushing force of a cart loaded with a 136 kg load on a carpeted floor. 100
Figure 5.32: Manual and assistive pushing forces applied during driving on a carpeted floor..... 101
Figure 5.33: Speed of Assistive Cart Sloped Driving, Up and Down Slope..... 102
Figure 5.34: Handle and Motor Forces Applied During Driving, On Slope..... 103
Figure 5.35: Cart Hauler during the assembly process. 104
Figure 6.1: Indoor sensor nodes mounted in MVS lab. 107

List of Tables

Table 3.1: Considered radial bearings..... 36
Table 4.1: Forces provided by single air cylinders of various sizes 54

List of Abbreviations

ASOC Active Split Offset Casters

CAD Computer-aided design

CCOHS Canadian Centre of Occupational Health and Safety

HR Hot-rolled

MDRD Medical Device Reprocessing Department

MVS Mechatronics Vehicle Systems

RF Radio frequency

List of Symbols

$A_{Bore\ Area}$ Bore area [m^2]

a Acceleration [m/s^2]

a_{Max} Maximum acceleration [m/s^2]

C_G Gradient factor

C_L Load factor

C_R Reliability factor

C_S Surface factor

C_T Temperature factor

C_{req} Required load capacity [N]

d_i Inner diameter [m]

d_o Outer diameter [m]

d_{patch} Patch diameter [m]

d_{wheel} Wheel diameter [m]

F Force [N]

F_{aero} Aerodynamic drag [N]

F_{bump} Bump force [N]

F_{ffront} Front rolling resistance [N]

F_{frear} Rear rolling resistance [N]

F_g Gravitational force [N]

$F_{N_{Max}}$ Maximum normal force [N]

$F_{Provided}$ Provided force [N]

$F_{Required\ Force}$ Required force [N]

F_i Inertial force [N]

F_r Radial force [N]

F_t Traction force [N]

f force [N]

f_{lift} Lifting force [N]

g Gravitational constant [m/s^2]

h Height [m]

$h_{compression}$ Height of compression [m]

I Moment of inertia [m^4]

l Length [m]

L Life [cycles]

L_R Required life [cycles]

$L_{Wheel\ Center\ to\ Bearing}$ Distance from wheel center to bearing [m]

l_1/l_2 Cart hauler lengths [m]

m_{bed} Mass of bed [kg]

m_{cart} Mass of cart [kg]

m_{Total} Total mass [kg]

$M_{Required\ Torque}$ Required torque moment [Nm]

M_1 Cart hauler moment [Nm]

M_{Lift} Lifting moment [Nm]

M_{Steer} Steering moment [Nm]

N Number of modules

$P_{Pressure}$ Pressure [Pa]

R Radius [m]

$r_{Motor\ Radius}$ Motor radius [m]

r_o Nominal radius [m]

S_n Endurance limit [Pa]

S_n' Fatigue strength [Pa]

S_u Ultimate tensile strength [Pa]

T Torque [Nm]

t Time [s]

v Velocity [m/s]

y Distance to neutral axis [m]

α_b Bearing constant

θ_{Max} Maximum angle of incline [degrees or radians]

θ Angle of incline [degrees or radians]

μ Coefficient of friction

σ Stress [Pa]

CHAPTER 1
INTRODUCTION

The demand for more efficient and convenient health care has surged in response to Canada's increasing population and was only magnified following the COVID-19 pandemic. The Mechatronics Vehicle Systems (MVS) Lab sees this demand as an opportunity to develop a state-of-the-art assistive mobility solution using its past experience with developing electric vehicle and robotic technologies.

1.1 Objectives

The aim of this thesis is to create mechatronic designs that improve the quality of the daily workflow of hospital and health care staff by alleviating the work that must be done to move equipment around facilities.

In order to do this, mechatronic modules are designed with the goal of retrofitting existing equipment. Commonly moved equipment such as beds, cabinets, and carts are considered as opportunities for a design to lessen the physical workload of health care staff due to repeated pushing, pulling, and steering. The designed solution contains a core universal drive unit with the ability of driving existing caster-wheeled equipment, and includes the components necessary to make the integration of the design into a health care workflow as non-intrusive as possible. The main focus of this thesis is to provide a framework design that can be easily adapted to various applications. The solution should be conscious of typical obstacles and limitations in its target environment, while minimizing costs and safety risks when possible. A practical assistive design will be assessed as part of this thesis, while enabling development of technology with higher levels of autonomy on the same platform in the future.

1.2 Motivation

Over recent years, the response to the COVID-19 pandemic has revealed a large opportunity for improvements in this sector. Both the quality and capacity of service required to match the demand were forced into consideration, and will likely be a point of contention for society in Canada over the coming decades.

Canada's census data from 2003 to 2023 has seen an increase of the average age of Canadians from 38.1 to 41.6 alongside an increase of the percentage of population over 65 years of age increasing from 12.8% to 18.9% over the same period of time [1]. This trend is expected to continue for decades to come, which will bring with it a necessity for innovations and optimizations to uphold the same or higher levels of quality in hospital and long-term care facilities. Another result that can be determined by this age demographic trend is that a smaller percentage of the population will in the working class in the future, if current population trends continue.

A driving motivator for researching the opportunities for mechatronic innovation in the health care industry as a whole is the fact that transportation and guiding of people and materials is one of the most cited areas for requests for assistance by health care staff [2]. The MVS lab aims to contribute to the introduction of mechatronic advancements and technologies with the motorized mobility systems it is developing. Autonomous and assistive systems have attracted a great deal of research opportunities for the health care industry over the past few years, and the solutions developed in conjuncture with this thesis aims to aid in this way.

1.3 Outline of Chapters

Chapter 2 describes the relevant literature to the scope of this project. Particularly the technology currently in use in hospitals and long-term care homes for moving people and equipment, existing semi-autonomous solutions develops for other environments, and assistive technology used in other fields. Previous MVS prototypes for mobility in health care is also be presented to better define the scope of this thesis.

Chapter 3 depicts the design process for developing the mechanical design aspects of an electromechanical module that can be used to retrofit an existing hospital or long-term care bed. The designing process required to select adequate components is described, and mechanical systems for operation are created.

Chapter 4 builds upon the assistive hospital bed design to create a more general assistive cart design that is easier to deploy in non-critical workflows for data collection and prototype testing. An alternative cart hauler system is also designed to add to the applications in which the technology developed can aid hospital and long-term care workers move materials involving tasks wherein the initial cart design may not be practical.

Chapter 5 presents the prototyping process and usage of the designs created to assist with mobility. Discussions and reflections are made involving the performance of the designs during tests as well as during use in their intended environments.

Chapter 6 concludes by summarizing the scope of the research performed as well as highlighting key areas that future work should be performed in.

CHAPTER 2
LITERATURE REVIEW

It is important to consider the existing bed and stretcher solutions on the market that also try to solve the problem that the assistive mobility project aims remedy. Reviewing the technology powering existing semi-autonomous and autonomous platforms is also essential when considering the future goal of autonomous robots moving people and materials in a controlled environment. In order to facilitate growth in the application of the technology developed for assistive mobility in health care environments, existing motorized carts are also investigated. Finally, an existing MVS lab prototype is assessed to facilitate further development of the mechatronic project that this thesis consists of.

2.1 Existing Beds, Stretchers, other Transportation in Health Care Facilities

Understanding the existing manual and electric transportation equipment used in health care facilities is crucial in determining the research that should be done to alleviate the day-to-day strain endured by workers.

Electric hospital beds are typically expensive while not offering any mobility-related technologies, resulting in them not being viable to replace a fleet of existing beds. Generally, the hospital beds use power to change the shape of the bed platform itself rather than any locomotion. This leaves the underside of most beds open, giving an opportunity for further technology to be added to the bed here in the future.

Weight capacities of beds also vary greatly depending on the intended application. From Vital Mobility, a Canadian hospital bed seller, smaller beds can be purchased with weight capacities under 200kg and are intended for only one patient while larger beds with limits of up to about 500kg intended for the patient as well as equipment also exist [3].

There are several features that are consistent with most types of beds available on the market. Each available bed from Vital Mobility features a mechanical frame connecting the bed platform to the caster wheels. The frames typically allow for bed height to be adjusted through the use of several pin joints. Positioning of the frame is usually aided either electronically or with the use of hydraulics, though cheaper options are fully manual.

The Vitalflex Home Hospital Bed is an easily dismantlable electric hospital bed option that features an electric drive to raise the head rest and foot rest and sells for $2490 [4]. The frame is fabricated using primarily powder coated metal with wooden accents for cover panels. Each caster wheel is lockable individually, and the bed can be raised and lowered to 10 positions with the help of a 9 V battery's power.

The $5425 Invacare Carroll CS Series CS7 Bed with Hi-Lo Lockout Package expands on the technology offered from the cheaper Vitalflex option. The two beds feature a similar weight capacity of about 225 kg in addition to their weights of just under 100 kg [5]. This bed features an enhanced user experience by allowing for movement at any bed platform height, and communicating this with an indicator light. The ten-button controller is waterproof and allows for various bed positions to be adjusted, including overall height, head rest, abdomen rest, and leg rest. The Invacare's bed frame is much heavier duty than that of the Vitalflex bed featuring eight smaller caster wheels, thicker metal beams, and a sturdier bed frame.

The VersaTech 1100 ULB Rotec Ultra Low Bed is a high-cost feature rich bed specifically designed for bariatric use [6]. This $21590 bed has a weight capacity of 500 kg and has an adjustable width for patient comfort. Four 5-inch anti-static double caster wheels connect the anti-microbial powder coated metal frame to the ground, and the siderails are constructed using a composite plastic material. Electronics are used to power the DC motor used to adjust the foot and head rests, notification features for patients and nurses, emergency lifting/lowering, and various other safety features.



(a) (b) (c)

Figure 2.1: (a) Vitalflex Home Hospital Bed [4]. (b) Invacare Carroll CS Series CS7 Bed with Hi-Lo Lockout Package [5]. (c) VersaTech 1100 ULB Rotec Ultra Low Bed [6].

Other forms of integrated technology in hospital beds are outlined in the HillROM Century Series P385A's operational manual. This model bed is available in the MVS lab and has been used for previous studies.

The referenced manual that covers features from all Century Series SKUs, some of which are not necessarily present on the P385A available in the MVS lab [7]. The manual, however, does describe in detail several common features used while designing beds for the health care industry.

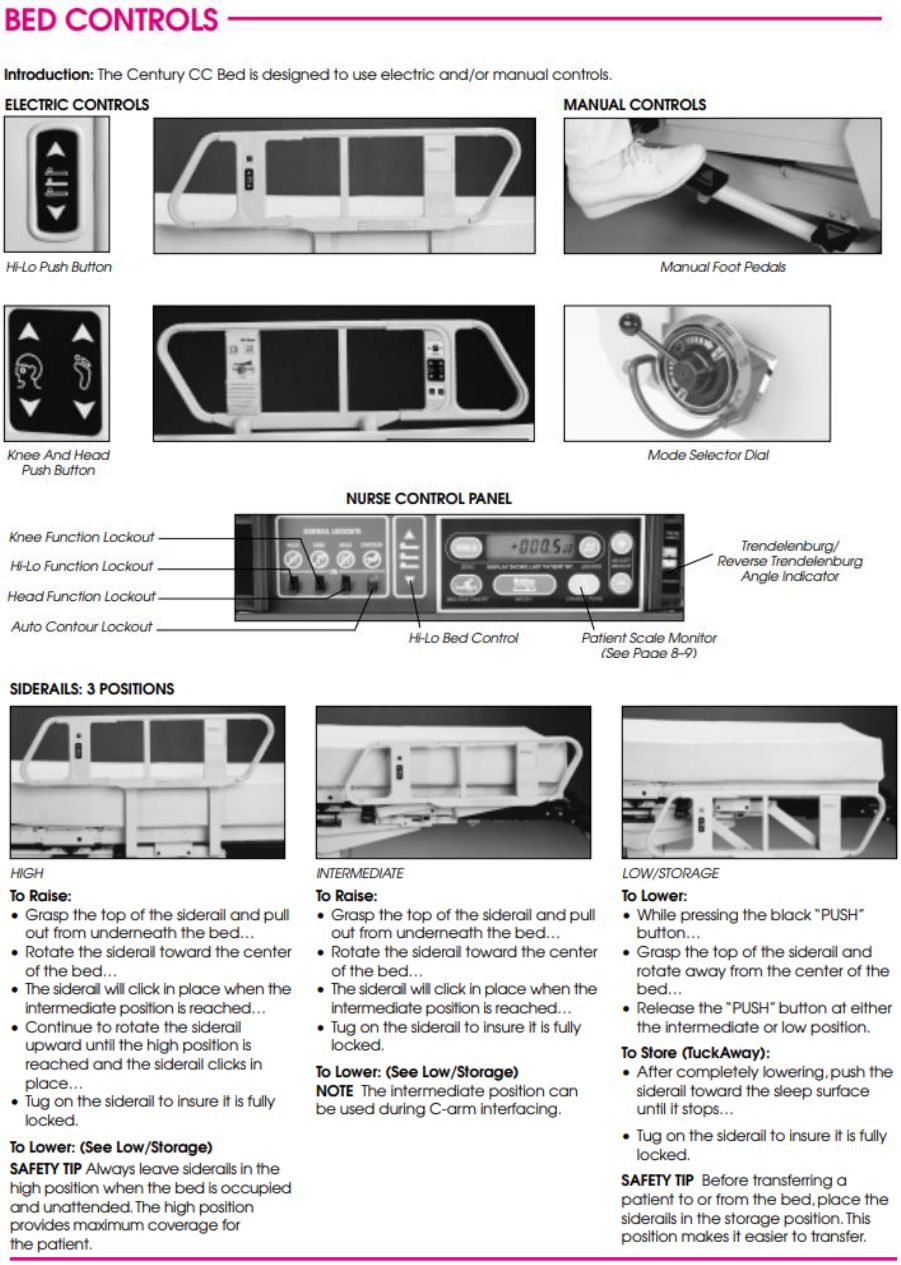


Figure 2.2: Controls and positions of HillROM century series hospital beds [7].

An Ergonomic foot pedal indicates that those working with transportation of people and materials currently have a foot available to make adjustments to the bed. In this case the adjustment is to lock and unlock the wheels to ensure that the bed is able to remain stationary. In addition to this, adjustable side rails allow for a comfortable pushing position to be selected by the nurse or doctor operating the bed.

A key takeaway from the design manual of the HillROM beds is that ease of use was considered during the initial design, and although long-term injuries still occur with use of manual beds throughout a worker's career, there are several features engineered to make the workplace environment safer. This supports the idea that this project should focus on an electromechanical system that can be retrofit to an existing bed, as it is not only a much less costly option than purchasing a completely new bed with a drive, but can also preserve the other features of existing beds specifically designed for medical professionals.

A robotic bed for transportation designed by Wang, Savkin, Clout, and Nguyen is also reviewed to become familiar with other research projects with similar goals to this one. Their publication, "An Intelligent Robotic Hospital Bed for Safe Transportation of Critical Neurosurgery patients Along Crowded Hospital" introduces the design of the Flexbed [8]. The design proposed in this study would replace existing beds completely, which allows for an original design to be created from the ground up.

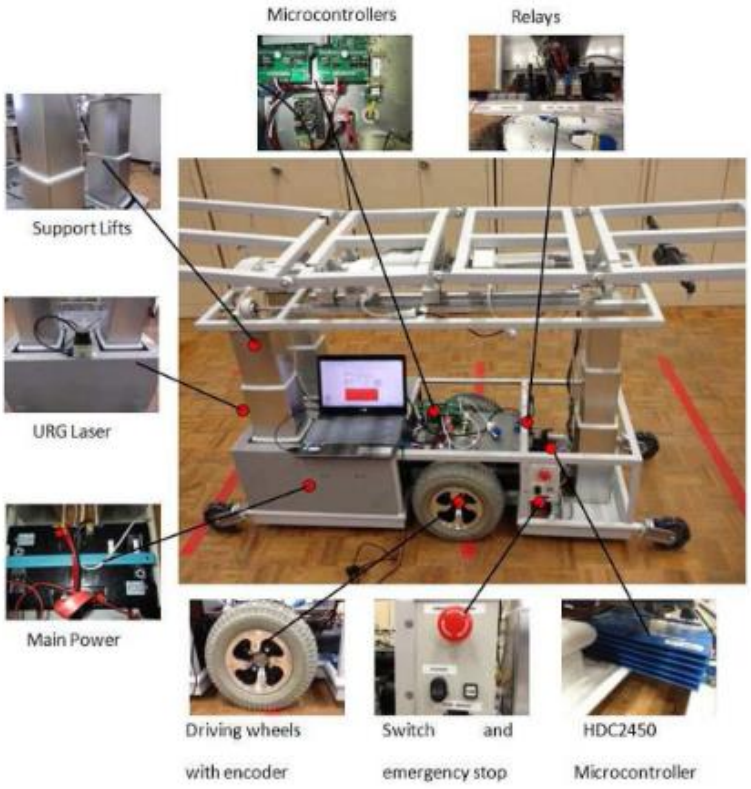


Figure 2.3: Flexbed design, used to transport neurosurgery patients autonomously from one location to a destination [8].

Autonomous navigation technology is used in this design to allow for the robot to move to a destination without the constant supervision of a worker or operator. The mechanical design of the Flexbed offers some insight on features of a successful solution for autonomous transportation. Two 320mm diameter driving wheels are featured on the design, which allow for a differential drive control scheme to be able to drive the robot from its center. Four additional smaller caster wheels are arranged in a rectangle around the key components. The driving wheels each feature encoders, which sense the direction and velocity of each wheel. This information is used for controlling and observing the state of the robot.

Three support lifts raise and lower the bed platform, as is a standard feature in hospital beds. Two 12V batteries in series are used as a power source, and a power switch and emergency stop are added at foot-level. A Hokuyo URG-04LX laser range sensor and Microsoft Kinect are used in order to effectively sense the area surrounding the robot during autonomous operation. A RoboteQ HDC2450 motor controller is used, which receives information through a serial or USB interface and controls the robot either autonomously or through manual input. A reactive navigation algorithm is used to maneuver in dynamically changing environments, which implements collision avoidance strategies to create a system that is more efficient and safer than conventional hospital beds.

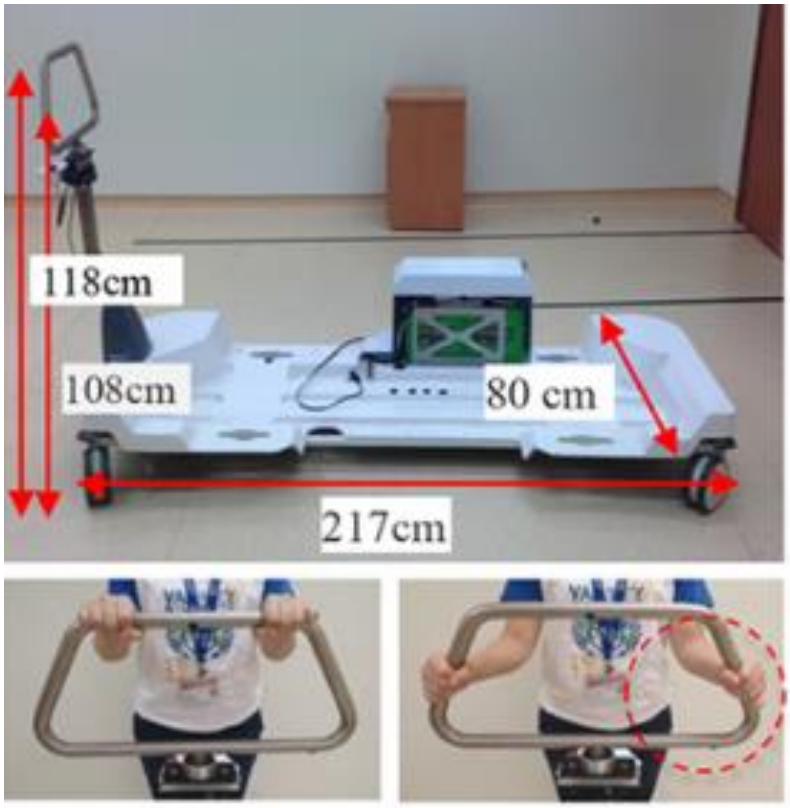


Figure 2.4: SESTO Robotic bed mover [9].

The SESTO bed mover, an omnidirectional robotic stretcher, is also reviewed to aid with developing a reliable system [9]. This solution is added to an existing hospital bed to allow for power-assisted movement. This study quantifies the reduction of manpower required to move hospital beds when robotic assistance is provided. Electromyography sensors are used to measure the different strain on four muscles as 14 subjects maneuvered the beds through various courses. The result of the experiment shows significant reduction in all four muscle groups observed during various maneuvers with the most significant reductions in the back-muscle groups. Some results also suggest a 50% reduction in required manpower, allowing for one person to be responsible for pushing stretchers that traditionally required two. The SESTO bed mover features both manual and driven modes and latches on to the bottom of a standard bed to allow for movement. Integration of several Active Split Offset Casters (ASOC) allows for omnidirectional movement in the final design.

2.2 Existing Semi-Autonomous robot platforms

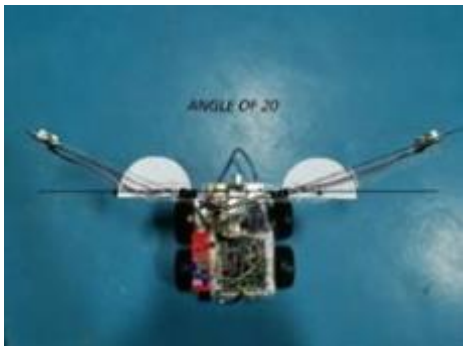
Different designations exist for the amount of autonomy that a robot operates at. SAE outlines these using levels 0 to 5 for automobiles, though this can be applied to any mobile robot [10]. Understanding these with respect to carts and beds in medical settings is important to communicate the degree to which a product requires its user to make decisions and be attentive. A level 0 autonomous robot has no driving automation, and must be operated manually. Most existing carts and beds fall within this category, as a manual input can be used to fully define their operation. At level 1 a vehicle gains some assistive properties. This can include helping with acceleration and deceleration, or with steering. A level 2 robot is similar to this, though is able to assist with steering and speed control simultaneously. Levels 0 through 2 all require constant attention from an operator to drive the vehicle. At level 3, the operator is no longer fully controlling the vehicle. At this level the vehicle can move without input given an adequate environment, such as an open room with a mapped floorplan. Level 3 robots retain the ability to be driven manually if necessary. At level 4, this ability is taken away, though the vehicle can still only operate under limited conditions. At level 5, the vehicle can drive autonomously under any condition and does not require a diver.

In order to issue controls to an autonomous system, a robust sensor platform must be developed. One of such systems is developed with the use of ultrasonic sensors for human-following, explored in a paper assessing the usefulness of ultrasonic sensors in this application compared to lidar and cameras [11]. A three-ultrasonic sensor setup rotates to sense in a sweeping motion for analysis in this example. This implementation for person-sensing is relatively simple, but is accompanied by potential problems such as following the target when multiple people are present in front of the robot's sensors. This would be suboptimal in a hospital or long-term care setting, as the bed losing track of the person it must follow can lead to undesirable behavior. This study does, however, outline the capabilities of standard 40 kHz ultrasonic sensors for object detection due to their smaller size, lighter weight, relative cost, lower power consumption, and low computational cost when compared to lidar and cameras, which will likely be useful in the future.

Another method of autonomous control is investigated in a paper that describes an autonomous robot caddie that is able to follow players in an outdoor environment [12]. This solution makes use of a radio frequency (RF) emitting device as well as an RF receiving device. The robot makes use of a manual

mode where it can be driven like a conventional caddie, as well as an autonomous mode based on velocity, heading, and angle between RF devices. This system is able to follow target in an outdoor environment successfully, though lacks robust obstacle detection, collision avoidance, and braking systems. If similar results can be produced indoors, it will be a suitable method for the navigation of a hospital bed indoors. The addition of a manual mode also greatly increases the safety and reliability of a robot system by allowing for requests for driver-control in areas with low visibility or a high density of obstacles.

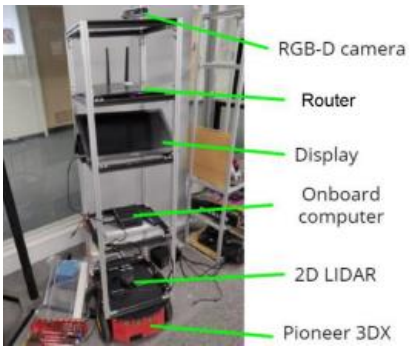
A final autonomous robot sensor system that is researched makes use of an RGB-D camera as well as lidar to detect individuals. The study by Chan uses a sequential nearest-neighbor machine learning algorithm to train and identify a specific person that the robot is to then follow [13]. Though this implementation identifies target destinations with great detail, it struggles with identification when the target individual is facing away from the sensors. In addition to this, the sensor setup and control complexity comes at a high computational cost which makes it expensive to implement. Implementing a similar system on a hospital bed system will likely require a much relatively powerful computer to be integrated in the design, which may be impractical due to power requirements in addition to the cost increases.



(a)



(b)



(c)

Figure 2.5: (a) Ultrasonic sensor for person following [11], (b) semi-autonomous golf caddie robot [12], and (c) autonomous person-specific following robot [13].

For the scope of this thesis, it is imperative to select a level of autonomy that allows for a confident deployment of the designed solution while minimizing costs to alter the design. As such, the initial prototypes are to be designed to be autonomous at a lower level, where they can confidently be implemented and used to collect usage data and determine any required improvements. Once adequate data is collected, the designs can be improved by adding or enabling additional sensors. This loop will ensure that each stage is feasible, and allow for reflection before a design of higher autonomy is deployed in a long-term care or hospital facility.

2.3 Existing Motorized carts

Products currently available in heavy duty and warehousing environments with electric powertrains are also investigated as a source for proven solutions in other industries.



Figure 2.6: MPC 2741 motorized platform truck [14].

The MPC2741 is a motorized platform truck cart that features four caster wheels and a center wheel drive designed to help transport heavy loads [14]. It is controlled using a throttle on the handle, where the emergency stop and charge level indicator are placed. This cart is available in multiple sizes to accommodate different loads of platform fixtures, which can be bolted, welded or clamped to the design.

The frame is constructed primarily out of reinforced tubular steel with a grey paint coating. The electronics are powered on a 24V battery contained within the center module, which also features a built-in battery charger. The carts automatically make use of dynamic regenerative braking to slow down, while also featuring an electro-mechanical parking brake.

This design is notable, as it allows for a high degree of customizability in warehouse and heavy-duty applications. The module itself can be placed under platforms of differing sizes to adapt to different applications, which is a design philosophy that can be beneficial in other fields containing several different cart loads. The control interface is within reach during operation, allowing for quick adjustments to speed.

Granite industries, another supplier of motorized solutions, has designed several electric utility carts for labor-intensive movement of materials and equipment [15].



Figure 2.7: Overland Electric powered 44” chassis [16].

The Overland Electric powered 44” chassis is an electric platform that can move a load of up to 340 kg [16]. The 13-inch wheels are driven by a 24 V DC motor, and the battery of 22AH can run the electric powertrain up to 6-8 hours. The design boasts easy operation using a handle-throttle, as well as low maintenance. Several safety features are also advertised in the design of this cart, including hill detection (likely using an internal gyroscope), an emergency stop button, controlled manual and automatic braking, an overload fuse, and an automatic wheel lock when idle.

The design is fully enclosed, protecting the components from hazards while also ensuring moving gears and axles do not pose a safety risk. The metal frame is powder coated after welding to preserve the metal and offer a durable finish. A differential drive control system is used, allowing for rotation in-place.

This $3095 design offers insight to a cart designed to be used for many different applications. The rigid build quality, simple control scheme, and intuitive design allow for easy adoption of the technology by professionals which should be strived for with a design for medical applications as well.



Figure 2.8: Overland Electric Powered Appliance Hand Truck [17].

The electric hand truck from Granite Industries is designed similarly to the cart, though can be easily used on different rectangular loads [17]. Designed for moving appliances, the hand truck lifts a load then allows for the user to engage the drive system.

The technical specifications of this design are the same as that of the electric powered chassis, and shows farther adaptability and reliability of the components used. The products designed for hospital and long-term care mobility would benefit from a similar setup, as maintenance, controls, and manufacturing are all shared between designs, which reduces costs while also providing a consistent user experience.

Immediate design improvements based existing manual and electric beds and carts can be used to enhance the performance of the designs of MVS lab's previous prototypes.

2.4 Prerequisite Assistive Bed Prototypes

Prior to the work done in this thesis MVS lab had produced two prototypes to test initial ideas for the design of a bed module.

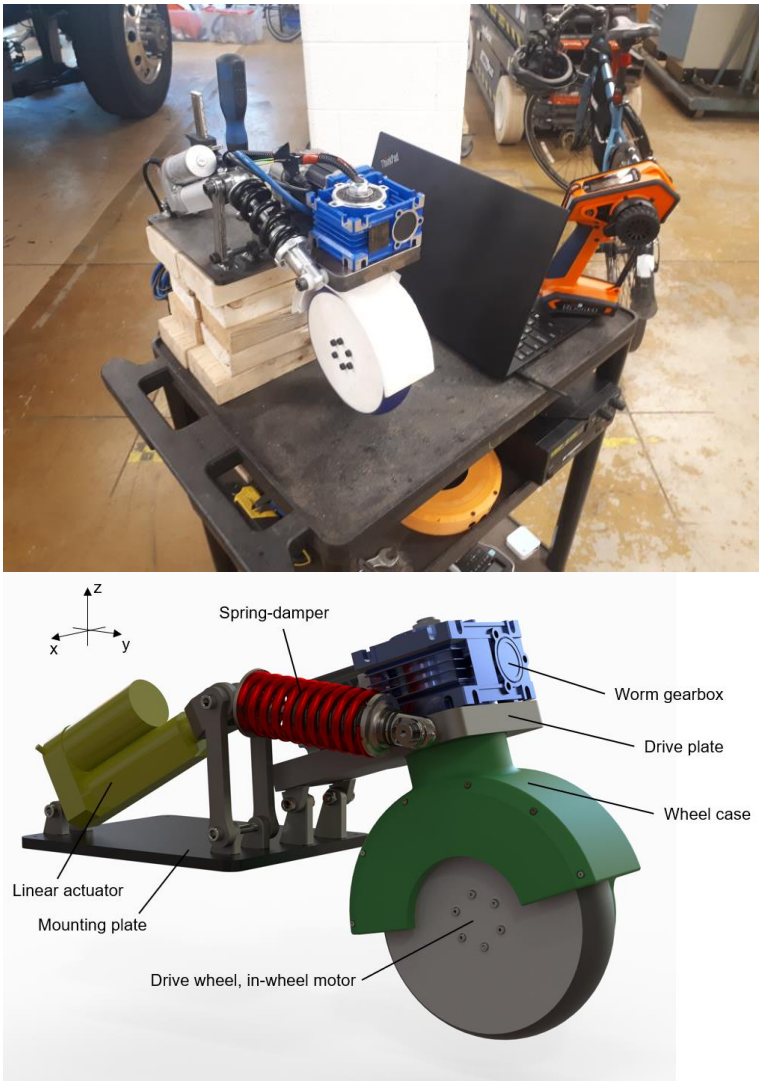


Figure 2.9: First MVS drive wheel prototype [18].

The first prototype is designed using preliminary load requirements and limitations in combination with a conceptual design framework that weighed possible features. It is decided that the design would place drives on two axles of the chassis to allow for a flexible steering system, as well as for simplicity in attaching to existing frames. An available lift platform is used to build the prototype upon and test its functionality. For this design, the suspension is controlled by an electric linear actuator paired with a

spring-damper system. An in-wheel drive motor is fitted to a custom designed wheel to move the system forward and backward, and a steering motor interfaced with a 1:30 gearbox is added for steering controls.

This system was able to achieve some success by being able to drive with adequate traction and precise steering on concrete flooring. The suspension system, however, caused several problems to arise when operating the robot. As the drive wheel is positioned in front of the existing caster wheels, all traction would be lost when driving over edge lip of a slope, causing complete loss of control of the cart. The forward and backward traction forces are also found to be unequal, as the drive plate rotated slightly around the mounting hinges. It is also observed that the system is unable to climb over 1-centimeter tall obstacles from a standstill. Though the drive wheel is able to climb over, the system is not powerful enough to move its caster wheels over the obstacles.

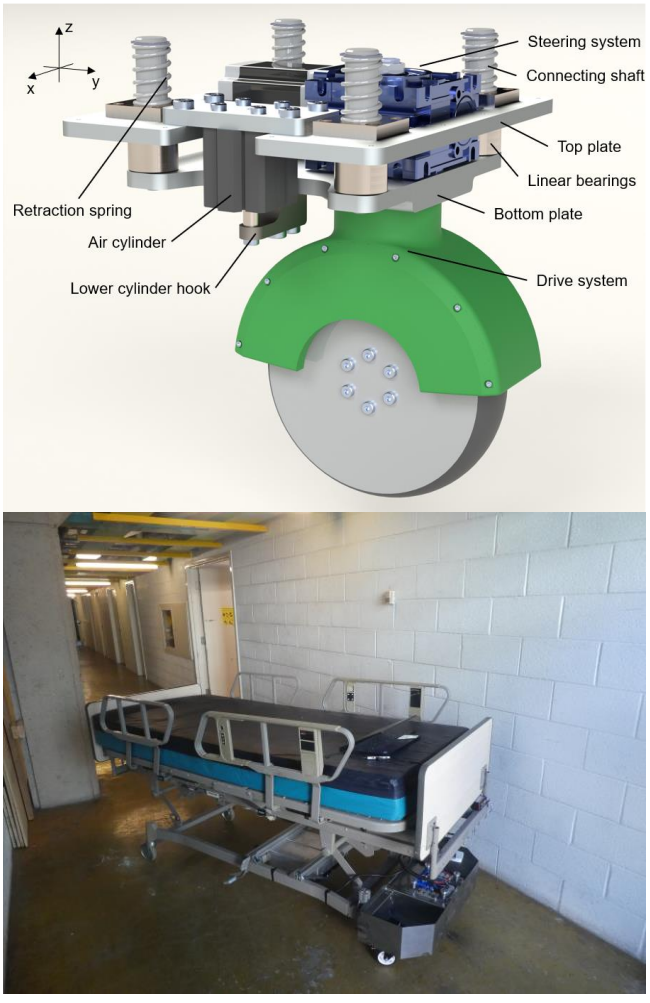


Figure 2.10: Second MVS drive wheel prototype [18].

The second prototype design is created with the intention of addressing the first prototype's mechanical shortcomings. The electric linear actuator suspension system is replaced with a pneumatic air cylinder solution, which allowed for the system to move directly up and down rather than rotating about a point. This design change immediately addressed the issue of loss of traction while operating on slopes, as the wheel could be placed in-line with non-powered caster wheels. The system is also placed in a module manufactured using steel sheet metal during the conceptualization of this design, which allows for it to be fitted to an available hospital bed. Two 40 x 40 mm aluminum profiles are embedded to the rear of the module to allow for simple attachment to beds and on-module casters are added to replace the existing hospital bed caster wheels.

Testing was also performed on this prototype to assess its improvement over the first prototype. Initial procedures confirm that the design is able to perform in single and dual module setups, while providing a maximum traction force of 441 N [18]. The vehicle is able to drive, stop, and steer on flat and inclined concrete surfaces, and is estimated to have a 10.41 h charge cycle. Though this design is able to operate more smoothly than the first prototype, some critical failure points are observed during usage. The in-wheel motor is prone to overheating and shutting off after continuous with reasonable amounts of accelerations and braking. The 3D drive system wheel case also tended to crack when the motor's full torque is used to accelerate or brake.

Within this thesis, the faults of past prototypes will be addressed and farther improved upon. The module will be redesigned and optimized, components will be reassessed, and decisions will be revised to create a more reliable system. Past studies by Yannik Volkert also recommend exploring weight reductions, control schemes, autonomous functionality, and sensor subsystems, which are all considered during further development of designs [18].

CHAPTER 3
DESIGN AND ANALYSIS OF AN ASSISTIVE HOSPITAL BED PLATFORM

In this chapter, the goals for the bed are reassessed, and changes made to better match the vision for the assistive bed and the hospital mobility project as a whole. The technical requirements are recalculated and parts are changed where it is determined to be beneficial.

3.1 Motivation for an Assistive Hospital Bed

Using the lessons learned from building and operating the prototype discussed in section 2.4, an updated assistive hospital bed design is to be created. The data collected about the user experience and prototype preparation are used to inform a conceptual redesign with the goal of making the necessary improvements to prepare for deployment in hospitals and long-term care facilities.

The assistive bed project strives to reduce the magnitude of the pushing and pulling forces that workers must exert when completing routing tasks. As most emergency service injuries are sprains, strains and tears, with the back being the most commonly injured part of the body, an opportunity to minimize incidents and absences exists by targeting this problem. About 35% of full-time workers become injured at some point each year, and 57% of these lead to lost workdays according to a study on these occupational injuries by Brian J Maguire [19].

The forces exerted when workers push wheelchairs and beds can reach unsafe levels. An average of 79N of force is used when operating a 240kg hospital bed or 135kg wheelchair, with a max force of 368N [20]. This figure sharply increases to a maximum of 856 N of hand force when a 100kg load is added to a wheelchair while climbing a step. During maneuvering, 80Nm of lumbar spine torque and 1800N of spinal compression force is experienced. For reference, the Canadian Centre of Occupational Health and Safety recommends that 110N is not exceeded during pushing and pulling [21]. From this recommendation, it can be concluded that the force magnitudes in the health care industry are well into the range for physical overexertion for less experienced or weaker individuals.

The assistive bed aims to address these issues utilizing the mechatronic engineering fundamentals found in heavy duty robot and electric mobile robot solutions to design a practical way to push heavy loads in long term care and hospital facilities. The design will first need to establish itself as reliable through

human-controlled operation, though will allow for work to be done to increase the solution from level 0 autonomy to level 4 autonomy as the prototypes mature.

3.2 Goals for Assistive Bed Design

An achievable goal concept is required for designing a bed module. Before technical guidelines are made some decisions are made to encompass the scope of the assistive bed design, as follows:

- The assistive bed module should be a tool that can be used to retrofit existing beds rather than replace them. This allows for more seamless integration of the design in workflows, while minimizing cost, and focusing on the mechatronic system rather than the health care features.
- The designed module should be reasonably easy to adapt to be fitted to different bed designs. The addition of the module should not be a hurdle in the workflow.
- In the event of required maintenance, the design must allow for parts to be repaired or swapped with ease to limit downtime. If standard parts with known reliability are available, they are to be selected over parts without a degree of confidence as high.
- The module will feature a driving motor as well as a steering motor to power the main drive wheel, as well as 2 caster wheels that replace the bed's original casters. This summates to 3 wheels per module.
- 2 modules must still be possible to ensure front and rear steering is available, as this greatly increases the maneuverability of the bed in tight spaces. A front and rear module allows for a combination of spinning, crab motions, and Ackermann steering models to reach a goal location. This will be particularly important as the controls are developed with future autonomous operation of the bed in mind.
- Suspension and downforce of the main wheel will be provided using a pneumatic system inspired by that of the second MVS prototype. This allows for the drive wheel to be lifted off the ground to enable a typical manual mode for pushing the bed, while also giving fine control of the normal force on the ground, thus the traction.
- Where possible, parts that are confirmed to be viable for the assistive bed application should be carried over between design iterations

These guidelines allow for an informed design to be created, and for an implementable scope for the bed.

3.3 Technical Requirements for Assistive Bed Design

The assistive bed platform technical requirements were initially set for the original prototype, though physical testing has shown that major improvements can be made [18]. As a result, a new set of technical requirements are created to better ensure the safe and easy functionality of the bed.

A total system mass of 500kg was initially set for the bed, but through redesigns and optimizations, the total weight for the prototype modules and retrofit bed during normal operation have been reduced greatly. This information is useful for quantifying a buffer between the expected typical use case of a hospital bed, which was observed during multiple trips to Grand River Hospital to a maximum design load. The maximum acceptable sum of load for a person and equipment on the bed is during operation is kept at 250kg, leaving approximately 240kg for the bed and modules. The total of this, 500kg, is again selected as the maximum system mass as it provides a large buffer for allowable patient and equipment masses while ensuring a reliable mechatronic assembly. It should also be noted that this is well above the typical masses for obese adults found by Statistics Canada's 2018 survey, therefore is expected to allow for use with the vast majority of human loads [22]. Though 63.1% of Canadians were found to be overweight in this study that classifies using BMI, the bed design should be able to accommodate these individuals without any changes to operation quality.

Similar studies can be used to determine other target parameters for the assistive bed's operation. A study comparing normal walking paces with recommended speeds for moderate physical activity found that all participants comfortably walked at a pace above 1.34 m/s [23]. The average walking speed of this study found the individuals walking at an average of 1.63 +/- 0.23 m/s, which falls into the recommended speed range of 1.34 to 1.79 m/s. As this pace is proven to be comfortable, 1.6 m/s will be used as a baseline for a minimum top speed for the mechatronic bed design.

Operation on a slope is also important for the operation of the bed. The user experience should not degrade whenever a typical indoor slope is encountered. A document published by the Canada Mortgage and Housing Corporation presents guidelines for accessible ramps in housing [24]. This source recommends 1:20 slopes, or about 3 degrees, for minimizing effort to climb. The maximum slope, however, is 1:12 (5 degrees) according to building codes. Steeper ramps are occasionally acceptable, but for very small changes in levels, for example a single step to a sunken room or through a sliding door. This 1:10 (6 degrees) slope should not be used for longer slopes, but the bed design should be able to overcome such an obstacle with ease. 6 degrees will therefore be used as the maximum slope that the bed should be able to overcome.

The materials used for the bed must be safe for operation in close proximity to immunocompromised individuals as it is expected to operate in this environment. As such, any potentially harmful materials are eliminated immediately if encountered in the module design. The selected materials must also be durable enough to allow for the bed to be used continuously. No mechanical issues should be tolerated while the bed is in use, whether this is in manual or powered operation.

The drive system must also enable for the bed to be able to roll over small bumps. Several ground obstacles are common in indoor settings, such as elevator gaps, cables, and floor transitions. A 20 mm bump is assumed to be a reasonably large obstacle, and will be used to complete calculations determining required torque.

Cleaning of the assistive hospital bed must be possible without damage. Though it is not intended for use in environments where it may come in contact with water jets or high wind speeds, it must be safe to keep the bed reasonably clean. As such, the bed and module must remain easy to disinfect by wiping or other low-force cleaning in order to minimize any health risks from germs or viruses. The design will attempt to use easy to reach outer surfaces using materials that prevent grime and dust from attaching to the modules.

In addition to this, operation of the bed must be physically safe in order to reduce any hazard to the user and those around them. Sharp edges and corners must be minimized to avoid any cuts. The mechatronic assembly must also not jut out from under the retrofit bed, as this would be a significant tripping hazard. Other methods of interfacing the operation to the user and those around them will be discussed according to specific features that are implemented later.

3.4 Assistive Bed Calculations

Calculations must be performed in order to select suitable components to ensure a successful design is achieved.

3.4.1 Driving Torque Requirements

As the past assistive bed prototypes struggled with climbing inclines, and motor overheating, a new motor must be selected to ensure reliable function of the assistive bed prototype. The torque required to overcome travel on up incline, as well as overcome steps must be provided by the new motor. The parameters used to determine these minimum motor specifications are as defined in section 3.3.

The motor torque required to climb a slope 1:10 slope (6 degrees) is calculated by requiring a net positive force along the incline, as depicted in the free-body diagram below.

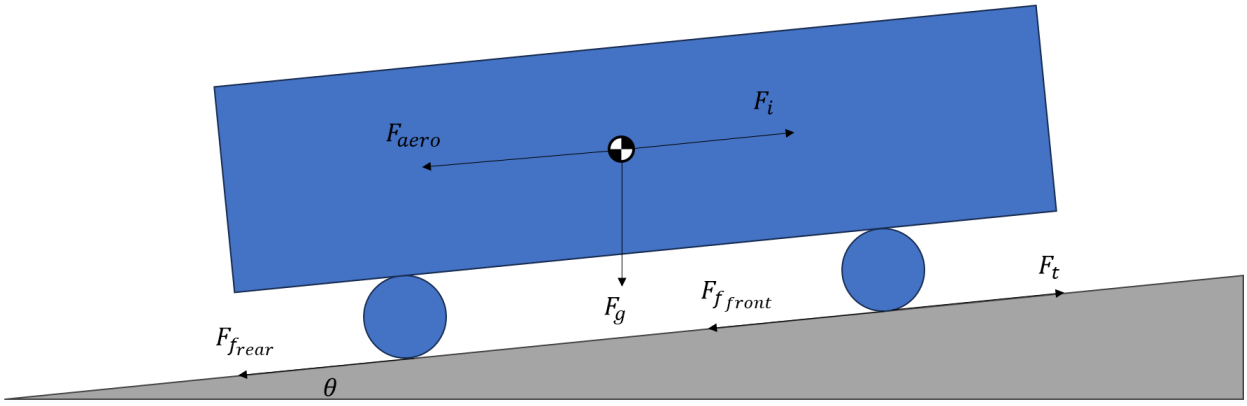


Figure 3.1: Longitudinal forces acting upon assistive bed on a slope

The force balance that results from this is adapted from other similar sources, such as "Modelling the Effect of Driving Events on Electrical Vehicle Energy Consumption Using Inertial Sensors in Smartphones" by Jiminez, which uses Newton's 2nd law to quantify the longitudinal dynamics of the system [25]. In the resulting equation, traction force is denoted by F_t, inertial force by F_i, aerodynamic drag by F_{aero}, friction of the front and rear rolling resistances by F_{ffront} and F_{frear}, gravitational force by F_g, and the angle of incline by θ.

$$F_t = F_i + F_{aero} + F_{f_{front}} + F_{f_{rear}} + F_g \sin\theta \tag{3.1}$$

As the expected operation speed of the assistive bed is not expected to exceed about 2 m/s, the contribution from the rolling resistances and aerodynamic drag are expected to be negligible, and will therefore be nullified to simplify the calculation. The force of gravity can be found by multiplying the maximum mass (m_{bed}) of the bed by the gravitational constant (g). The resulting equation is given below.

$$F_t = m_{bed} a + m_{bed} g \sin\theta \tag{3.2}$$

The acceleration in the equation above is used to define the length of time that the bed takes to reach its operating speed. An acceleration time of 1.5 seconds is selected to ensure that the motor is powerful enough to respond to manual and software control schemes effectively. The value for acceleration can therefore me determined, as shown below.

$$a = \frac{\Delta v}{\Delta t} = \frac{1.6 \text{ m/s}}{1.5 \text{ s}} = 1.07 \frac{\text{m}}{\text{s}^2} \tag{3.3}$$

This value can be used to complete the right side of equation (3.2), and solve for the traction force that must be provided by the motors to climb a slope.

$$F_t = 500\ \text{kg}\left(1.07\,\frac{\text{m}}{\text{s}^2}\right) + 500\ \text{kg}\left(9.81\,\frac{\text{m}}{\text{s}^2}\right)(\sin 6°) = 1046\ \text{N} \tag{3.4}$$

This result of about 1050 N can be used to determine the motor torque by multiplying the value by the radius of the selected wheel motor, however, before a selection can be made, the traction force required to climb a 20 mm bump must be found. The larger of these two forces should be used to select a motor with adequate performance.

The torque required for climbing a 20mm must be checked to ensure that the bed does not struggle to maneuver over small indoor obstacles such as door frames and elevator gaps. To find this, the forces acting on the wheels when it comes in contact with the edge is considered.

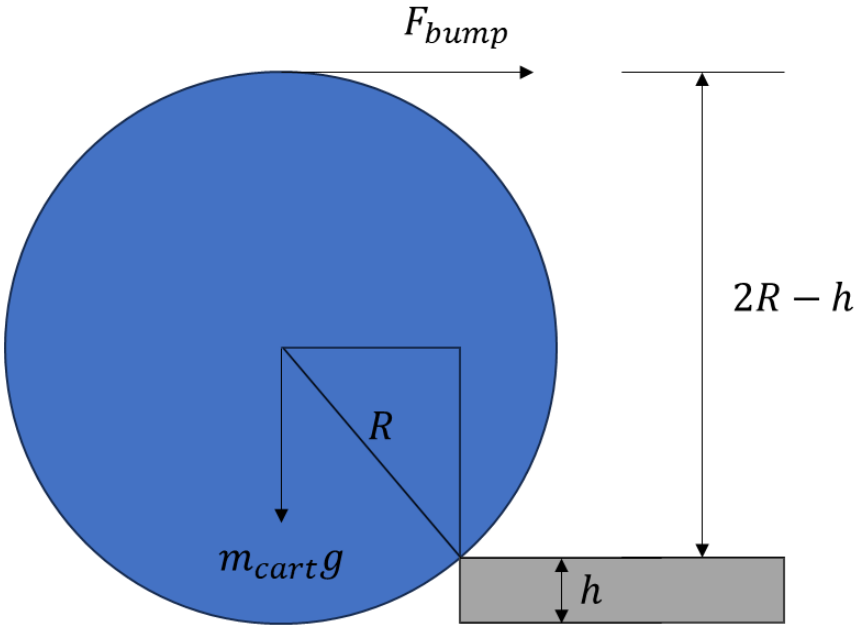


Figure 3.2: Forces acting on assistive bed wheels, directly after coming in contact with a bump.

In order to simplify the calculation of the required force to overcome the bump, some assumptions are made. The bed is assumed to always be horizontal while scaling the 20mm obstacle resulting in the force of gravity always acting straight down when compared to the orientation of the bed's wheel. Additionally, a single wheel axis is expected to be in contact with the obstacle, meaning that the second module is available to provide additional torque without affecting the geometry of the front wheel. Finally, the wheel is assumed to begin from standstill, though with all normal force being provided by the bump. This means that the flat ground surface has a normal force of 0 N when summating the forces.

The geometry of the wheel is also critical when calculating the force required to scale a bump. As the design is expected to preserve as much of the original bed as possible, typical caster wheels for medical applications are considered for calculation. A wheel diameter of 125mm is therefore selected, resulting in the following force balance.

$$F_{bump} = m_{bed} g \frac{\sqrt{2Rh - h^2}}{2R - h} \tag{3.5}$$

$$F_{bump} = 250\ \text{kg}\left(9.81 \frac{\text{m}}{\text{s}^2}\right) \frac{\sqrt{2(0.0625\ \text{m})(0.02\ \text{m}) - (0.02\ \text{m})^2}}{2(0.0625\ \text{m}) - 0.02} = 1070\ N \tag{3.6}$$

The above result provides the peak force when comparing the required force to climb a 6-degree incline to the required force for scaling a 20 mm bump. This can then be used to calculate the required torque by using the radius of a selected motor's wheel.

$$M_{Required\ Torque} = \frac{F_{Required\ Force} r_{Motor\ Radius}}{2\ motors} \tag{3.7}$$

The previous prototype featured a 3D printed tire of diameter 170 mm, and an RMDX10 in-wheel motor. This is used to validate that the new motor selection will be adequate, the result of which is shown below.

$$M_{Required\ Torque} = \frac{1070\ \text{N}\left(\frac{0.170\ \text{m}}{2}\right)}{2} = 45.5\ \text{Nm} \tag{3.8}$$

The resulting required torque from the motor dimensions used in previous prototypes is very close to the 50 Nm peak torque that this motor could provide [26]. This is a possible explanation as to why this motor is observed to have difficulty driving the bed, while also reinforcing that a new motor more suited for the application should be selected.

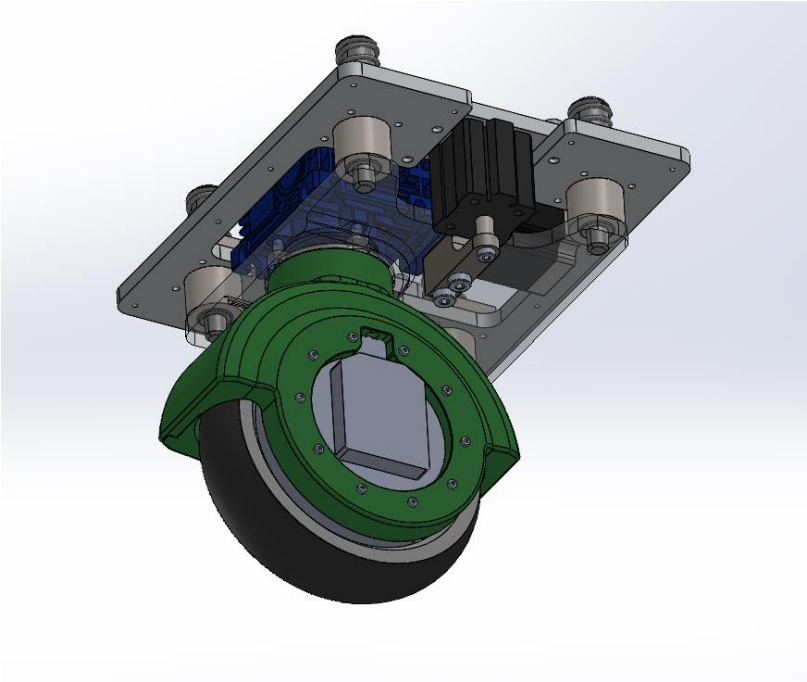


Figure 3.3: Previous drive assembly featuring in-wheel motor [18].

The 200mm diameter ZLTECH ZLLG80ASM800 is selected as a replacement following review of the capabilities of motors on the market as well as in-house production capabilities [27].

$$M_{Required\ Torque} = \frac{1070\ \text{N}\left(\frac{0.200\ \text{m}}{2}\right)}{2} = 53.5\ \text{Nm} \tag{3.9}$$

This in-wheel hub servo motor presents advantages over the previous in both design intent and specifications. This selection increases the torque safety margin when compared to that of previous prototypes, featuring a peak torque of 60 Nm, which exceeds that which is required based on the above calculation [27]. In addition to this, the wheel is included in the motor design, which reduces the complexity of the design by nullifying the need for an original tire design, while also offering IP65 protection. This motor is also originally designed for mobile robots such as delivery robots, handling robots, AGVs, and cleaning robots, which is likely to perform better under continuous use than the previous motor, which is designed for robotic arm use.

3.4.2 Steering Torque Requirements

The torque required to steer the driving wheel of the modules is also reconsidered as part of the component design of the assistive bed's modules. This value can be found by determining the forces of

friction that must be overcome to rotate a tire patch (a flat circular portion of the wheel in contact with the ground). The force of this tire patch varies as more or less of the tire is in contact with the ground, so the worst case, featuring a fully compressed tire is considered.

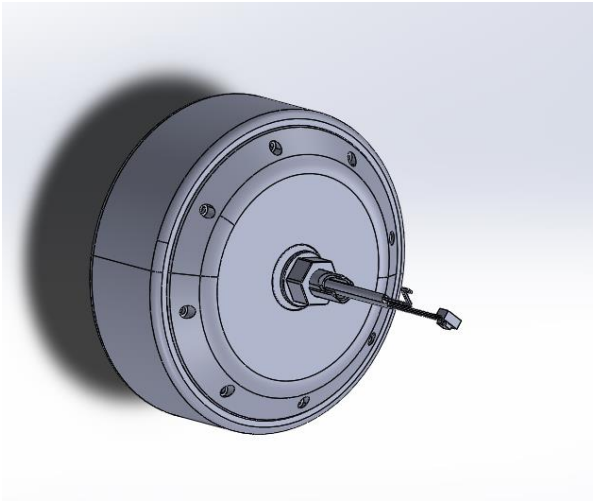


Figure 3.4: Computer-aided design (CAD) model of ZLTECH ZLLG80ASM800 motor and its polyurethane tire.

The thickness of the polyurethane tire is about 10 mm, which can be used to estimate a circular patch diameter. This is done by assuming that the contact area is a circle featuring a diameter equal to that of the length two-dimensional length of wheel in contact with the ground. In the equation used to determine the patch diameter, d_{patch}, below, d_{wheel} represents the diameter of the wheel, and $h_{compression}$ represents the height of the wheel that is compressed.

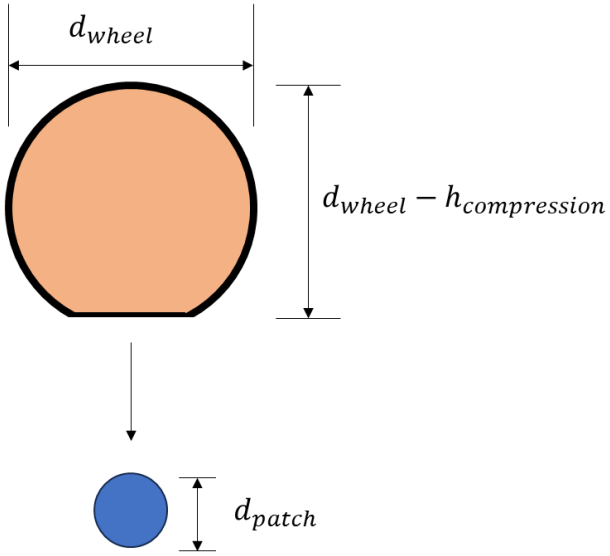


Figure 3.5: Compressed wheel and patch diameter.

$$d_{patch} = 2\sqrt{\left(\frac{d_{wheel}}{2}\right)^2 - \left(\frac{d_{wheel} - h_{compression}}{2}\right)^2} \tag{3.10}$$

$$d_{patch} = 2\sqrt{\left(\frac{0.2\text{ m}}{2}\right)^2 - \left(\frac{0.2\text{ m} - 0.01\text{ m}}{2}\right)^2} = 0.0872\text{ m} \tag{3.11}$$

The patch diameter can then be used to find the frictional force that must be overcome to rotate this patch about its center axis. For this calculation an average range for the friction coefficient between a polyurethane wheel and flooring ranges from 0.04 to 0.08 is considered [28]. The worst case of 0.08 is used for calculation in order to ensure adequate capabilities of the selected steering motor.

The friction between a surface and a solid circular shaft can be considered in order to determine the required torque [29]. In this frictional force balance, μ is the friction coefficient, F is the normal force between the surfaces, r_o is the outer radius of the circle, or half of the patch diameter, and M_{Steer} is the input moment or torque required for equilibrium. Half of the total system mass of 500 kg is used for calculation. This is the maximum theoretical force that can act on the driven wheel at the front or rear axis, though during regular operation, it is expected that caster wheels aid with supporting this mass.

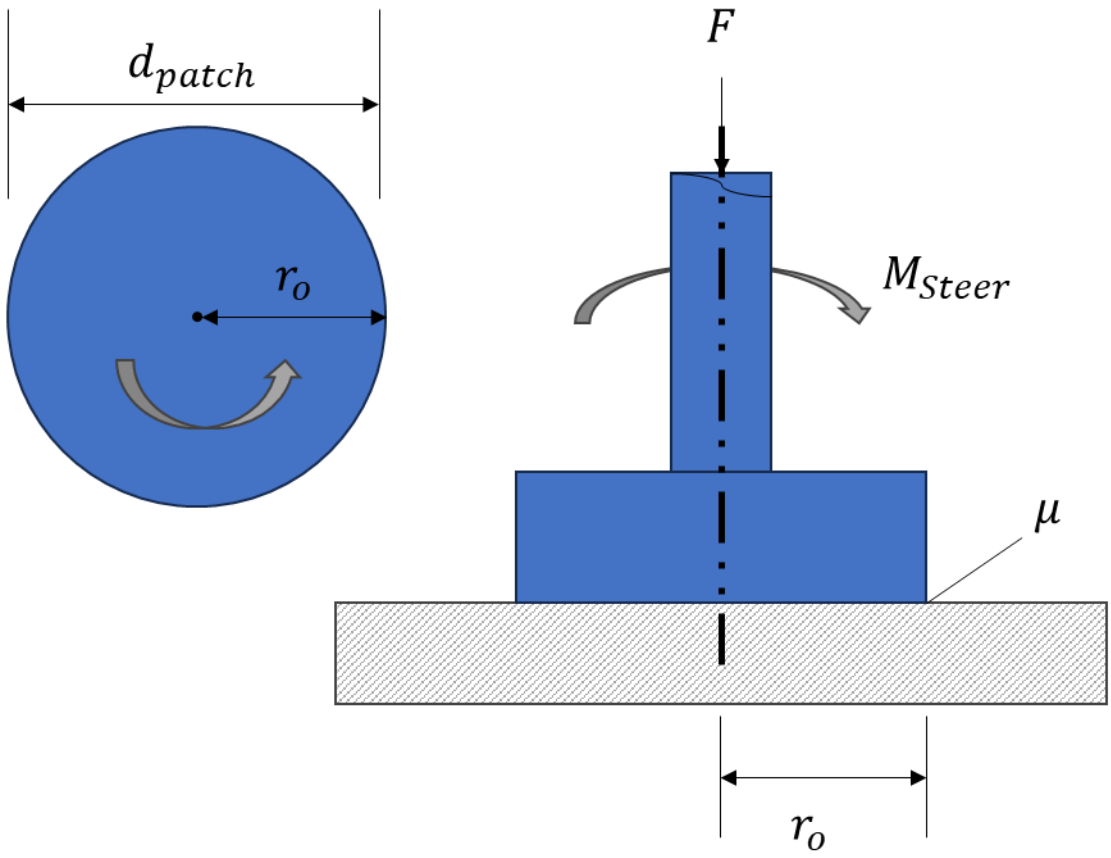


Figure 3.6: Diagram depicting steering moment required to overcome force of friction.

$$M_{Steer} = \frac{2}{3}\mu F r_o \tag{3.12}$$

$$M_{Steer} = \frac{2}{3}0.08\left(\frac{500\text{ kg}\,(9.81\frac{\text{m}}{\text{s}^2})}{2}\right)\left(\frac{0.0872\text{ m}}{2}\right) = 5.70\text{ Nm} \tag{3.13}$$

With this result dictating the performance specification target, the ZD motors Z4BLD60-24NL2-30S-MB brushless DC motor is selected. This motor features a rated torque of 6.97 Nm after a 50:1 gear reduction [30]. This is selected to replace the CPM-MCPV-2311SRLS from Teknic Inc, as it features a higher peak torque by approximately three times, and does not require an additional gearbox for integration [31]. The selected motor from supplier ZD Motors also features some protection with an IP20 rating, which indicates that it is resistant to large solid object of 12 mm.

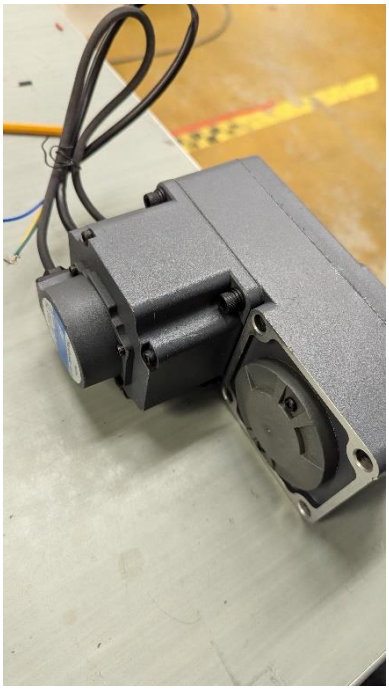


Figure 3.7: Z4BLD60-24GNL2-30S-MB brushless DC motor.

3.4.3 Pneumatic Calculations

The pneumatic system is responsible for lowering and the drive wheel to and from the ground, as well as controlling the magnitude of normal force transferred through the drive wheel. A pneumatic system is selected for this application over an electric lift or mechanical design due to its compactness, design complexity, maintenance, and suitability for a health care environment. A manual lift mechanism would add physical activity to the operation of assistive bed, which is counterintuitive towards achieving the goal of reducing strain on workers and simplifying their workflows. A manual lifting mechanism would also unnecessarily expand the footprint of the bed, as it requires an easily accessible location in front of or beside the module. As discussed in section 2.4, an electric lift is also tested in an early prototype, and it is found that it is difficult to design a compact and reliable system that avoids slipping during operation.

The previous prototype's drive system found success by using a pneumatic system featuring 4 linear bearing shafts between two 10mm thick aluminum plates. These aluminum plates are separated by two air cylinders, which pressurize to separate the plates and push the drive wheel to the ground. This mechanism is used to control the normal force and traction of the wheel. Springs are added along each linear bearing lift the wheel off the ground when the system is depressurized.

The pneumatic system featured in past prototypes are found to be reliable and offer better performance than the electric lift systems designed prior to those, though the latest system is complex to manufacture and assemble, while also being bulky. This offered an opportunity to redesign an effective drive with a smaller overall profile. The first conceptual change that is made is replacing the function of one of the aluminum plates by securing two air cylinders directly to the module chassis or frame. Though this solution eliminates the plate, alignment of the cylinders and plate is crucial for reliable operation of the air cylinders and avoiding buckling. To help alleviate this concern, the single rod air cylinders will be replaced with dual guide rod air cylinders. The dual-guide rod air cylinder features rods on both sides of the main pneumatic cylinder, which prevent the actuated rod from rotating, thus increasing the accuracy and repeatability when extending the air cylinder under load. These air cylinders are also typically more buckle-resistant, allowing for smoother operating when lateral forces are present, which are expected to occur while steering and maneuvering over different terrain.

The spring-linear actuator system is also simplified by changing to double-acting air cylinders. Double acting cylinders give more precise control on the pressure of the system as pressure can now be used to create both tension and compression. The traction of the system can be better controlled in this way using a 5-way 3-position pneumatic valve, which increases the tunability of the system for user comfort, while also allowing for more customizability in a future fully autonomous system. The ability to pneumatically raise the drive wheel also completes the role of the spring, so the four springs and actuators are removed from the system. Although the removal of the spring reduces the system's ability to lift without any powered intervention, the design allows for the wheel to always be lifted when the assistive features are disengaged, returning the drive characteristics to those of a manual bed.



Figure 3.8: New pump and air valve selected for use in the assistive bed.

The 12V pump used in previous designs is replaced by the more compact 24V BD-08AB-D micro air pump which provides a maximum of 7 bar of positive pressure [32]. This pressure can be used to calculate the bore size of air cylinder required.

$$F_{Provided} = P_{Pressure} A_{Bore\ Area} \tag{3.14}$$

The maximum total force is calculated as a baseline for bore size, which would be half of the 250 kg of mass of the front or rear end of bed being lifted by each air cylinder. This results in a force of 1226.25 N being experienced by each air cylinder, and a minimum bore area of 1751.8 mm^2. Assuming a circular bore, the minimum diameter is therefore 23.6 mm. With this knowledge, market options of 25 mm, 32 mm, and 40 mm are purchased for consideration. The 32 mm double-acting air cylinder is ultimately chosen as it offers a safety factor of 1.4, and reduces the concern for buckling during operation as the larger bore is more resistant to buckling at the expected ranges of pressure for operation.

A 30 mm stroke is selected for use, as it allows for a 10 mm gap from the ground to the disengaged, raised wheel when the maximum allowed bump of 20 mm is encountered during manual operation. This also allows for adequate tunability of the suspension stiffness when maneuvering over rougher terrain such as thick textured carpets or tile flowing.

A fast stroke speed is desirable for fast disengagement of the mechatronic module to return to manual operation in a swift fashion. A lifting time of 0.1s is used to determine an estimate of the expected stroke speed of a purchased air cylinder.

$$\frac{Stroke\ Length}{Lifting\ Time} = \frac{30\ \text{mm}}{0.1\ \text{s}} = 300\ \text{mm/s} \tag{3.15}$$

Using these results, the MGP M30x30 air cylinder from supplier, XCPC, is selected for integration in the assistive bed design as it features a 40 mm bore size, 32 mm stroke, 50 to 500 mm/s piston speed, and 1.2 to 10 bar operating pressure [33].

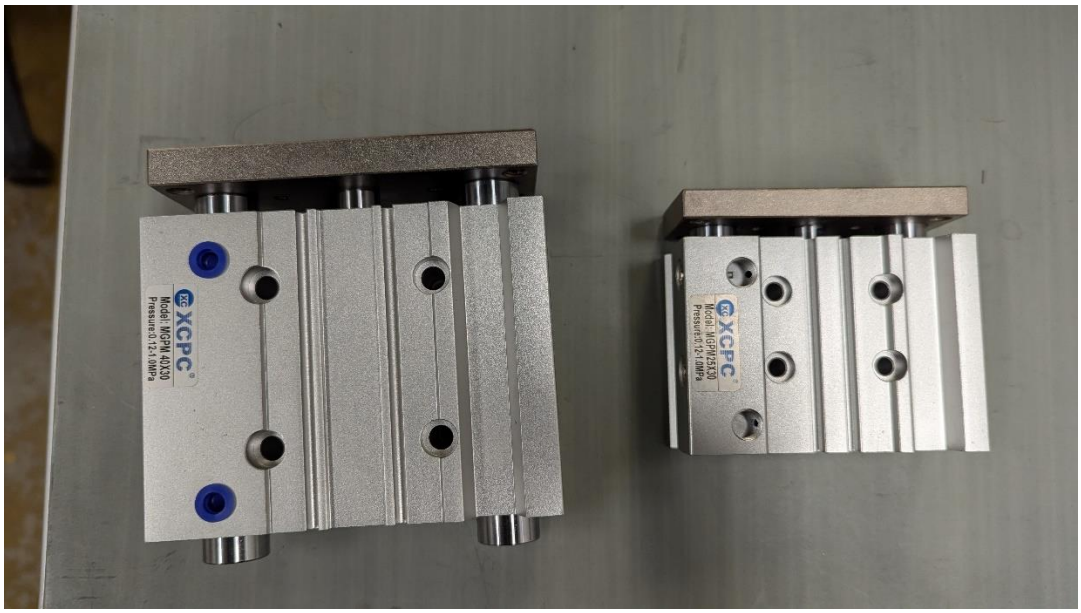


Figure 3.9: 25 mm and 40 mm air cylinders from XCPC.

3.4.4 Bearing Calculations

With changes made to the pneumatic system, driving wheel, and steering motor, compatible bearings must be selected. During initial design of the new bed mechatronic system, it must be proven that bearings of an adequate size feature acceptable lifetimes.

The design takes inspiration from previous bed prototypes by using a thrust bearing as well as a radial bearing, that will be integrated into the driven wheel system to allow for smooth rotation around a shaft when controls are sent to the steering motor. Estimates for dimensions are made based on the motors selected prior to bearing design, the locations of which are outlined in figure 3.10.

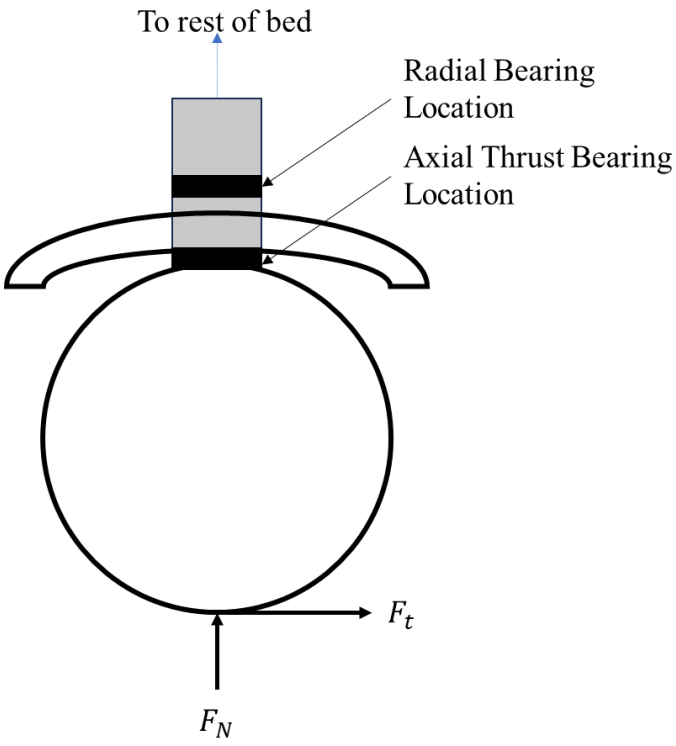


Figure 3.10: Diagram showing rough locations used for calculating thrust and radial bearing specifications.

The process for calculating is taken from Shigley's Mechanical Design textbook, which suggests that the only failure mode for properly cleaned and lubricated bearings operated at a reasonable temperature is fatigue [34]. The life of a bearing is commonly listed as the number of revolutions before the effects of fatigue become present, or the number of hours at a standard angular velocity before fatigue becomes present. Definitions for life also exist which observe the useful life of a bearing. The most common ratings for life provided by suppliers are for the load capacity for operating a bearing for 10^6 revolutions. The 90th percentile reliability rating (L_{10}) is typically used for defining these bearing life load capacities, and will therefore be used to calculate the allowable forces of select bearings.

The load life equation for radial and thrust bearings is typically defined by an empirical logarithmic regression equation. In this equation, F is the expected force, L is the Life, and α_b is a bearing constant. The bearing constant is typically 1/3 for ball bearings and 10/3 for cylindrical and tapered roller bearings.

$$FL^{1/\alpha_b} = constant \tag{3.16}$$

The thrust ball bearing load is tested first. The thrust bearing is responsible for allowing rotation about the steering shaft while being compressed by an upper and lower metal plate. The 51109 used in previous is compared with the smaller 51106 bearing of the same style for this application. This bearing is considered, as it would allow for a slightly more compact design.

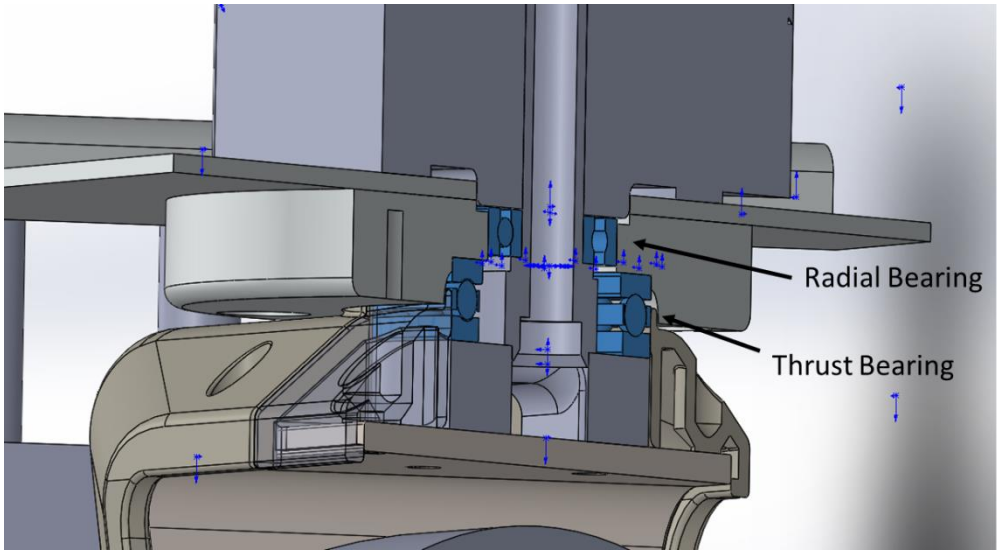


Figure 3.11: CAD model depicting location of bearings.

Initial calculations are performed using the 51109 bearing, which features a 65 mm outer diameter, 45 mm inner diameter, and 14 mm height [35]. The manufacturer lists a 26.5 kN dynamic capacity and 69.5 kN static capacity. The similarly-designed 51106 thrust ball bearing, which has a 47 mm outer diameter, 30 mm inner diameter, and 11 mm height, will then be compared. The 51106 bearing features aa smaller 43 kN dynamic load rating and 19 kN dynamic load rating [36].

The total force that may be experienced by the thrust bearing is found by setting the required traction force as the maximum force. This results in the equation:

$$F_t = \frac{m_{Total}(a_{Max}+g\ sin(\theta_{Max}))}{N} \tag{3.17}$$

In the above equation, m_{Total} is the total mass of the robot, a_{max} is the maximum acceleration of the robot, g is the gravitational constant (9.81 m/s^2), θ_{Max} is the maximum incline that the robot must overcome, and N is the number of motorized wheel modules on the robot. As each of these values are available the equation can be solved directly. The above equation is identical to that which is solved to determine the traction force required from the driving motor and once again results in a force of 1023 N for a one-module setup, and 523 N for a two-module setup.

The traction force must then be transformed into a normal force to find the load that the thrust bearing must support during normal operation. The one-module force of 1023 N is used for calculation from this point. Though the two-module setup is the intended operation setup, a rigorous design is sought to avoid any large failures if one module becomes damaged. A 0.08 coefficient of friction between the polyurethane wheel and flooring is once again used.

$$F_{N_{Max}} = \frac{F_t}{\mu} \tag{3.18}$$

$$F_{N_{Max}} = \frac{1023\ \text{N}}{0.08} = 13\ \text{kN} \tag{3.19}$$

Assuming the dynamic capacity of the bearings will be the limiting factor during operation, this result can be used in equation (3.16) to find the life of the bearings. A safety factor of 1.5 is also applied.

$$26.5\ \text{kN} * (10^6)^{1/1/3} = 1.5 * 13\ \text{N} * L^{1/1/3} \tag{3.20}$$

$$L = 1.1\ x\ 10^6\ \text{cycles} \tag{3.21}$$

The result exceeds the 1 million cycles that is typically given as acceptable when designing for a bearing. The same can now be applied for 51006 thrust ball bearing.

$$19\ \text{kN} * (10^6)^{1/1/3} = 1.5 * 13\ \text{kN} * L^{1/1/3} \tag{3.22}$$

$$L = 0.99\ x\ 10^6\ \text{cycles} \tag{3.23}$$

This result is slightly under the acceptable life of 1 million. Though it should be noted that the normal force is larger than realistically expected during operation as it exceeds the expected maximum gravitational force of the assistive bed the 51109 bearing can be more confidently deployed. For this reason, as well as its availability for testing in the MVS lab, the 51109 bearing is selected for this design over the 51106 bearing.

The minimum allowably bearing capacity is also calculated for reference if in the future the size or application of the technology undergoes changes.

$$F * (10^6)^{1/1/3} = 1.5 * 13\ \text{kN} * (10^6)^{1/1/3} \tag{3.24}$$

$$F = 19.5\ \text{kN} \tag{3.25}$$

This reveals that a dynamic capacity of 19.5 kN should be adhered to in order to ensure long lives of these components and to remove a significant failure point.

Similarly, the value for the radial bearing can be evaluated in the same fashion. As inner diameter of the radial bearing is limited by the size of the steering motor shaft, the previous prototype's radial bearing is not suitable for application. As a result of this, two radial ball bearings of 20 mm inner diameter are compared. The 6004 and 16004 bearings from SKF are selected for consideration [37] [38].

Table 3.1: Considered radial bearings

Specification	**6004**	**16004**
Inner Diameter (mm)	20	20
Outer Diameter (mm)	42	42
Width (mm)	12	8
Dynamic Load Rating (kN)	9.95	7.28
Static Load Rating (kN)	5	4.05

The governing equation (3.16) can be rearranged for radial bearings to determine the required capacity directly. In the following equation C_{req} is the required load capacity, F_r is the radial force, L is the standard life, L_R is the required life and α is the bearing constant.

$$C_{req} = F_r \left(\frac{L}{L_R}\right)^{1/\alpha_b} \tag{3.26}$$

The radial force can be calculated using the maximum wheel torque and its moment arm to the radial bearing.

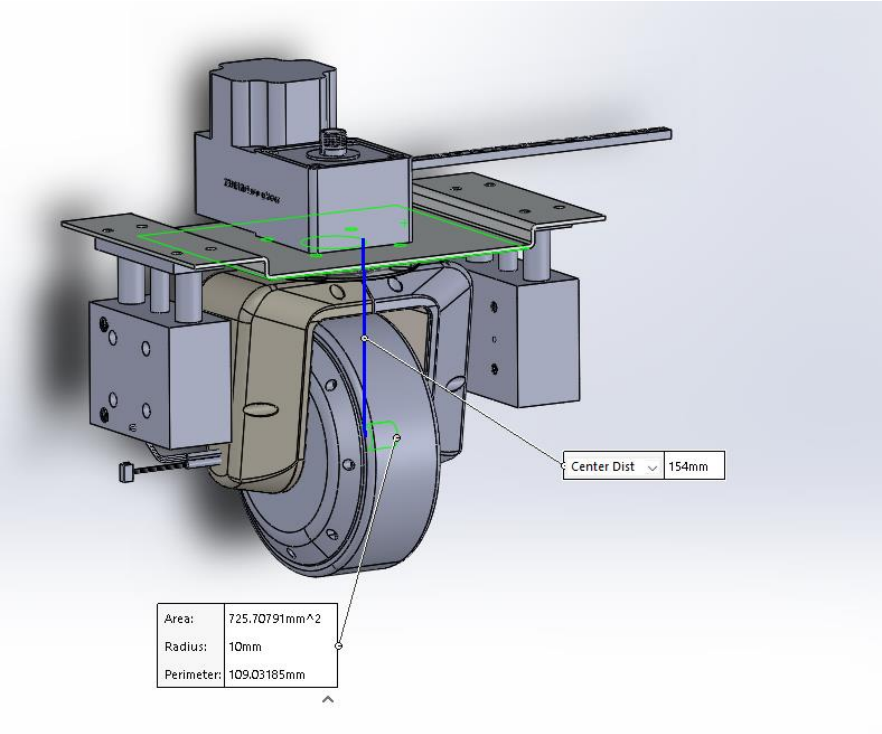


Figure 3.12: Distance from center of wheel to radial bearing location on CAD model.

$$F = \frac{T}{L_{Wheel\ Center\ to\ Bearing}} \tag{3.27}$$

$$\frac{60\ \text{Nm}}{154 \times 10^{-3}\ \text{m}} = 390\ \text{N} \tag{3.28}$$

Plugging this into the required capacity with a safety factor of 1.5, we find:

$$1.5\ (390\ \text{N}) \left(\frac{10^6}{10^6}\right)^{1/3} = 585\ \text{N} \tag{3.29}$$

This result of about 0.6 kN shows that the static and dynamic load capacities of radial bearings are an order of magnitude higher than what is required for safe integration into the design for 1 million cycles. As such, it is not expected than the radial bearing will be a significant point of failure, and both options feature adequate load capacities. The SKF 16004 bearing is therefore selected, as it is 4 mm smaller, and allows for a more compact design.

3.4.5 Other Design Elements

Wheel Case

The wheel case is redesigned to directly address a common failure that is observed when dealing with the original prototype. In the past, the part responsible for connecting the driving wheel, shaft, bearings, and steering motor was 3D printed, though several iterations of this design failed following a few hours of operation. To ensure that this problem does not cripple the performance and life of the design, a metal wheel fork is designed to act as the skeleton for connecting these parts, with a 3D printed. Interior metal is responsible for carrying the majority of the load, while the 3D printed exterior enhances the aesthetics, and protects any wiring from the wheel from contact with external debris.

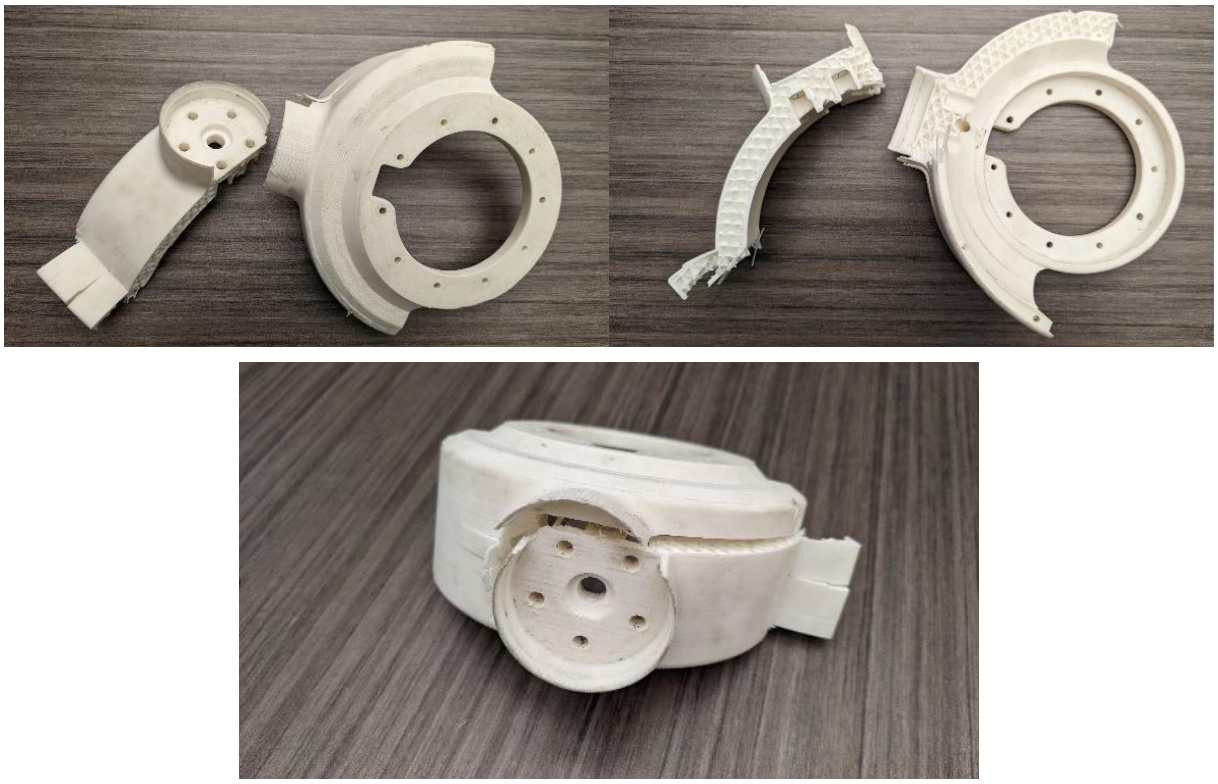


Figure 3.13: Fractured 3D printed wheel case.

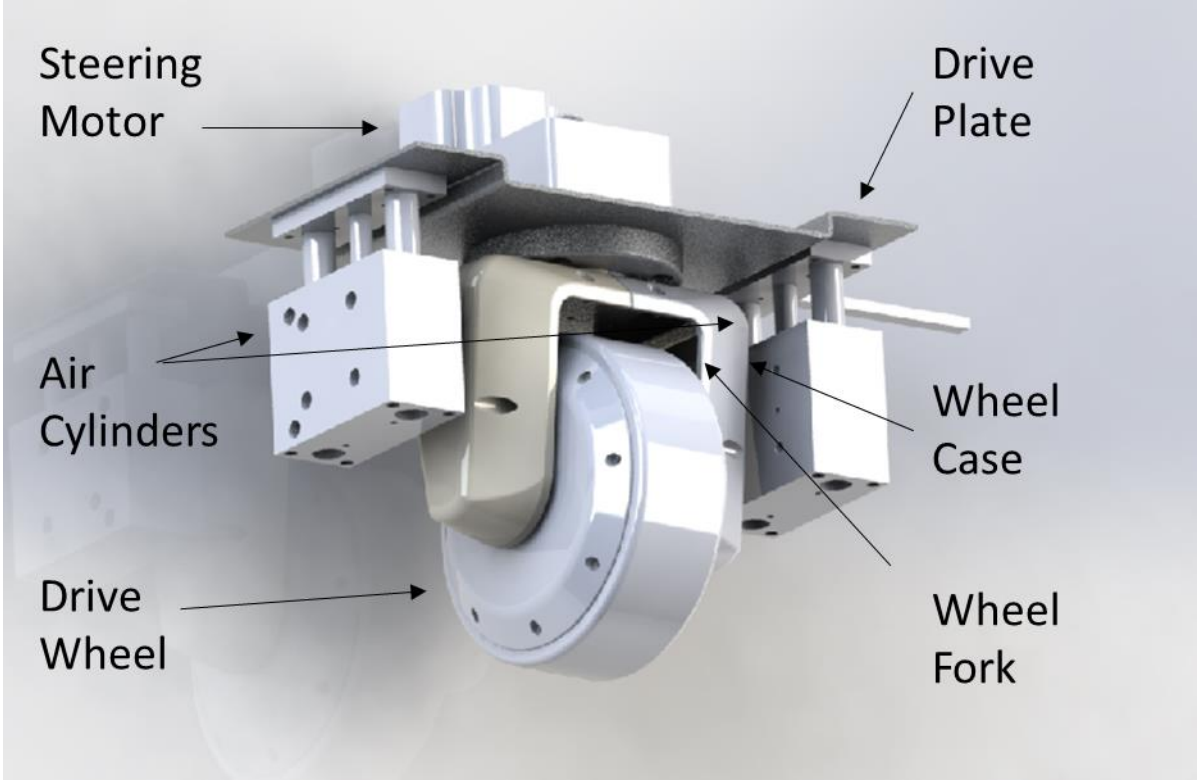


Figure 3.14: CAD Model of main drive assembly, featuring in-wheel motor, air cylinders, and steering motor.

Prior to manufacturing the wheel fork, the 60 Nm maximum torque of the steering motor and 1070 N maximum traction force are simulated. The result of this informs the choice of thickness and material for the wheel fork, and ensures that static failure is prevented under normal use.

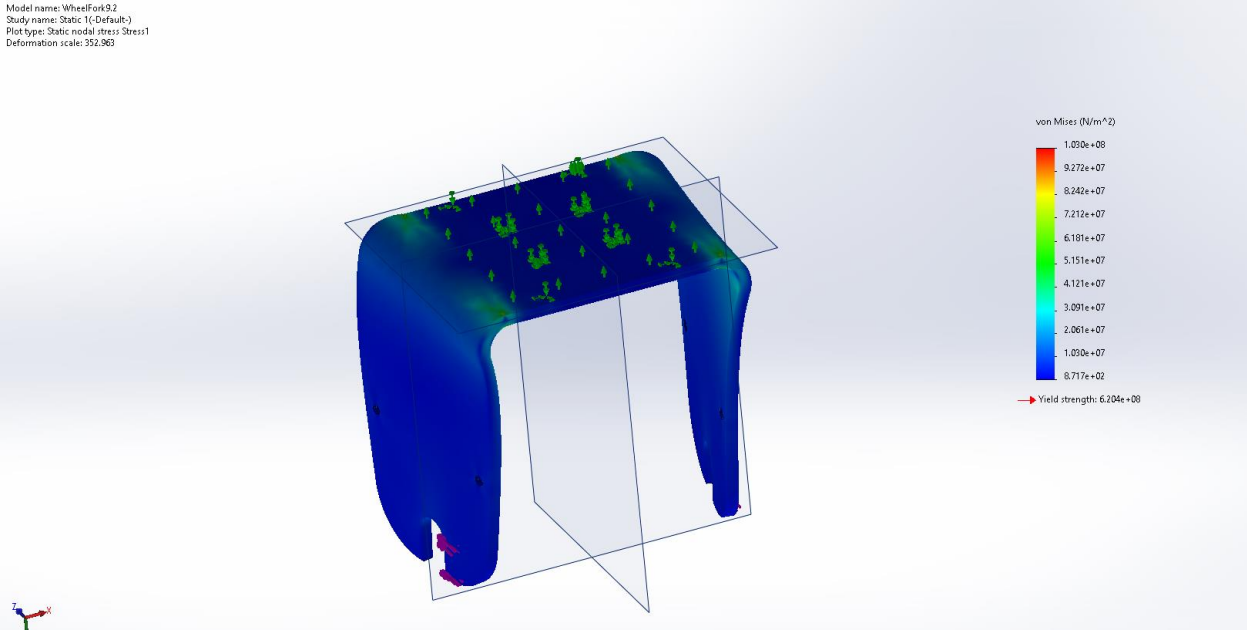


Figure 3.15: Wheel fork with 1070 N from the in-wheel motor exerted.

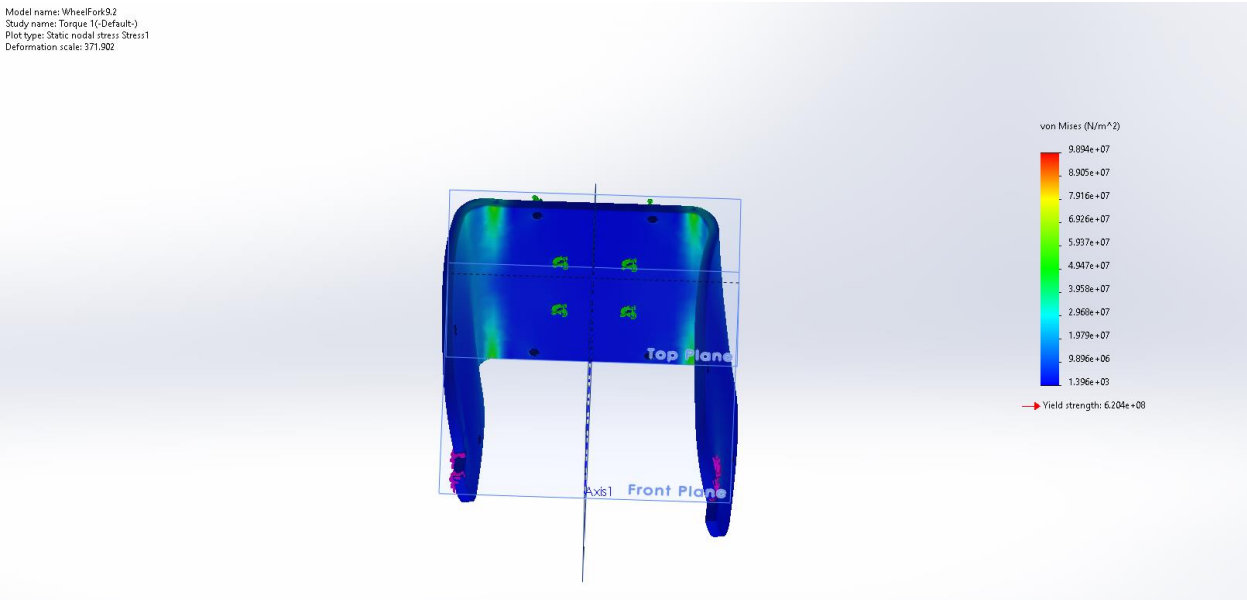


Figure 3.16: Wheel fork with 60 Nm of torque from the steering motor exerted.

The maximum stresses determined using the SolidWorks FEA tool reinforce that the wheel fork at 5 mm thickness will perform more reliably than its 3D printed counterpart. The locations of higher stress are in the corners and connection points, as expected, though the maximum stress is an order of magnitude lower than that which would cause yielding in mild steel.

Overall Mechatronic System

The new overall mechatronic system is designed to be compatible with the new parts, while also serving as a guideline for integration in the existing casing for testing. Though the width and connection mechanism are preserved, a bus bar and terminal block mounting location is added to aid with wiring. Direct access for wiring is also added to the rear of the module.

The layout of the internal components is modelled, and battery expanded to 48 V and 35 Ah to fill available remaining space. The overall sheet metal profile is kept similar to the previous model to allow for quick deployment of new parts into existing technology, though the steering motor size requires a lid with a cutout or top feature to accommodate. 40 x 40 mm strut profile are also maintained for the attachment mechanism that allows for quickly retrofitting existing beds. This allows for compatibility between the old casing and new design, to allow for faster testing after this redesign by changing components, rather than requiring all parts to be purchased again.

As casters wheels are simple to replace, generic casters are modelled, and holes left for assembly using options on the market. Different caster wheels exist for different heights, weights, rotating resistance, and wheel frictions, allowing for several options to be tested later.

Many of the components related to control are carried over from past designs to this one. An Audesse Flexcase S microcontroller is used in this design, as it is powerful and versatile [39]. Although its original design intention is for automotive applications indicates that it is more powerful than what is needed for this application, its reliability allows for its use for this design so that a cheaper option can be selected in the future. This microcontroller is paired with an Arduino, which is used to interface the main microcontroller unit with the sensors. The EPAuto Air Compressor Tire Pump is also carried between designs initially for its reliability, though the BD-08AB-D micro air pump is also purchased for its preferred size and as a readily available alternative. The EPAuto pump operates at 12 V, with a maximum working pressure of about 480 kPa [40]. An air tank is also paired with an air reservoir tank with a maximum operating pressure of 1.2 MPa and volume of 0.5 L. This allows for some pressure to be stored to ensure that the drive wheel can be lifted from the ground even in the case of a pump failure, while also regulating the system pressure to more efficiently run the pump. New servo motor drivers are also included this design for the drive motor and steering motor, though these are provided alongside their respective motors from the motor manufacturers.

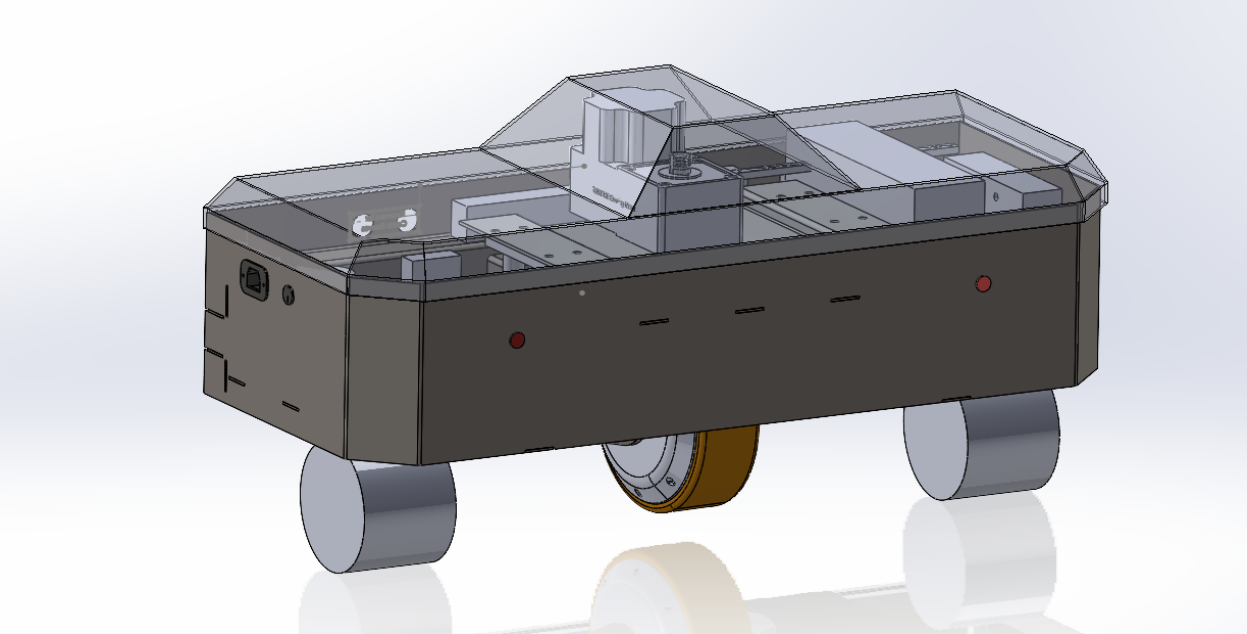


Figure 3.17: Front view of the assistive bed module CAD model.

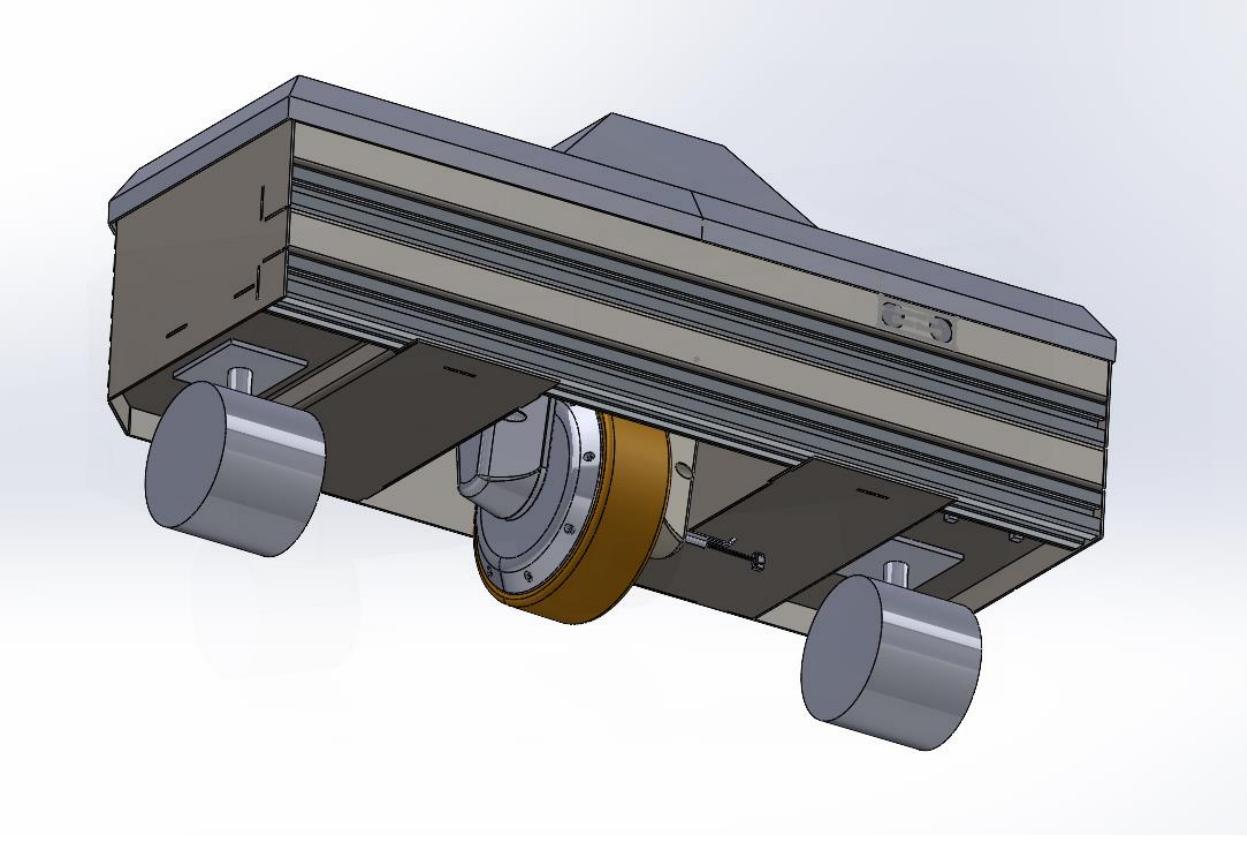


Figure 3.18: Rear view of the assistive bed module CAD model.

Non-Steering Version

A non-steering 1-module design is also conceptualized to show the adaptability of the design. This module features all the same technology of the full design, aside from the removal of the steering motor, shaft, and bearings. This design offers the ability to assist workers with only longitudinal movement. This idea is used as a simpler use case to verify the performance of the remaining parts, and ensure ease of use with a simpler robot. It is found that workers can quickly switch from manual to this assistive mode seamlessly, which is used to justify farther designs.

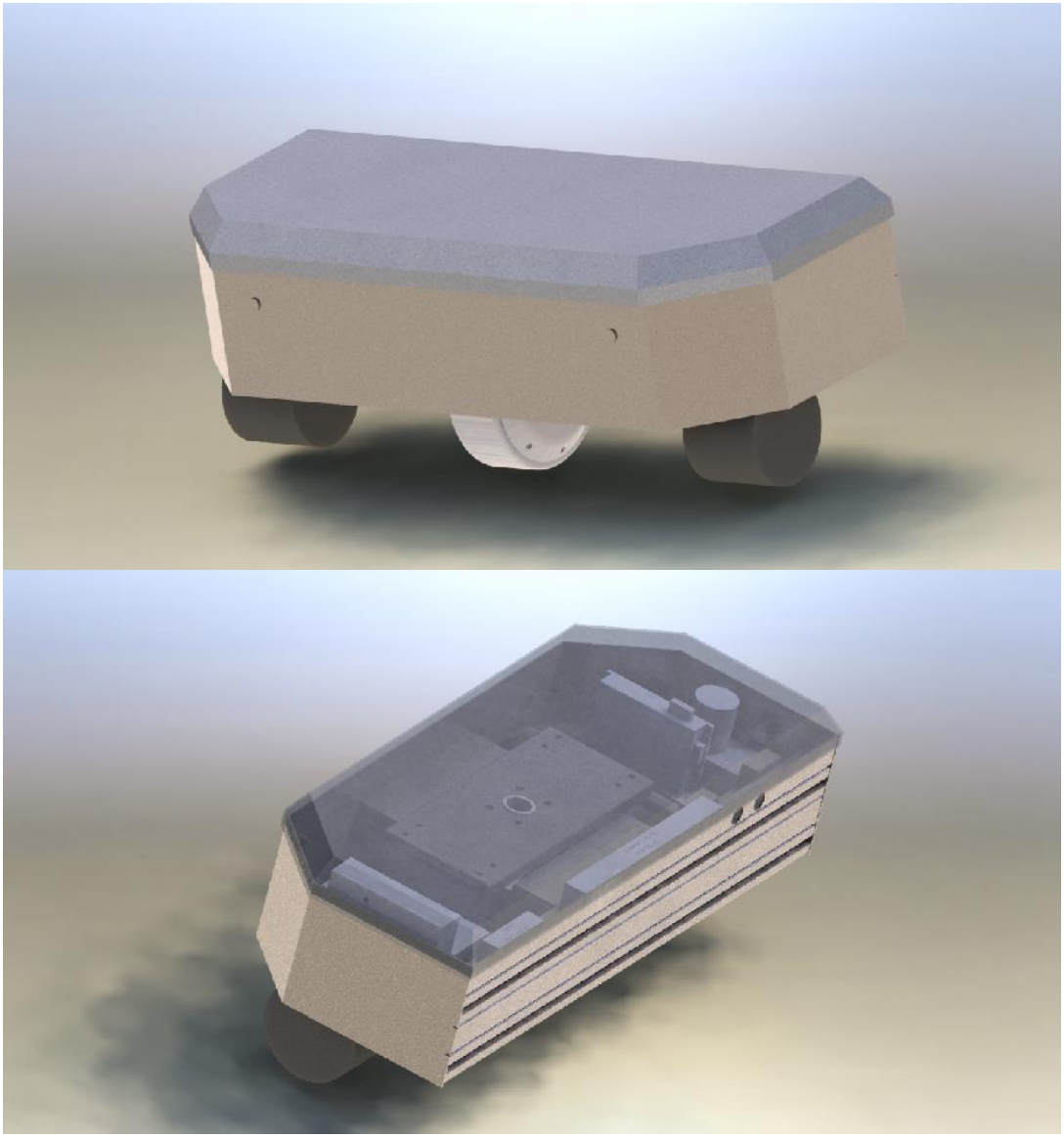


Figure 3.19: CAD model of non-steering bed module.

CHAPTER 4
DESIGN AND ANALYSIS OF ASSISTIVE CART AND CART HAULER

Using the lessons learned through the design, fabrication, and testing of the assistive bed prototype, a larger scope design is initialized with the goal of more universality for applications in health care mobility. The following section will present the necessary calculations and designing that are required to build assistive modules that can be quickly adapted for use in applications other than carts. The daily workflow of health care workers features several potential opportunities for routing transportation of materials outside of patients on beds, including but not limited to laundry carts, medical equipment carts, and food carts. The following designs aim to create a solution that can be quickly adapted to for the need for any of these frequently pushed apparatuses to further reduce the potential strain on workers.

4.1 Design of an Assistive Cart

An assistive cart is designed to expand the mobility in health and long-term care project. Though the cart shares the goal of lowering the levels of strain experienced by workers routinely pushing equipment, the types of equipment that this project's solutions apply to is expanded.

4.1.1 Design Goals and Motivations

The assistive cart concept expands upon the assistive bed's design by attempting to create a more general design that can be adapted to other apparatuses that require movement. While conducting field research with a long-term care home partner of the lab, it is observed that the technology can be useful in many applications. Heavy food carts, laundry carts, medicine cabinets, medical carts, and several other types of caster-wheeled carts are moved between several points within the facilities to be loaded and unloaded. Some of these carts can be moved several times an hour, with a more variable weight than the bed.







Figure 4.1: Various carts observed at Schlegal Villages Retirement Home and Schlegal-UW Research Institute for Aging.



Figure 4.2: Various carts observed at Grand River Hospital

With the fundamental differences in the construction of the carts, a new design is required. The goal of this design is to be easily adaptable to any equipment that uses caster wheels in health care and long-term care facilities. As such, the dimensional profile must be easy to deploy on carts of varying heights, lengths, and widths.

The cart is designed to be quickly deployable in non-critical workflows where data can be collected on the user experience and it can be switched for an existing manual cart without disruption. The platform will consist of similar core components to the bed for future research on autonomous operation of various degrees, though it is designed with assistive capabilities taking precedence. A simple-to-use control scheme is required at this point in the design, as past bed prototypes have been controlled from a computer or controller, which is not practical for its intended use.

The first prototype of these will be designed for Schlegal's encore series treatment cart, though will be easily adapted to the other carts mentioned. This type of cart is used at long-term care homes to deliver medicine and tablets to residents several times a day and thus makes several stops.



Figure 4.3: Vintage Encore Series Treatment Cart from Cancard [41].

4.1.2 Required Parameters

A new set of qualitative and quantitative design guidelines are required to meet the altered design goals of the assistive cart. The nontechnical guidelines are used to initialize the design process while also providing reasoning for weighing options and selecting solutions. They are as follows:

- The assistive cart technology should be contained within a module similar to the bed. The module should be simple to retrofit to carts of different sizes. As a result, the length, width, and height should be minimized.
- Ease of maintenance should be maintained or improved by allowing for simple access to the main electrical components for swift changes to be made. Standard parts are preferred over custom parts as they are more plentiful and can typically be held to a high standard of quality.
- The module will feature a driving motor but no steering motor.
- Original caster wheels should be used during the retrofitting process if possible.
- Suspension and downforce of the system will still be provided using a pneumatic system, as this method has proven to be compact on previous prototypes.

The assistive cart's smaller size also necessitates adjusted technical requirements.

The maximum system weight can be informed by guidelines provided by the Canadian Centre of Occupational Health and Safety (CCOHS). CCOHS provides the weights and frequencies at which carts should be operated at in order to minimize injuries related to overexertion, including strain injuries in the lower back, shoulders and arms, slips trips and falls, and toes and fingers being caught or crushed by the cart [42]. As the defined goal of the assistive cart is to retrofit rather than replace, the limits can be defined using manual parameters. This leads to a maximum load of 227 kg for a 4-wheeled cart, with a maximum of two hundred 33 m transportations during an 8-hour shift.

The desired design speed of about 1.6 m/s of the assistive bed is shared with the cart as a walking pace is desired. The acceleration time to reach this speed will also be shared at 1.5s. The indoor operation setting is also shared between these two designed, so the maximum incline of 1:10 will be used for design in accordance to the Canada Mortgage and Housing Corporation building guidelines. Additionally, the cart must overcome the same indoor obstacle as the bed, so a bump of 20 mm will be used to aid in calculating the required torque of the system.

Like the bed, the materials used for the assistive cart must be safe for operation in long term care and hospital facilities. Durability is essential for a long lifespan of the product, and to avoid debris and moisture damage. The cart must also be able to withstand light surface liquid use for cleaning.

4.1.3 Required Torque

In order to select a suitable motor for the assistive cart, the minimum required torque must be determined. The torque provided from the motor must be able to overcome travel on an incline, as well as overcome bumps from a stand-still, similar to the bed.

Following a similar process used when calculating the torque required for travel up an incline using a model involving the sum of the forces acting upon a vehicle, the required torque can be found. The maximum angle θ is taken to be the 1:10 ratio outlined in section 3.3, which is the maximum that should be encountered indoors, where the cart should be operating. F_t denotes the traction force required to be provided by the motor in order to accelerate the cart forward. F_i denotes any inertial forces that the cart exhibits. This can be calculated using Newton's second law of motion as the target maximum mass is known, and acceleration can be found by assuming a walking speed should be achievable in a short timeframe of about 1.5 seconds. F_{aero} denotes the aerodynamic drag, while F_{ffront} and F_{frear} denote the front and rear frictional rolling resistances respectively. The final necessary force for determine the force required to be provided by the motor is the component of the gravitational force parallel to the ground surface. Figure 3.1 can also be used to describe the cart body.

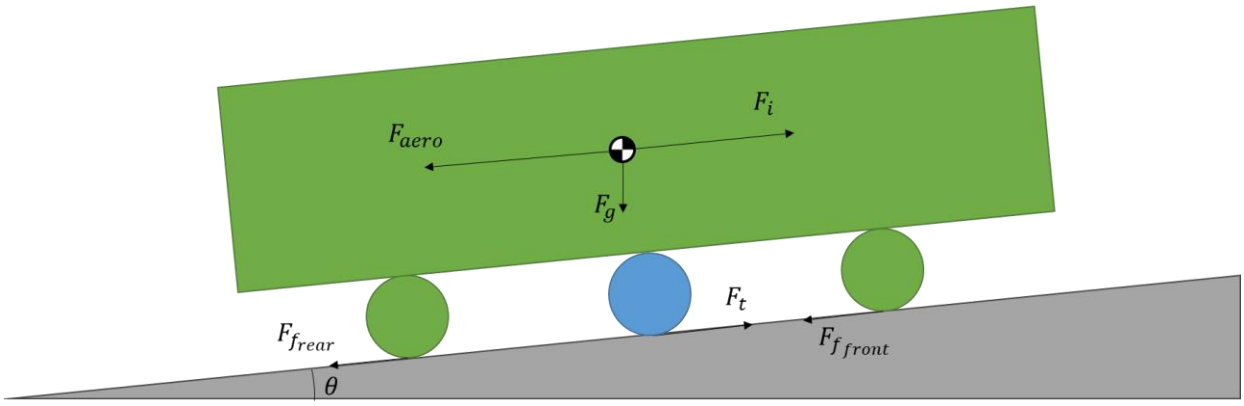


Figure 4.4: Free body diagram depicting the force balance for calculating the required torque for the cart's climbing of a 1:10 incline.

$$F_t = F_i + F_{aero} + F_{f_{front}} + F_{f_{rear}} + F_g \sin\theta \tag{3.1}$$

Due to the relatively low speed operation environments that the carts are expected to operate in, the effects of the aerodynamic drag and frictional rolling resistances are assumed to be negligible and thus set to 0. This simplifies the equation to:

$$F_t = m_{cart}a + m_{cart}g \sin\theta \tag{3.2}$$

As stated above, the acceleration used to determine this is determined by assuming a 1.5 second acceleration to the desired walking speed of 1.6 meters per second. The g variable is the gravitational constant.

$$a = \frac{\Delta v}{\Delta t} = \frac{1.6\ \text{m/s}}{1.5\ \text{s}} = 1.07\,\frac{\text{m}}{\text{s}^2} \tag{3.3}$$

This can then be implemented in the full torque equation (3.2) and solved for the traction force.

$$F_t = 227\ \text{kg}\left(1.07\,\tfrac{\text{m}}{\text{s}^2}\right) + 227\ kg\left(9.81\,\tfrac{\text{m}}{\text{s}^2}\right)(\sin 6°) = 474.90\ \text{N} \tag{4.1}$$

Before selecting a motor with an appropriate diameter and rated torque suitable for providing this traction force, the force required to overcome a small obstacle or bump must be checked. This calculation may potentially produce a smaller value which would make it the limiting factor. Unlike the 2-module layout that the bed featured, the cart design is planned to only have 1 driving motor without any steering capabilities, so ideally the selected motor can push the front caster wheels over a bump.

The bump height under consideration is selected to be 20 mm in order to ensure robustness and confidence when deciding on a motor and wheel. This will trivialize the difficulty of moving the cart over door frames, elevator steps, wiring, and other small obstacles that it may be required to maneuver over. To calculate the required force and torque a few assumptions must be made:

- The vehicle will always be horizontal throughout the duration of the calculation scheme, ensuring that gravity acts vertically
- Only wheel axis is experiencing the obstacle, and will thus experience a maximum of half of the cart mass, 113.5 kg
- The wheel at the step is only in contact with the step and not the ground surface. The normal force from the ground surface is therefore 0N

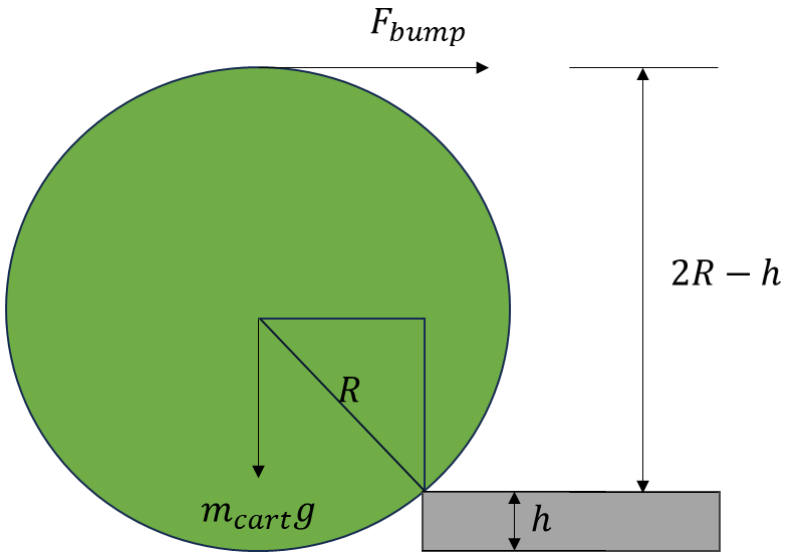


Figure 4.5: Forces acting on wheels when in contact with an obstacle.

In order to calculate the force required to rotate the wheel up this step, a wheel radius must be selected. As the front and rear axles of the cart are planned to be separate from the motorized module, the radius of the casters found on these axles are expected to cause the maximum force requirement. In order to be consistent with the standard caster size used for the bed previously, a radius of 62.5 mm is used for calculation. A force balance of the wheel depicted above is used to determine an equation for the required force:

$$F_{bump} = m_{cart}g\frac{\sqrt{2Rh - h^2}}{2R - h} \tag{3.5}$$

$$F_{bump} = 113.5\text{ kg}\left(9.81\frac{\text{m}}{\text{s}^2}\right)\frac{\sqrt{2(0.0625\text{ m})(0.02\text{ m}) - (0.02\text{ m})^2}}{2(0.0625\text{ m}) - 0.02} = 413.5\text{ N} \tag{4.2}$$

As can be observed by the above result, the peak force that will be required to be provided by the motor is expected to be limited by its ability to overcome small obstacles. With both results, the torque rating of the motor can be calculated by taking a moment about its center, which gives the equation:

$$M_{Required\ Torque} = F_{Required\ Force}r_{Motor\ Radius} \tag{4.3}$$

As reference for motor selection purposes, the ZLLG80ASM800 motor selected for the bed is used as a baseline. This wheel-motor assembly features a diameter of 200 mm.

$$M_{Required\ Torque} = 556.72\text{ N}\left(\frac{0.2\text{ m}}{2}\right) = 48.6\text{ Nm} \tag{4.4}$$

The resulting torque rating of about 49 Nm is under the peak torque of 60 Nm listed for the ZLLG80ASM800 motor. As the peak torque is expected to only be required for small durations of time, selecting a motor with a marginally higher rating will serve most expected scenarios well. Knowing this a motor is selected with a rigid requirement of requiring a higher peak torque than that which would be required to overcome a 20mm bump, as well as other qualitative parameters:

- Preference is given to other ZLTECH motors, as the motor used for the bed is shown to perform well on the bed prior to this selection
- Preference is given to smaller wheel diameters, as it directly affects the overall dimensional footprint of the design, which should be minimized
- As the design will operate in an indoor setting, high RPM ratings are not required
- Preference is given to more robust motors featuring resistance from dust or water

These considerations lead to the selection of a slightly smaller model of motor from ZLTECH, the ZLLG65ASM500. This motor features a diameter of 165 mm and 44 Nm peak torque. When equation 4.3 is used to determine the required torque for a wheel of this size to move the casters and cart frame, a result of 40.1 Nm is found, which is adequate for meeting the parameters outlined above.



Figure 4.6: ZLLG65ASM500 motor.

4.1.4 Pneumatic Requirements

The pneumatic system also requires a redesign to better accommodate the smaller mass, smaller size, and universality of the cart module when compared to the existing assistive mobility bed. Initial results from the assistive bed confirmed that the pneumatic system is adequate for lifting and lowering the motor safely without the need of a supportive spring system when a double acting air cylinder is used instead of a single acting cylinder. This also gives more precise control over the traction force while operating, as the amount of normal force can be controlled by adding pressure to the cylinder in the direction that pushes the wheel into the ground.

The main pneumatic components that must be selected and designed around are the pump and cylinders. The pump used for the bed will be used for calculation purposes then changed if performance or size does not meet the requirements for the cart. Preference will also be given to a larger two 3-shaft air cylinder rather than four smaller air cylinders.

The BD-08AB-D micro air pump used for the bed featured a maximum positive pressure during operation at 24V DC of 7 bar. This operating pressure can be used to determine the maximum force that can be provided by the air cylinder in either of its acting directions using a force-pressure balance.

$$F_{Provided} = P_{Pressure} A_{Bore\ Area} \tag{3.14}$$

Using the pressure of the micro motor, the force provided using 3 readily available bore sizes for cylinders is found.

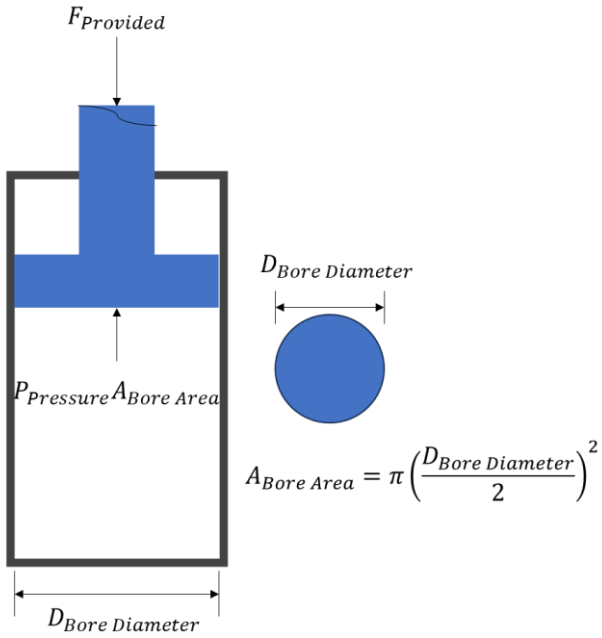


Figure 4.7: Air cylinder equilibrium free-body diagram.

Table 4.1: Forces provided by single air cylinders of various sizes

Bore Size (mm)	**Force Provided (N)**
25	343.6
30	494.8
40	879.6

These forces can then be compared to the required traction forces found in section 4.1.3 of about 475N. Though the magnitude of the forces found using a single 25 mm or 30 mm bore cylinder configuration are both less than that of the required traction force, it is expected that either will be able to surpass this when a two-cylinder configuration is designed as this will double the provided force. In order to narrow the selection further, the maximum mass of the cart of 227 kg is considered. The wheel should be able to lift slightly more than half of the mass for flexibility for the drive quality when going over rougher uneven terrain. The force of gravity on the ground from the total cart is calculated prior, and half of this is about 1113 N. Of the three bore sizes under consideration, only a configuration featuring two 40 mm air cylinders would meet this force requirement. This bore size is therefore decided upon, as it meets the upper end of the requirements, and will be able to operate with a large buffer under normal conditions when frictional losses and pressure losses of the system are considered.

The stroke and speed requirements of the air cylinder are selected qualitatively based on prior experiences. A 30 mm stroke is selected to ensure the travel distance is adequate in the downwards direction for keeping contact with the ground over bumps, while also leaving distance to be lifted so that the assistive cart can still operate as a non-motorized cart when the system is turned off. The speed of the air cylinder should be able to cover this stroke length quickly, so a time of 0.1 seconds is used for a basis for speed selection.

$$\frac{Stroke\ Length}{Lifting\ Time} = \frac{30\ \text{mm}}{0.1\ \text{s}} = 300\ \text{mm/s} \tag{3.15}$$

This result is used to select the MGP M40x30 air cylinder from XCPC, which features a 40 mm bore size, 30 mm stroke, 50 to 500 mm/s piston speed, and 1.2 to 10 bar operating pressure. This meets each of the guidelines presented in this section, and is expected to operate well based on successful integration of a smaller air cylinder from the same manufacturer in the assistive bed.

4.1.5 Assistive Handle

An assistive handle is also designed for the cart. This is an improvement to the initial control interface used for the bed, which used an Xbox Controller. Though the controller served as a useful tool for testing that the mechatronic assembly is working as intended, it would not be a viable option for deploying the assistive bed or the cart for testing in a health care or long-term care home.

The assistive handle as presented below is chosen, as it is the most natural user interface possible. The handle's usage mimics a non-powered cart's operation, to minimize any operational training required for this design to replace an existing cart. The assistive cart's new human-robot interface responds to a natural push of the handle by assisting to move the robot forward.

The introduction of the seamlessly controlled handle is a natural progression of the design, facilitated by the use of strain gauges. Strain gauges are arranged in a full bridge setup to sense the bending stress on the vertical legs of the handle in the locations shown in figure 4.8. Two full-bridge strain gauges sets are placed on each leg to measure forward pushing force, as well as in the side direction to monitor any twisting on the handle. Though the cart is only able to assist with longitudinal locomotion, the information from the additional set of strain gauges allows for data to be collected regarding the typical torque input to the handle by the user. This rotation-monitoring strain gauge standardizes the handle design for future any future models that include steering capabilities. A full bridge strain gauge is selected, as it offers greater sensitivity, while minimizing any effects of temperature changes in the handle

metal. It also allows for a linear output from the strain gauges, which simplifies the required data processing for controls.

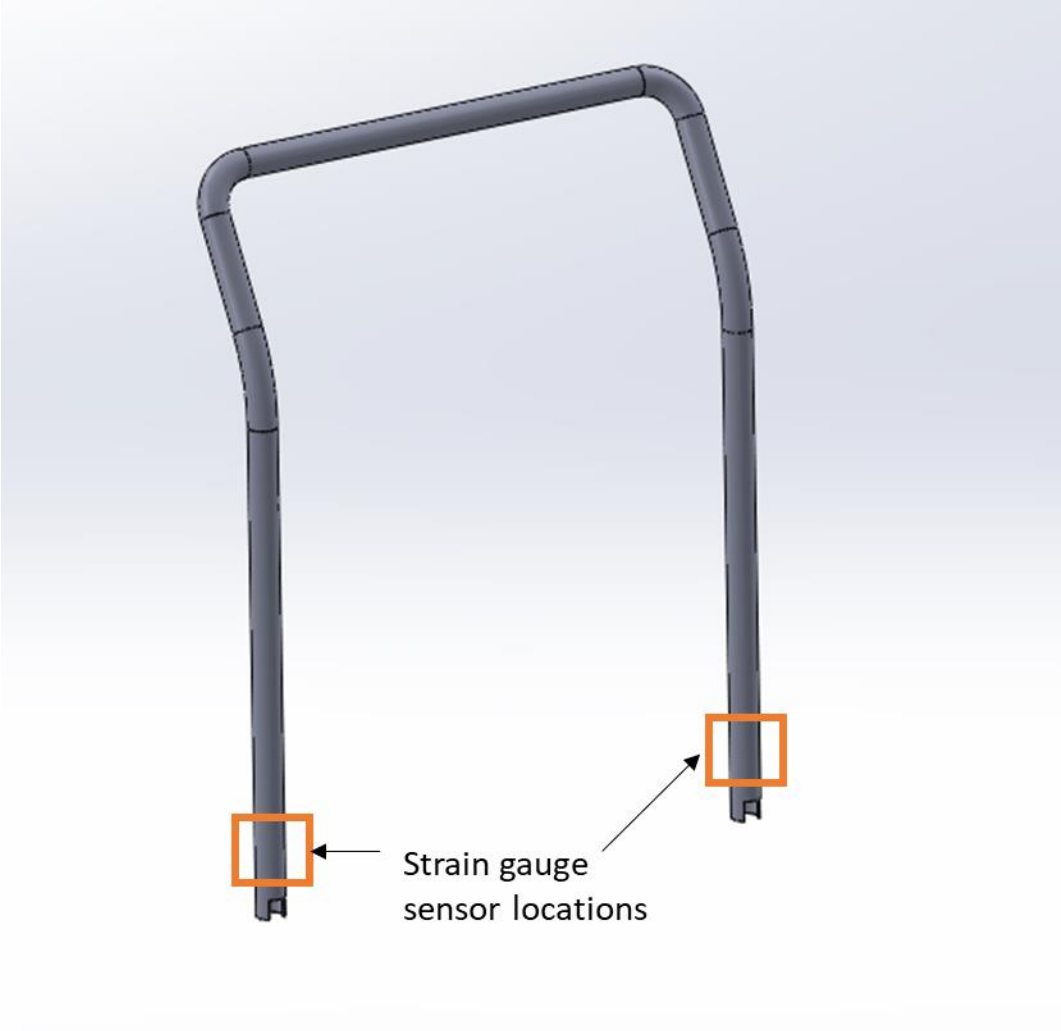


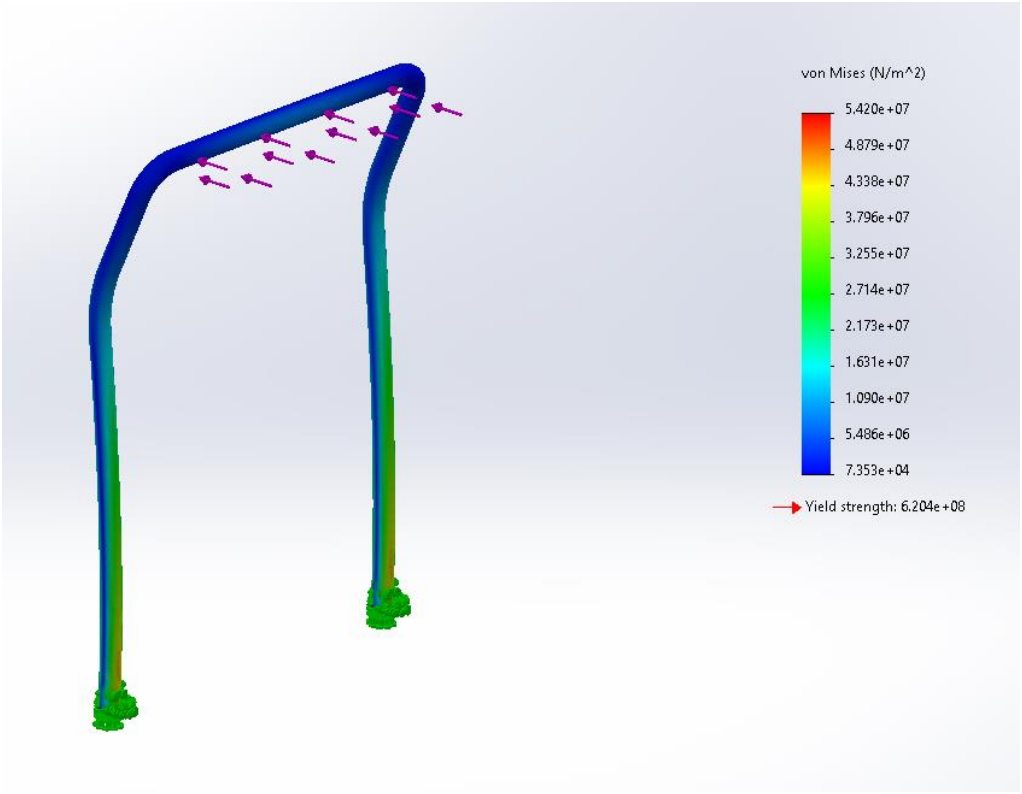
Figure 4.8: Assistive handle hollow circular bar and strain gauge locations.

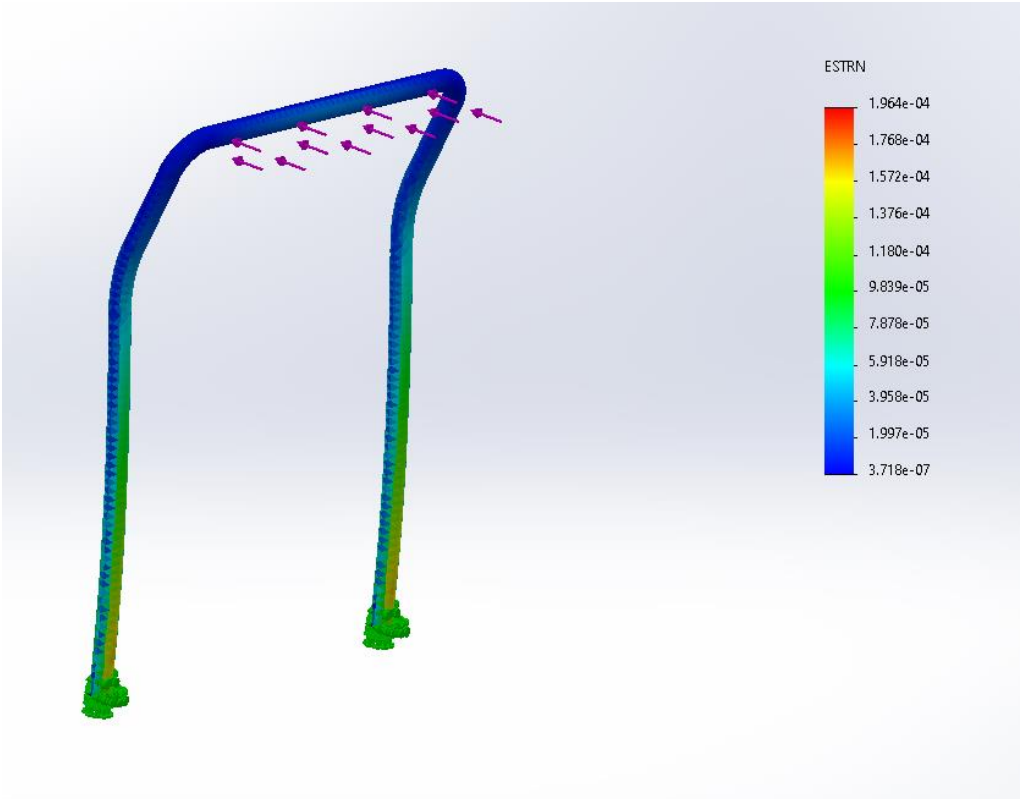
As the handle is designed to be rigid with measurable bending stresses due to pushing and pulling, a stress simulation is performed using Solidworks. Strain gauges on the market typically have a maximum strain between 0.01 and 0.05, though typically work best under 0.005 in/in [43]. The handle design, therefore aims to pick a comfortable outer diameter for grasping, with a thickness that allows for measurements under this 0.005 threshold. A maximum pushing force of 225 N is assumed, as per CCOHS's recommended upper limit for cart handling [21]

This leads to the selection to use a bent metal pipe with standard dimensions, 1-1/4" OD, 1/8" thickness, that allows for an acceptable amount of strain to be read. Though 1 inch was found to be comfortable, 1-

1/4 inches is selected for this design as it allows for easier routing of cables from the screen to the mechatronic assembly.

A general alloy steel is used for simulation of static stresses of the handle. This metal features an elastic modulus of 0.21 GPa, ultimate tensile strength of 7.24 MPa, and yield strength of 6.20 MPa. This is more ductile than an average steel such as AISI 1020 which will also be used for handle calculations, though gives a good baseline of the order of magnitude expected during operation, as well as if material changes will make a large impact on the static reliability of the handle.


von Mises (N/m^2)
5.420e+07
4.879e+07
4.338e+07
3.796e+07
3.255e+07
2.714e+07
2.173e+07
1.631e+07
1.090e+07
5.486e+06
7.353e+04
Yield strength: 6.204e+08


ESTRN
1.964e-04
1.768e-04
1.572e-04
1.376e-04
1.180e-04
9.839e-05
7.878e-05
5.918e-05
3.958e-05
1.997e-05
3.718e-07

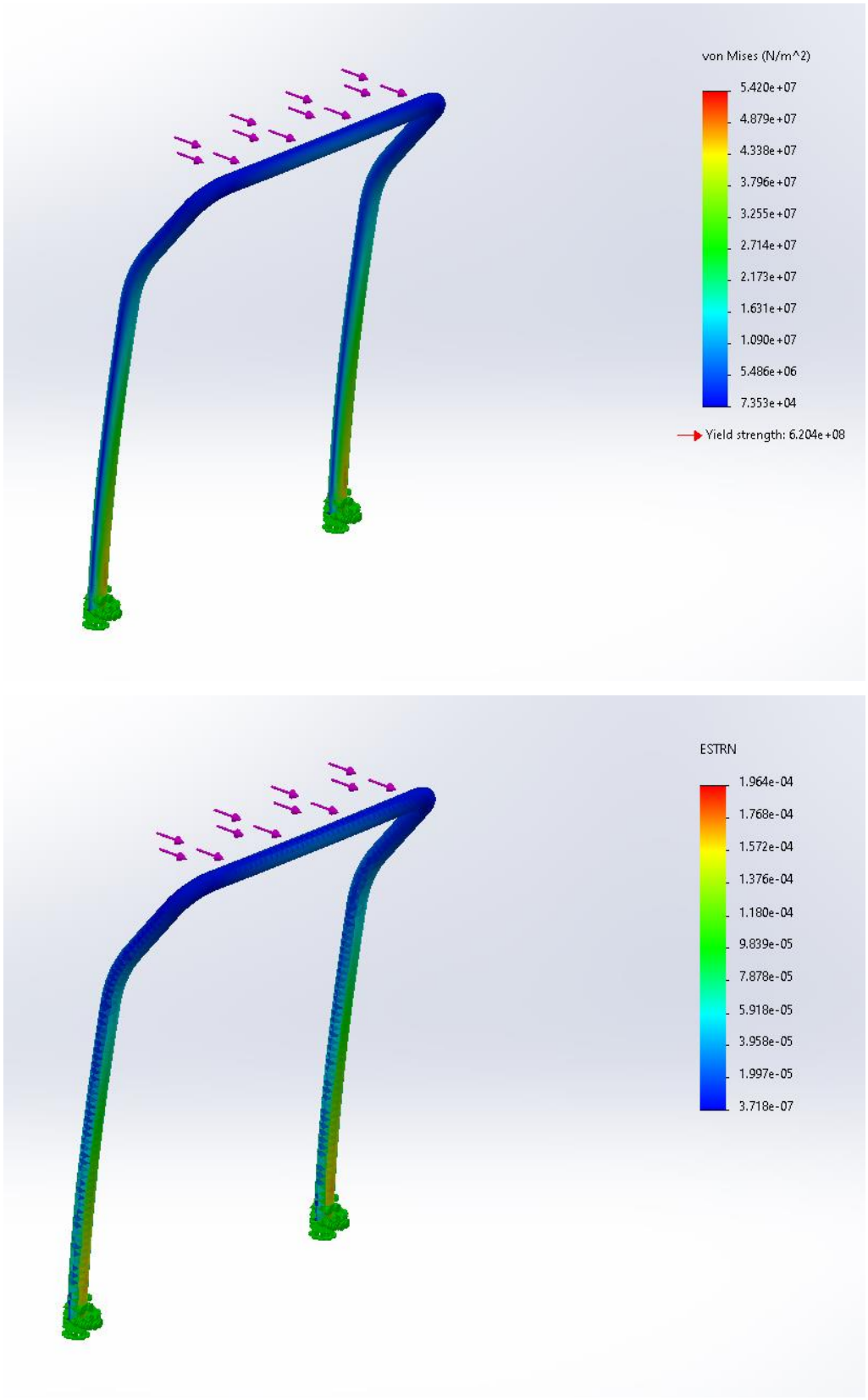


Figure 4.9: Stress and strain results of assistive handle under expected loads.

From these simulations, it can be seen that the static stress observed is an order of magnitude under the yield stress of the selected metal with the selected dimensions. It is therefore not expected that a static failure will occur with metals of a wide range of strengths during normal operation.

As the expected operation of the cart involves frequent pushing and pulling, a fatigue analysis is also performed. Fatigue is the gradual failure of a material under a cyclic load due to local plastic deformation. Fatigue usually manifests in metal parts in the form of crack or fracture propagations, and can eventually lead to a fatal failure in the design. Often in metals, fatigue does not manifest until hundreds or thousands of cycles, and typically occurs beginning from a small imperfection plastically deforming while the overall shape is still in the elastic region.

In order to reduce the risk of a fatigue at the attachment location, which is shown to coincide with the highest stresses during operation, a bending analysis is performed. Juvinall's Fundamentals of Machine Component Design textbook is used to collect the factors and constants required for this calculation, as well as properties for AISI 1020 hot-rolled (HR) steel, which is a typical average steel that the handle can be constructed from [44]. For the values determined in this estimation to be deemed accurate, it is assumed that the actual fatigue data for the material is not available for the dimensions used, figure 4.10 can be used to estimate the surface factor, and a gradient factor of 1 can be used for calculation.

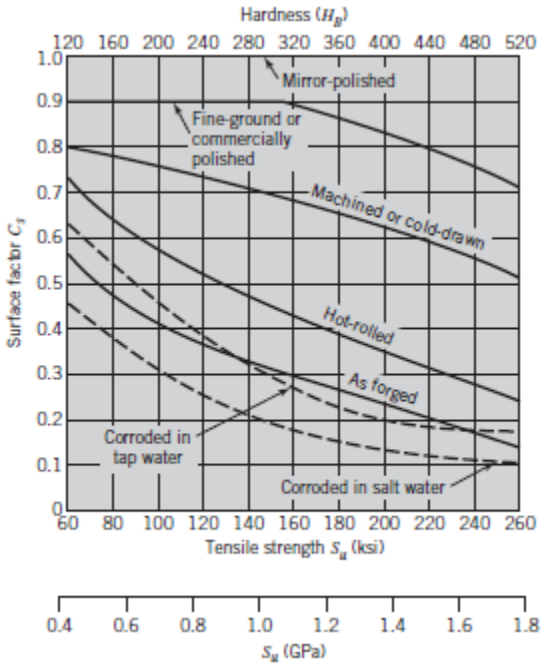


Figure 4.10: Reduction of endurance limits caused by various surface finishes [44].

The maximum bending stress of the handle is recalculated manually given the geometry from above, as well as the AISI 1020 properties. In this calculation, the handle is idealized to a cantilever beam where the force of pushing and pulling is exerted on the tip. The reaction moment, *M*, is then used to find the stress at the maximum distance from the normal axis, y_{max}, using the moment of inertia, *I*. The moment of inertia can be found using the inner and outer diameter of the tube, d_o and d_i respectively.

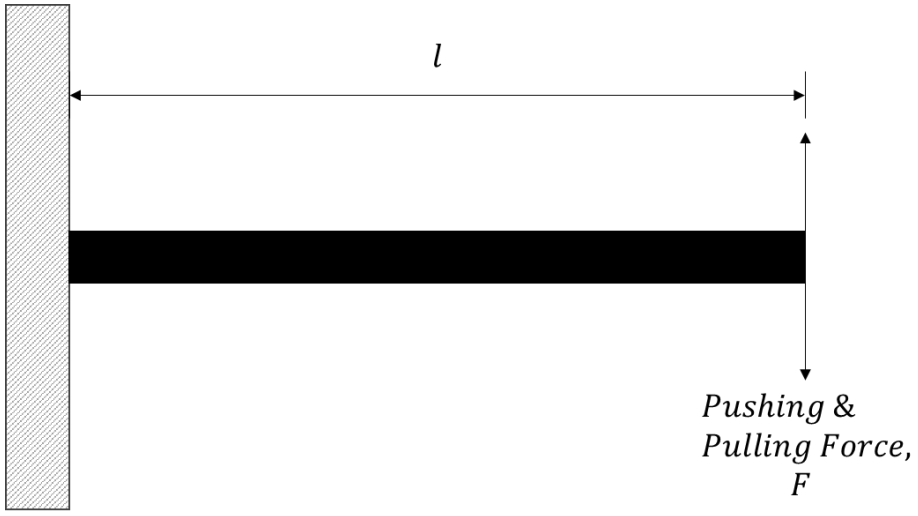


Figure 4.11: Free body diagram of bending cantilever representing the assistive handle.

$$M = Fl = 225\ \text{N}(810\ \text{mm}) = 181.25\ \text{Nm} \tag{4.5}$$

$$I = \frac{\pi}{64}\left({d_o}^4 - {d_i}^4\right) = \frac{\pi}{64}((31.75\ \text{mm})^4 - (25.4\ \text{mm})^4) = 2.945\ \text{x}\ 10^{-8}\ \text{m}^4 \tag{4.6}$$

$$\sigma = \frac{My}{I} = \frac{182.25\ \text{Nm}\ (\frac{31.75\ \text{mm}}{2})}{2.945\ \text{x}\ 10^{-8}\ \text{m}^4} = 98\ 240\ 396\ \text{Pa} \tag{4.7}$$

The result for the maximum bending stress of 98 MPa is higher than that found statically using SolidWorks, likely due to the simplified geometry and material change. The result is, however, still within an expected range, and a fraction of the 290 MPa yield stress for 1020 HR steel.

This maximum stress can then be used to determine the resistance of the handle to fatigue failure in an ideal scenario for greater than 1 million cycles. 10^6 is selected as a cycle benchmark, as this is commonly considered infinite life, and will be ensure that the handle performs well throughout the life cycle of the assistive cart.

For a fully reversed bending load, the fatigue strength, S_n', is taken as half of the ultimate tensile strength.

$$S_n' = 0.5S_u \tag{4.8}$$

$$S_n' = 0.5(455\ \text{MPa}) = 227.5\ \text{MPa} \tag{4.9}$$

The endurance limit, S_n, which communicates the maximum allowable stress for 10^6 or infinite cycles can be found by applying several factors to the fatigue strength. C_L, the load factor, is determined by the type of load that the metal is subject to. For a bending load, this factor is 1. C_G, the gradient factor, signifies the variance of the endurance of a material based on its size and loading type. For a tube of diameter greater than 10 mm, this factor is 0.9. C_S, the surface factor, decreases the endurance strength based on the surface finish and its irregularities. A hot-rolled steel part with a 455 MPa ultimate tensile stress has a surface factor of about 0.725. C_T, the temperature factor, reduces the endurance limit in high-heat applications. As the assistive cart operates at room temperature, this factor has a value of 1. C_R, the reliability factor, lowers the endurance limit based on the desired reliability of the calculation. For a 99% reliable calculation, this factor is 0.814.

$$S_n = S_n' C_L C_G C_S C_T C_R \tag{4.10}$$

$$S_n = 227.5\ MPa\ (1.0)(0.9)(0.725)(1.0)(0.814) = 120.8\ \text{MPa} \tag{4.11}$$

As the calculated endurance strength of 121 MPa is greater than the maximum expected stress exerted on the handle during use of 98 MPa, fatigue is not expected to contribute measurably to the failure of the system with the inner and outer diameters selected. This is also found to be true when reducing the size of the metal tube to an outer diameter of 25.4 mm and inner diameter of 21.4 mm, which is about the smallest it can be while preserving the ability to route the various cables required for function through it.

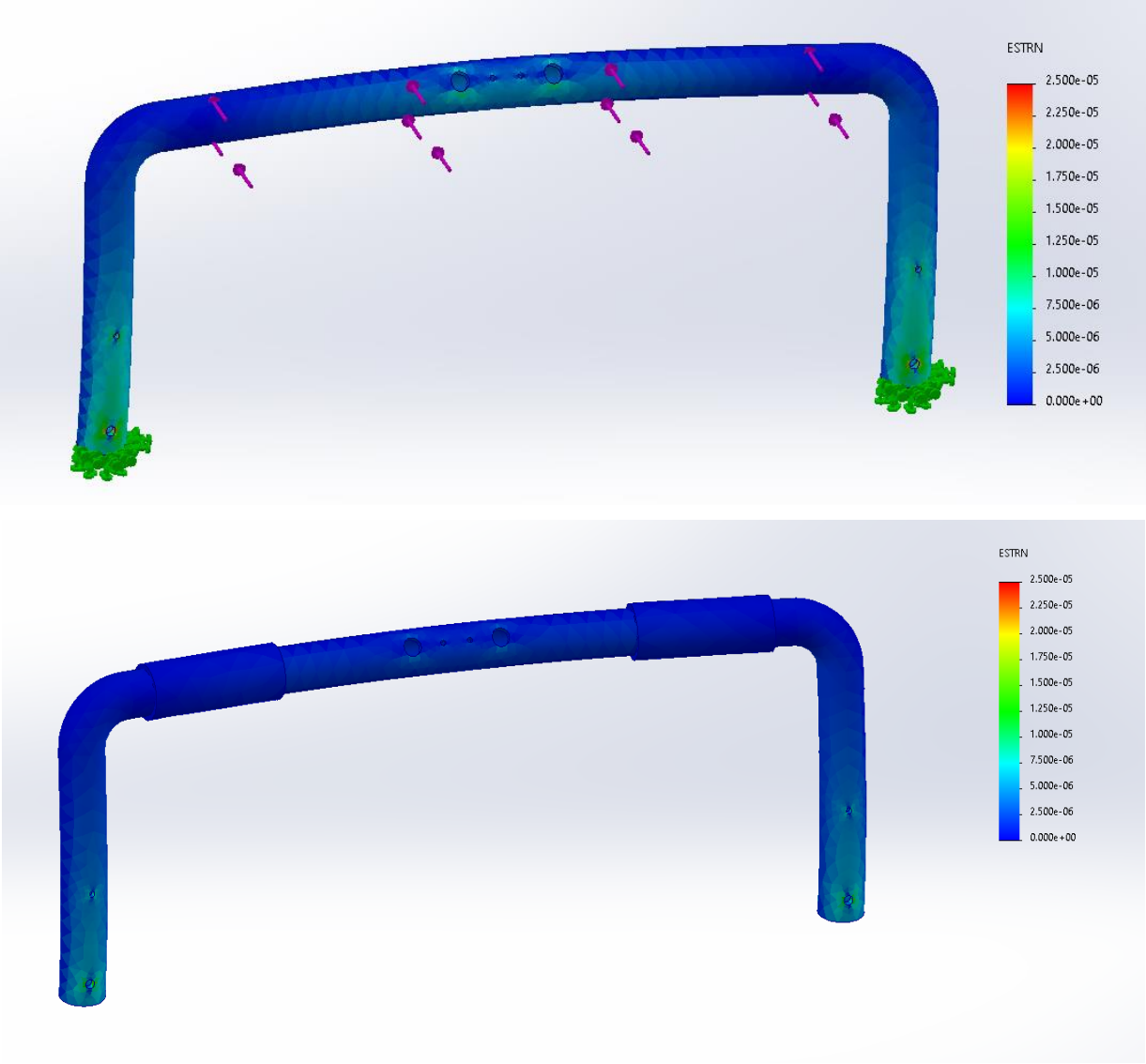


Figure 4.12: The stress and strain for a handle is also designed with the bed dimensions in mind. It is, however, simpler to attach the stain gauges directly to the frame of the bed to avoid outfitting the bed with new parts.

4.1.6 Other User Interface and Safety Features

Additional safety features are added to the mechatronic system to help with safe integration of the assistive cart into health care workflows.

A screen assembly is added at the top of the handle. This screen allows for a user interface to be added to the assistive cart to succeed the use of a laptop or game controller. This allows for basic functions such as data input, information presentation, live battery charge levels, and lift/lowering of the drive wheel to be

performed much more seamlessly. In addition to this, it is possible to use the screen to tune operation characteristics, such as the strain gauge value relation to the motor speed, or aggressiveness of automatic breaking.



Figure 4.13: CAD model of the assistive cart's screen assembly

An on/off switch is added to the screen assembly to offer a more convenient method of toggling the power of the assistive cart when compared to the on-module power button of the bed. In this design, the mechatronic assembly is not easily accessible from the ends or sides of the cart, necessitating a new location for this switch.

An emergency-stop button is also added to the screen assembly. Rather than turning off the full system, the emergency-stop button cuts power to the motor, causing it to stop. The screen and pneumatic system are still engaged, so the cart can be controlled manually while the motor is not engaged in this mode. Functionality can be resumed by switching the emergency stop button to re-enable power to the motor.



Figure 4.14: Manufactured screen assembly.

Four infrared sensors are installed in the front of the cart, which determine the distance to any oncoming obstacle. This data is used to safely avoid collision with any walls, equipment, or humans that pass in front of the cart while in operation. This is an essential feature for building trust between the operator and the assistive cart when being used in busy hospital hallways, as it directly addresses concerns with collisions at speed.

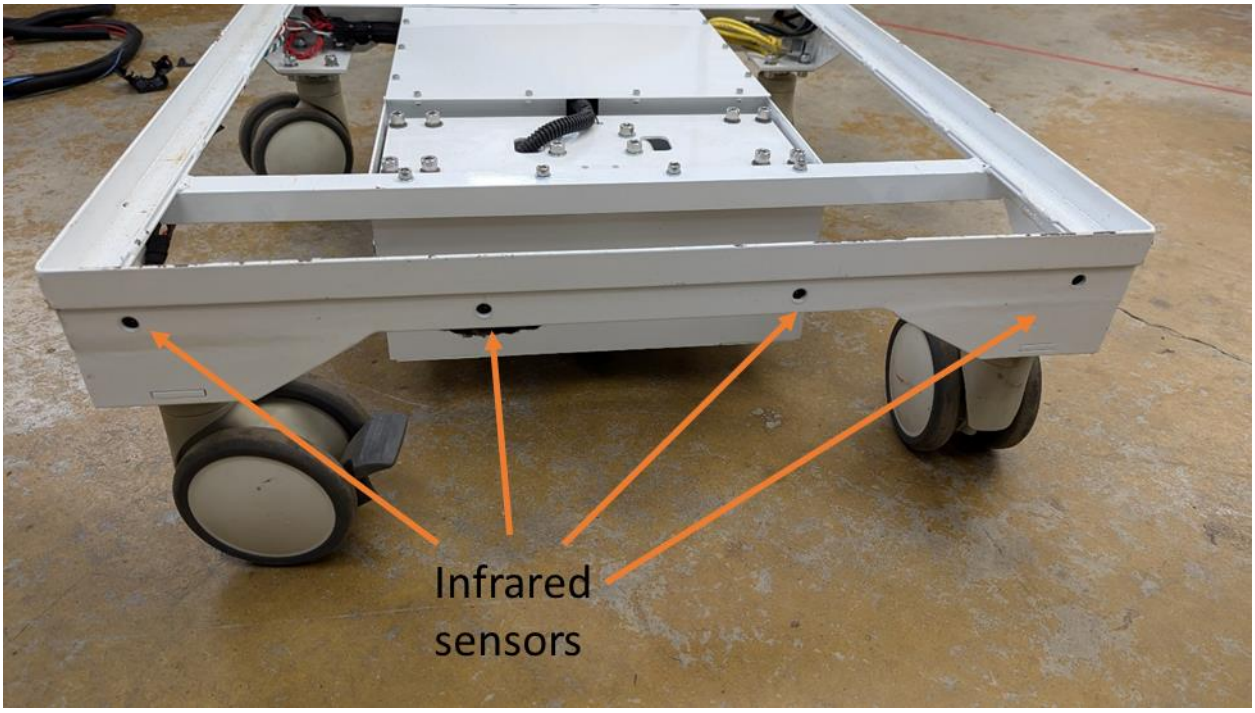


Figure 4.15: Cart infrared sensors, as viewed from front of cart.

4.1.7 Complete Assistive Cart Assembly

With the considerations for design parameters of critical subsystems completed, a complete assembly is created. This system integrates the motors, pneumatics, handles, and a frame to accommodate retrofitting a medicine cart. It is decided to house the main components in a smaller module near the center of the full assembly, then connect it to a frame that can be adjusted to fit the size of any existing cart larger than the module.

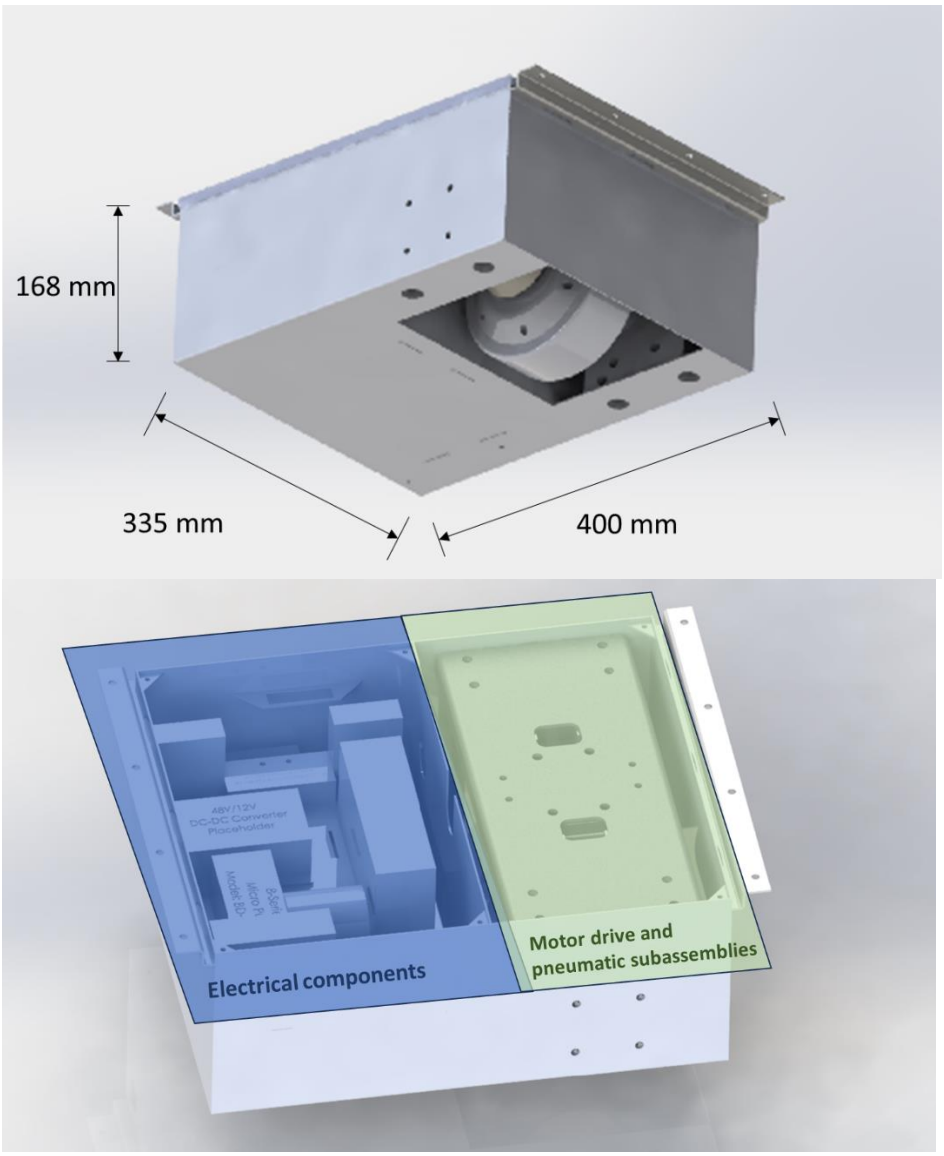


Figure 4.16: Cart main component assembly.

Many of the outstanding electric components are shared with the bed, though significant changes are made to allow for a more compact design. The frame is split up into two sides, one featuring the drive wheel and air cylinders, and the other containing the rest of the electronic components. This allows for a separation between these parts that minimizes that threat of dust and debris from the wheel dirtying the rest of the components. A 48 V, 40 Ah battery is included at the bottom of the component side, and a removable plate acts as the mid-frame where the other components can be secured to. A 48V to 12V DC to DC converter is added to simplify providing adequate voltages to each of the components. A more compact automobile mini pump is used to replace the pumps used in previous designs and for some

assistive bed design testing, which features similar specifications, operating with a maximum pressure of 600kPa [32]. A Raspberry Pi 4 is also used to replace the Audesse MCU used in previous designs as it is less expensive and much more compact, while preserving the computational power required for operating the cart module.

4.2 Design of a Cart Hauler

A modified version of the cart is designed based on observations made while collecting data from medical partners at Grand River Hospital.

4.2.1 Motivation for Cart Hauler

While researching the intended use environment for the products designed as to help with lessening the magnitudes of force experienced by workers while pushing equipment routinely, it is observed that many more opportunities for improvements exist than initially speculated. Several carts of the same type are used across a hospital's various operational teams that may not be practical for completely retrofitting in the methods best used for the main assistive cart design. As an example, the surgical equipment case carts are used by the Medical Device Reprocessing Department (MDRD) to move surgical equipment from sanitization stations to rooms around the hospital. These case carts are a significant strain on the workers responsible for moving them to and from dozens of operation rooms daily. The masses of the carts are able to reach and exceed the recommended limits outlined by CCOHS, and workers routinely take thousands of steps daily moving these carts.

Though these types of carts offer a large opportunity for the improvement of working conditions, the exertion is caused by the need to move several carts rather than one cart continuously. Rather than outfitting tens of carts with an electromechanical module, a module that can be removed from a cart and reattached to another is designed. This avoids the long periods of idling that any single cart may undergo while waiting to be used or cleaned, while vastly reducing the number of products that are needed for moving the carts. As each of the MDRD carts share a base platform, a design can be made that can follow a worker's movement.



Figure 4.17: Hot food delivery cart and surgical equipment case cart at Grand River Hospital. These carts share a platform.

4.2.2 Dynamics of Lifting with Cart Hauler

As this design is removable, it must be intuitive to attach and detach the electromechanical module from the carts that that require movement. As such, the design must be in a visible location, unlike the main assistive cart design. The cart hauler is thus to be attached in an external position. Inspiration is taken from dollies and hand trucks, which are commonly used by warehouse and delivery workers to move heavy packages. The cart hauler will be similar to this by slightly lifting one side of its cart-load, then

acting as a new wheel axis. This necessitates caster wheels to be present on the design, as well as a reliably strong design for the lift motion.

The acceptable forces for lifting and pushing are used in conjunction with the mechanics of a dolly to inform the design of the cart hauler. Based on the CCOHS recommendation for muscle exertion with primarily arms of 110N, the amount lifted can be calculated using the comfortable height of handle used in previous designs [21].

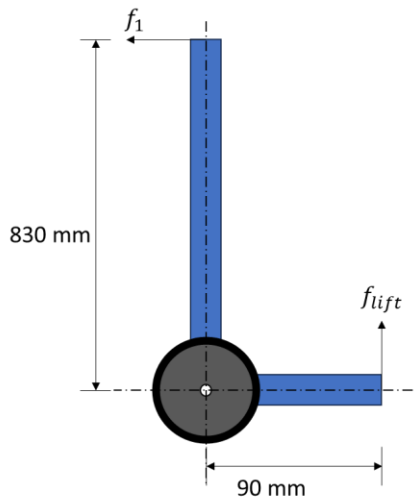


Figure 4.18: Free body diagram depicting forces of dolly lifting.

By selecting dimensions based on the previous cart design, a moment balance about the wheel's center of rotation can be performed.

$$\sum M = 0 \tag{4.12}$$

$$0 = M_1 + M_{Lift} \tag{4.13}$$

$$-f_{lift} l_2 = f_1 l_1 \tag{4.14}$$

$$f_{lift}(90 \text{ x } 10^{-3} \text{ m}) = 110\ N\ (830 \text{ x } 10^{-3} \text{ m}) \tag{4.15}$$

$$f_{lift} = 1014.4 \text{ N} \tag{4.16}$$

This result dictates that about 1014 N can be safely generated to lift using the cart hauler at dimensions reflecting the overall size of the cart design. This translates to the ability to lift 103kg, or half of a 206 kg cart, which is slightly lower than the recommended load for pushing with purely arms, though a foot is typically used to aid with dolly lifting, making this an acceptable result.

4.2.3 Complete Cart Hauler Design

The cart hauler is designed to share all of the electronic components of assistive cart, to ensure availability of parts and to streamline the design process. The module design is adjusted to a vertical orientation rather than one that attempts to fit under an existing cart. This allows for the overall profile of the design to be minimized by placing the majority of components between the two handle legs, while also allowing for the frame to aid in force transfer. The components are, again, secured to a removable 20-gauge sheet metal plate which also serves the purpose of securing the battery. The screen assembly is identical to that used in the assistive cart design. The bends in the handle are adjusted to increase the width where an operator would grip it. The wider available area here allows for less force to be exerted in order to generate the moment required to steer the cart.

A locking mechanism is added to prevent unlocking during operation. 3/16-inch sheet metal is used to create a bar which unlatches when the operator presses their foot on the 3D printed pedal in the front of the design. A fixed bar is also added alongside the locking mechanism which help with positioning and lifting the cart using the mounting locations. Both of these attachment locations are designed to be able to sustain loads greater than expected during normal use to ensure no failure occurs that causes the cart to no longer be secure during operation.



Figure 4.19: Renders of complete cart hauler design.



Figure 4.20: Render of cart hauler design, showing internal component placement.

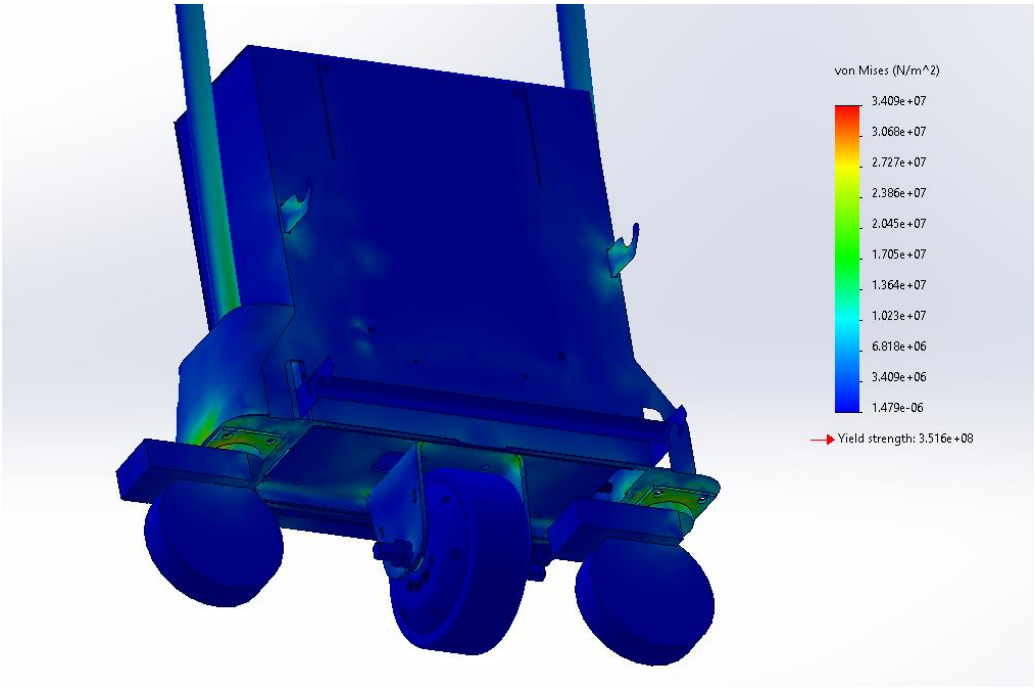


Figure 4.21: Stress analysis of cart hauler under expected load.

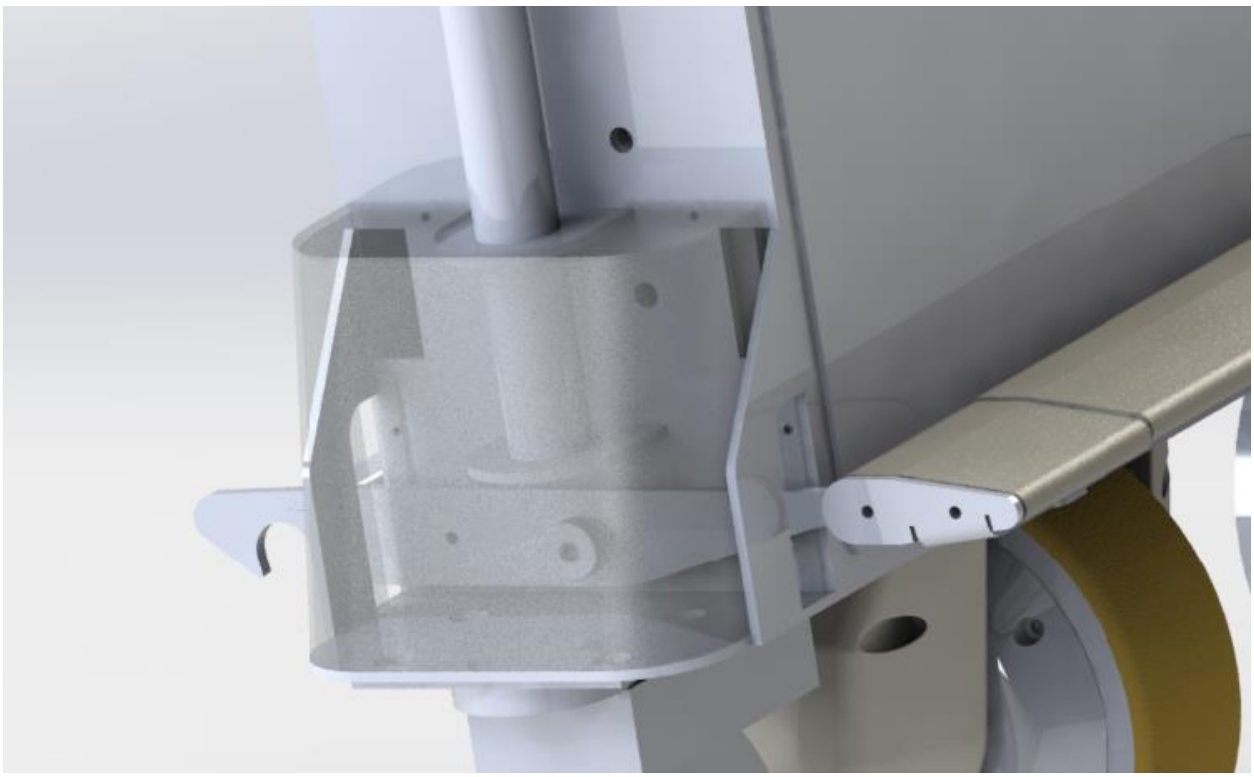


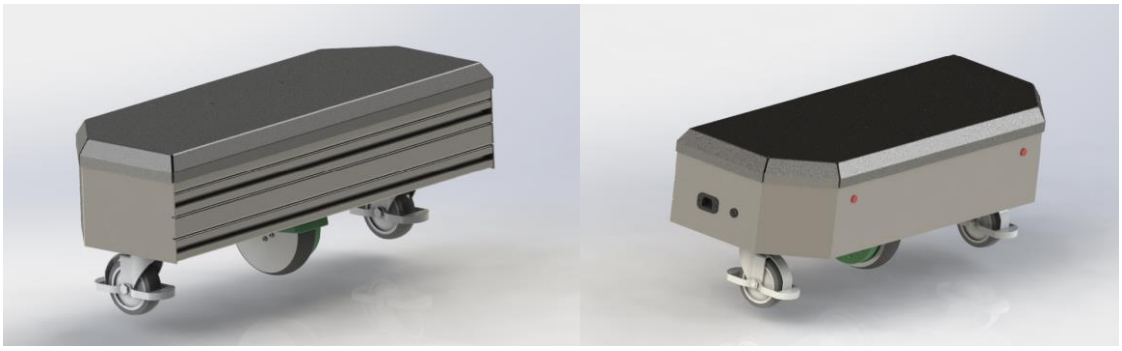
Figure 4.22: Rotating locking bar.

CHAPTER 5
PROTOTYPING AND TEST RESULTS

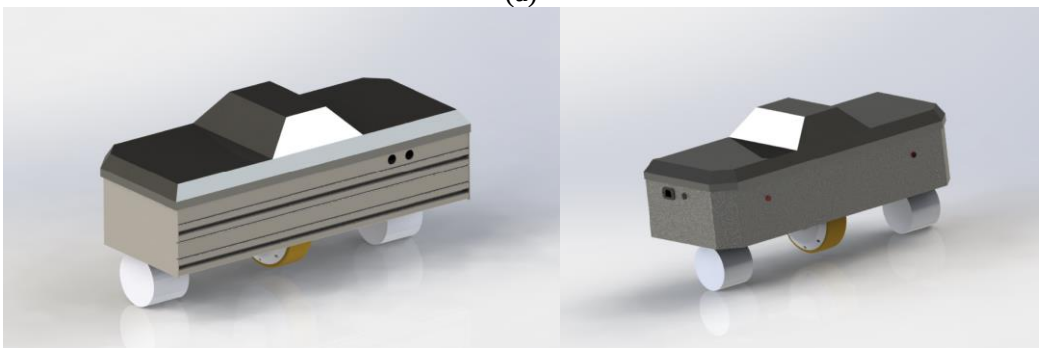
In this chapter, the designs of the assistive bed, assistive cart, and cart hauler modules established in previous sections are prototyped and experimented upon. Experiences involving their usage and testing is presented.

5.1 Prototyping of the Assistive Bed Design

The fabrication of the assistive bed is completed using many of the previous prototype's parts. Though compatibility would be better with the updated frame and internal spacings presented below, the reduction in component sizes allows for quick integration into a slightly smaller chassis at the expense of cable management and fixed component locations. The old lid remained as the only fully incompatible part between the designs due to the protruding steering motor and larger battery, however, this is not a critical part to the operation of the bed, allowing for testing of the new parts to still be performed.



(a)



(b)

Figure 5.1: (a) previous bed module and (b) new bed module designs. The profile of the new module is slightly larger at 805 x 325 x 210 mm when compared to the previous prototype's 805 x 315 x 190 mm.

5.1.1 Fabrication and Assembly of the Assistive Bed

As many of the parts are compatible, the previous bed chassis is used for testing the newly designed components of the assistive bed. As stated previously, the newly selected components are able to fit within the profile of the previous design, although with a protrusion of the steering motor preventing the use of the lid. Additional features not shared by the designs are added to the sheet metal frame, however, including the cable-routing holes, busbar, and terminal block.

During the assembly process, performing maintenance and changing components on the overall module is confirmed to be a relatively quick process for those familiar with the design. The module is attached to the bed frame using 40 by 40 mm aluminum strut profile that allows for easy attachment with the addition of an simple attachment fixture to the original frame. This is a crucial design goal to meet, as a bed is critical in the operation of hospitals and long-term care homes. As a bed's main purpose is to support or carry patients, it is imperative that and out-of-service bed is returned to use as quickly as possible as to not reduce capacity or disrupt workflows.

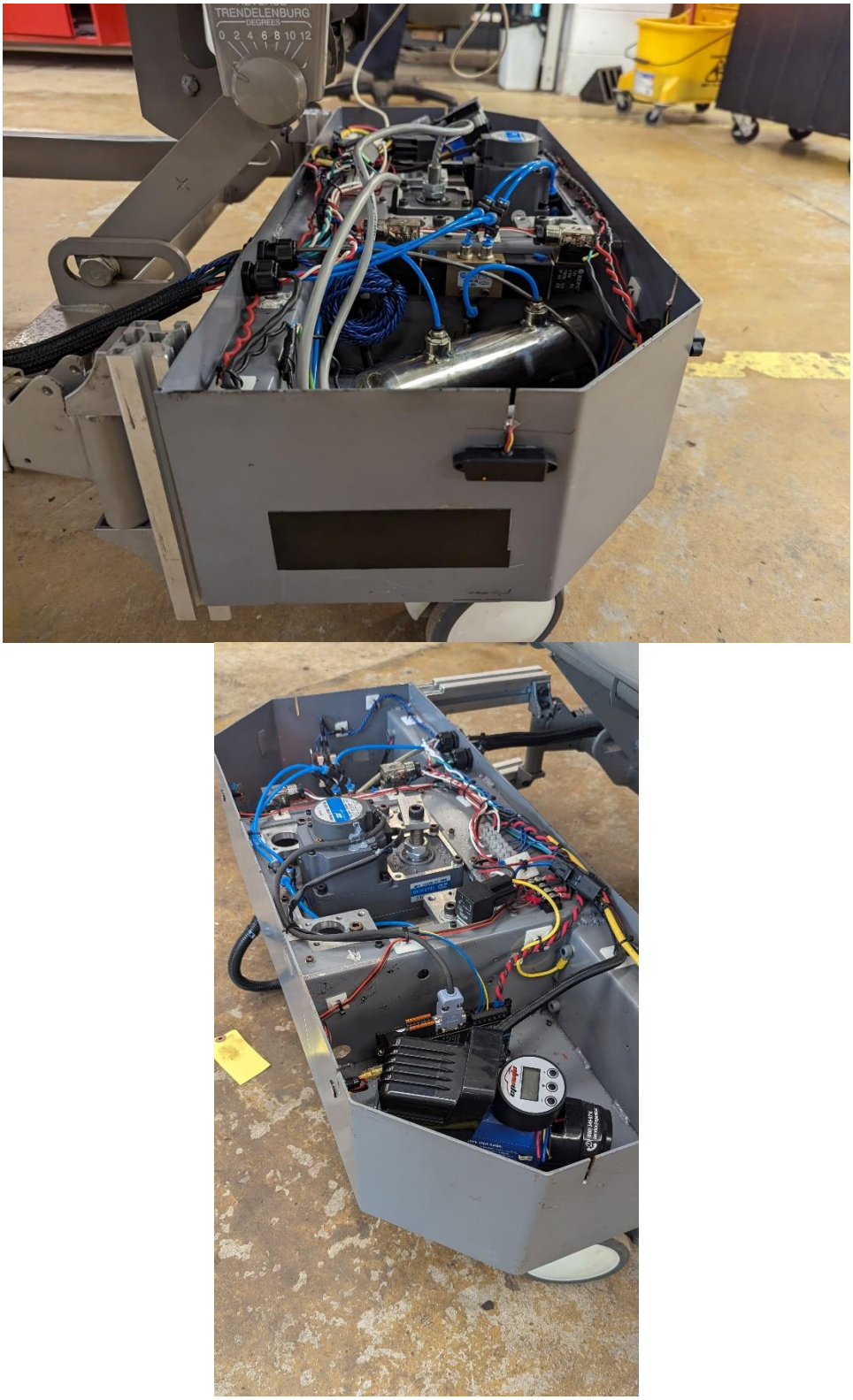


Figure 5.2: Updated bed module prototype featuring new core system components and additional technology shared with assistive cart.

5.1.2 Assistive Bed Operation

The testing performed on the bed largely pertained to confirming its abilities to operate in the situations that the previous prototype was not able to. With the updated drive system, steering system, and pneumatic system, the bed must be able to perform well in all environments that are considered during design.

The assistive bed is successful in each of the various driving modes considered. Forward and backward operation occur with no issues on both concrete and carpeted flooring, without any diminishing function when used for an extended period of time. Like the previous prototype, the bed is able to start, stop, and steer on an incline without problem. When paired with the new assistive handle outfit with strain gauges, the force required to push the bed up an incline is trivial and the required muscle exertion remains comparable on sloped and flat terrains.

The new pneumatic system is also successful in function, with pressures and tractions being tunable. The assistive bed does not have difficulties generating the traction force required for acceleration and deceleration on low-coefficient of friction concrete flooring. In addition to this, it is successfully able to be pushed into and out of elevators.



Figure 5.3 Assistive bed after the updated components are installed. As stated, the larger battery and steering motor prevent the usage of its lid.

The front and rear steering system paired with the assistive control through strain readings caused some difficulty in controlling in different driving modes. Feedback from the control system designer indicates that the sensor setup does not allow for easy switching between longitudinal, lateral, and pure rotational motions. Though operation in longitudinal directions with considerable steering is functional, intuitiveness sharply declines when the other front and rear steering options are added to the control system. As a result, the assistive handle is a success in one-module operation as well as longitudinal operation, but requires further investigation to design a method with which steering modes can be better distinguished.

Occasional servo motor driver failure when testing autonomous operation, though this is likely due to large changes in controls issued during initial testing. As this does not occur during the manual and assistive-controlled operations, it can likely be prevented by making changes to the autonomous control system. In order to prevent critical failures such as these in the future, improvements of market parts should be monitored with any revision to the system hardware, and any deviation from expected operation should be noted for future review.

5.1.3 Assistive Bed Test Results

Results verifying the assistive bed's movement capabilities are collected in the form of motor speed data from the driving motor and steering motor. The bed assembled with two modules has a mass of 201 kg and is controlled by issuing commands manually to the motors to verify its ability to operate in different steering modes. The tests are performed in the MVS lab area to confirm adequate performance at low speeds.

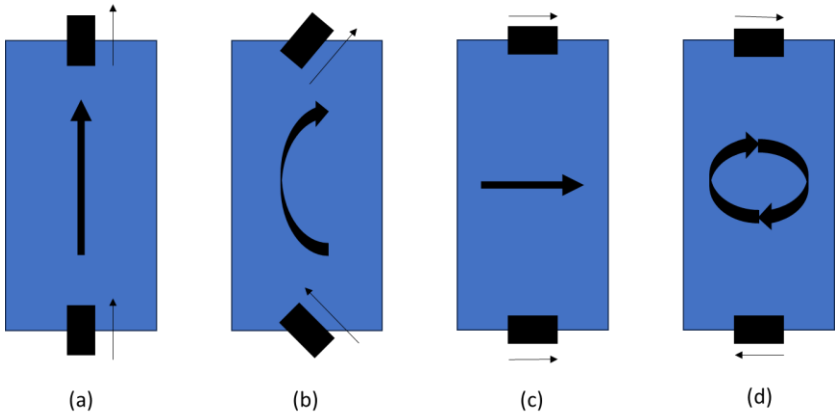


Figure 5.4: Four main assistive bed steering modes. (a) Linear motion, where both wheels are aligned longitudinally with the bed, (b) mixed linear and steering motion, where the wheels are not in line with the bed, (c) crab motion, where the wheels are aligned transversally with the bed in the same direction, and (d) spinning motion, where the wheels are aligned transversally with the bed in opposite directions.

The figure below depicts the assistive hospital bed performing a forward, then backwards movement with minimal steering corrections. The speed of each motor is limited to about 0.3 m/s during this testing, as lower speeds than initially designed for allow for a more controlled trip, increasing comfort through the minimization of longitudinal and angular accelerations.

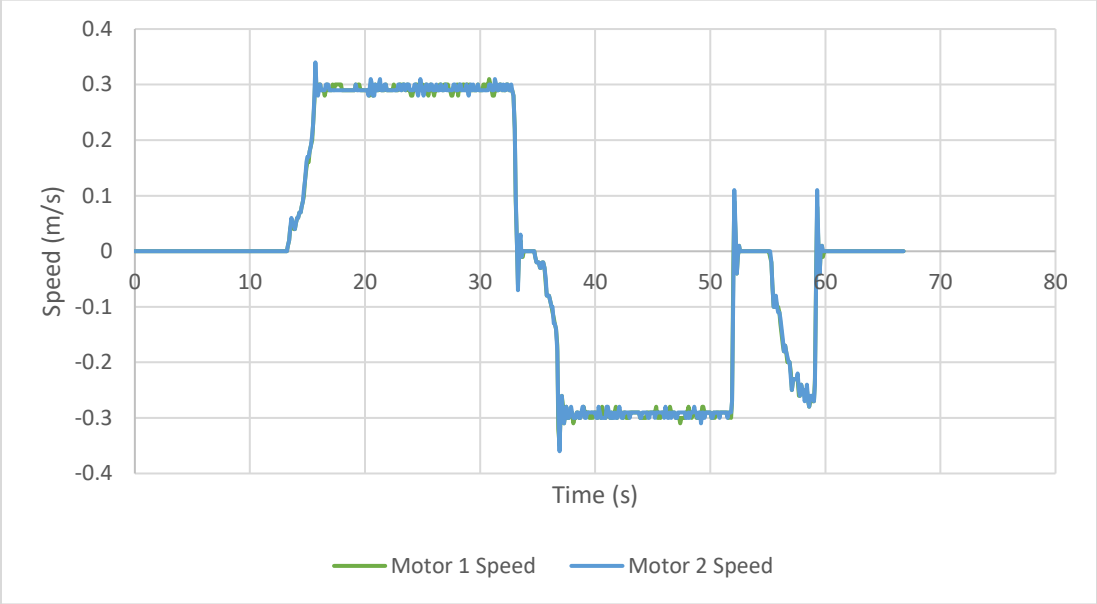


Figure 5.5: Speed of the assistive bed motors during linear travel forward and backward.

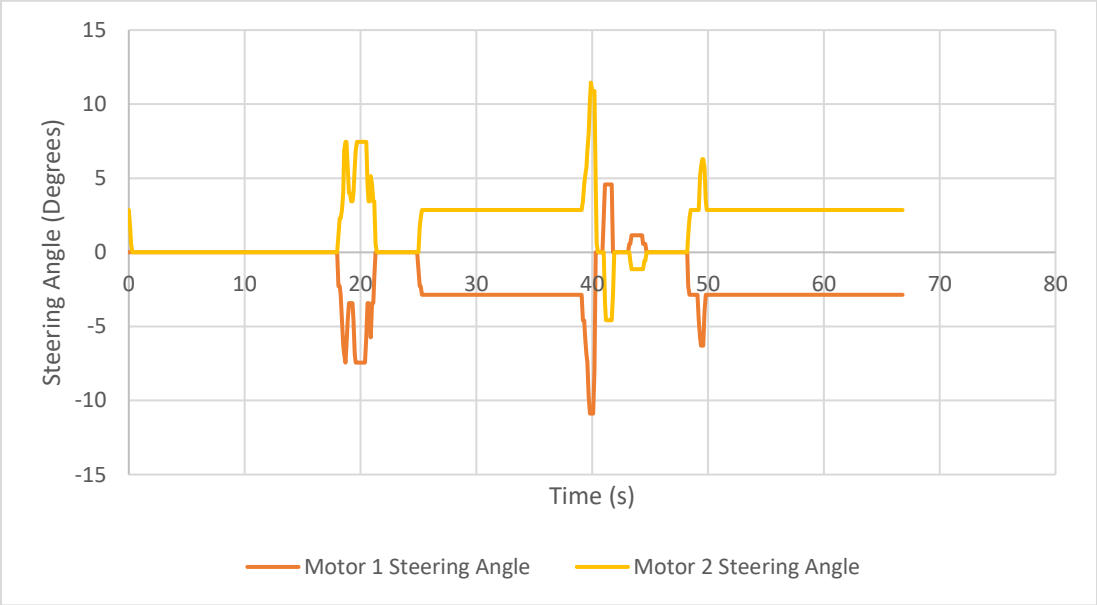


Figure 5.6 Steering angles of the assistive bed motors during linear travel forward and backward.

The second series of graphs depicts the speeds and steering angles of a typical crab motion. The bed is able to successfully move in this motion in addition to the regular trips. This motion is useful as it allows for the bed to park adjacent to walls and avoid obstacles more simply.

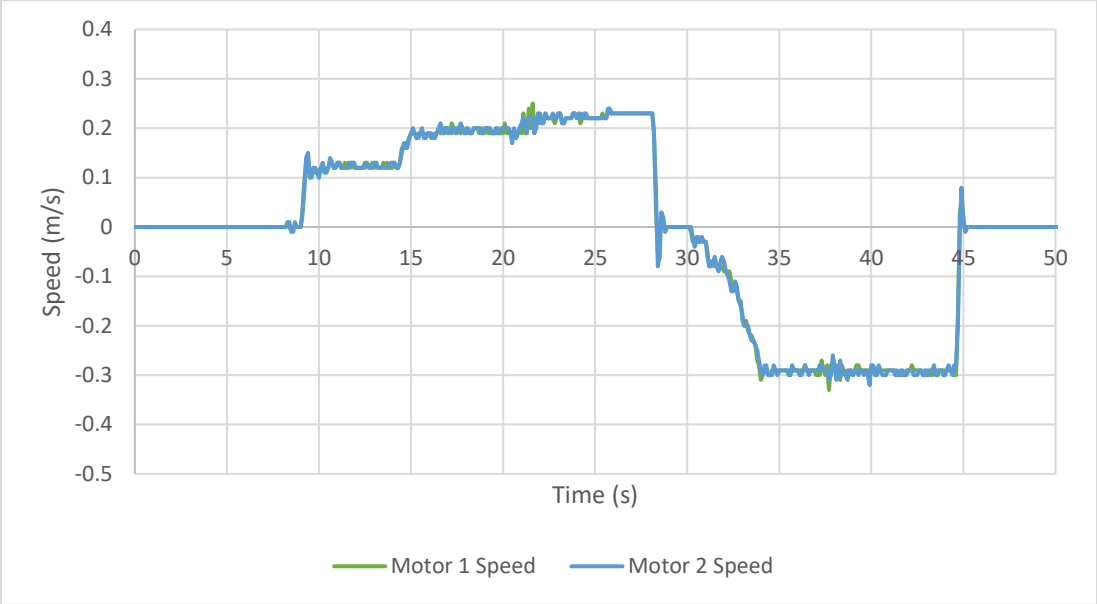


Figure 5.7 Speed of the assistive bed motors during crab motion.

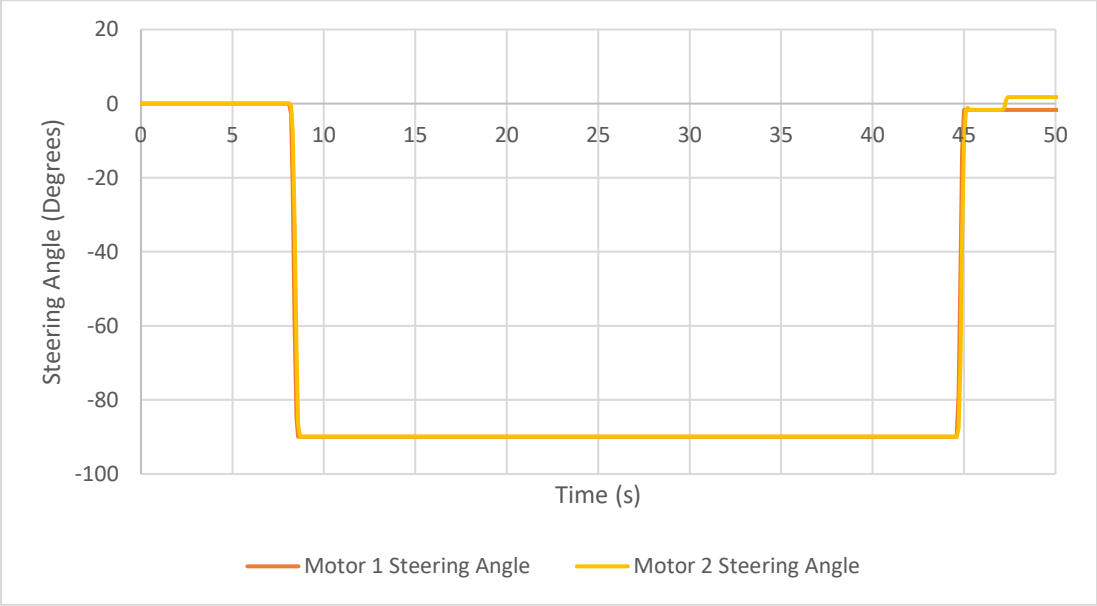


Figure 5.8: Steering angles of the assistive bed motors during crab motion.

The following figures show the fully rotational capabilities of the assistive hospital bed. As the steering angles of the wheels are opposite from one another, the bed rotates about its center. This is useful for repositioning and navigating tight corners in congested hallways.

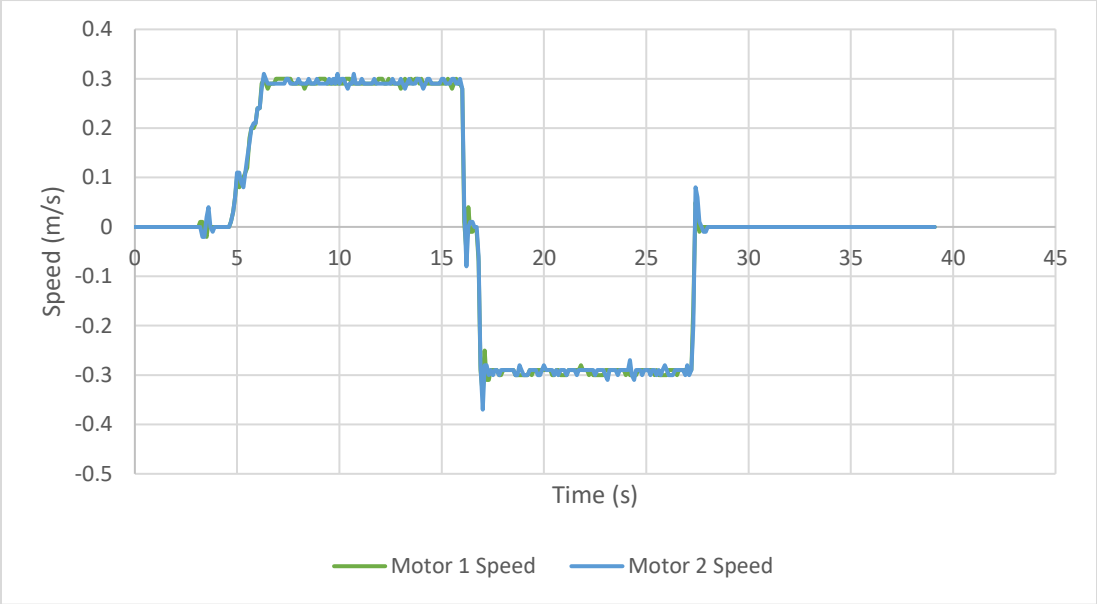


Figure 5.9: Speed of the assistive bed motors during spinning motion.

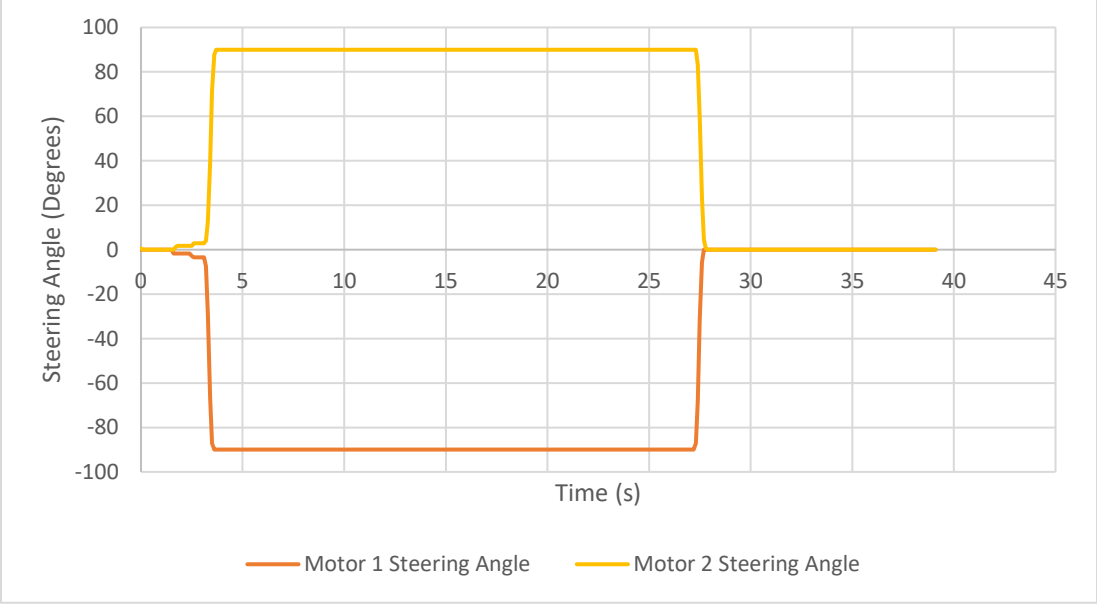


Figure 5.10: Steering angle of the assistive bed motors during spinning motion.

The final test begins in a crab motion, then moves to a longitudinal motion with a slight bend at the end. This test serves to show that the bed is capable of switching steering modes during operation. Though this did not feel intuitive when operating the bed using the assistive handle, the motion is able to change without problems when motor commands are issued directly.

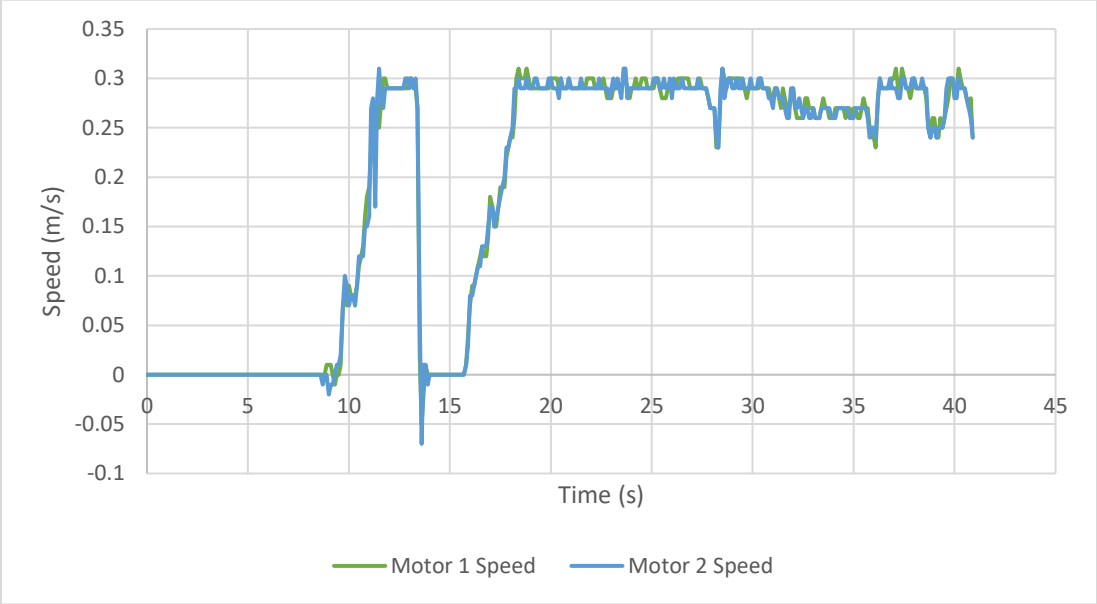


Figure 5.11: Speed of the assistive bed motors during mixed motion.

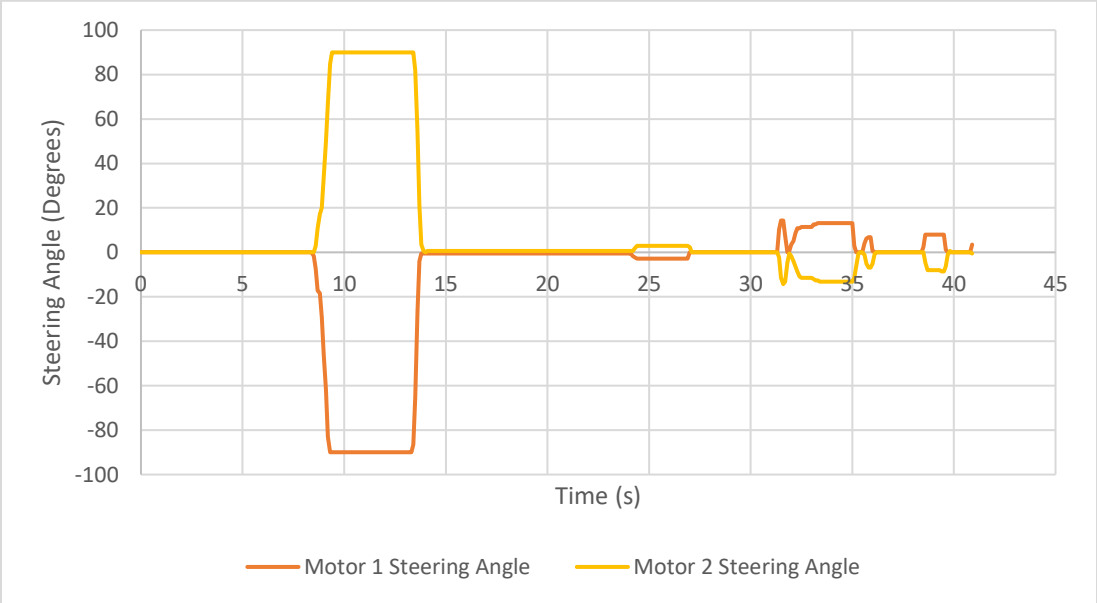


Figure 5.12: Steering of the assistive bed motors during mixed motion.

To conclude, the new components on the retrofitted assistive bed are able to complete the motions that justified adding front and rear steering. The ability to control the motors manually in this way demonstrates that it will be possible to later design an autonomous control system to integrate into the assistive bed.

5.2 Prototyping of the Assistive Cart

The assistive cart is the design that generated the most interest from partner long-term care facilities and hospitals. As a result, the manufacturing process and design saw some revisions between builds. Each cart shares the design goals previously outlined and use the same module, leading to similar functionality. The exterior and presentation, however, are altered to better match various applications.

5.2.1 Fabrication and Assembly of the Assistive Cart

As no previous hardware existed to simplify the cart fabrication process, the new parts component required to manufacture the full design. As per the design discussed in section 4.1, the main module is attached to a frame created using 1-inch angle members to support a treatment cart. This frame is also responsible for rigidly connecting the main mechatronic module with the assistive cart and screen assembly.



Figure 5.13: CAD model of the assistive cart and frame for a medication cart.

Metalwork

The majority of the load-bearing parts are fabricating using mild steel. Hollow metal pipes are bent and welded to the frame and screen. The frame consists of angle members welded in a rectangular arrangement with each edge being made from members in a “T”. This creates a thicker outer edge platform on which the medical cabinet can sit on without deforming the metal. 5-inch medical cart caster wheels are bolted under each corner of the frame on the first prototype. Additional angle beams are used to bolt the module containing the drive motor and electrical components to the rest of the welded frame

The screen cover and module chassis are fabricated using sheet metal. Both subassemblies require laser cutting and metal bending. Tolerancing for these processes are set at +/- 0.01” for laser cut features and +/- 0.5 degrees for bend angle as well as 0.01” for bend length as per industry standard and machinist recommendation.



Figure 5.14: Bent sheet metal parts used for module frame, as received from external supplier.

During the metalworking process for the assistive cart fabrication, a few opportunities for improvement are observed. The spacing required for the swivel of all four caster wheels is obstructed by the frame when wheels with diameters larger than 5-inches are used. Although this did not prevent successful fabrication for this prototype, it should be noted for frames featuring different dimensions. In addition to this, cable routing from the handle to the motor and component module should be designed in more detail. Despite these potential improvements, the fabrication of the metal required for this prototype is completed without the need to overcome any significant hurdles, indicating a sound design.



Figure 5.15: Welded cart frame.

Powder coating and Painting

Over the span of time that the cart is used, powder coating is observed to keep its finish better than its painted counterparts. Powder coating gives the metal a professional-grade finish that looks and feels better to use and clean.

The painted parts, however, had the advantage of being much cheaper and faster to apply. Though the finish was not as uniform and high-quality as the powder coated parts, it still protected the metal from rust.

Both methods are not completely resistant to scratching which leads to the conclusion that the cheaper painted parts should be used for internal prototyping and testing, while the powder coated part should be used for any products that are deployed.

Along with this, stainless steel parts are also used for a fabricated cart, which bypasses the painting or coating process by instead transferring the cost to the initial steel part procurement. Stainless steel offers many of the durability advantages that powder coating provides, in terms of preventing steel from rusting or corroding though is more expensive than its mild steel counterparts.



(a)



(b)

Figure 5.16: (a) Powder coated drive plate and fork and (b) painted drive plate.

3D printing

Fuse deposition modelling 3D printers are used to fabricate non-load bearing parts for the weight and complexity advantages the plastic filament offers. The rear plate of the screen assembly, strain gauge covers, and wheel fork covers are fabricating using this method. Each part is printed using white PLA to the powder coating or paint on the carts they are to be installed on

As the name implies, the strain gauge cover protects the strain gauges used to sense the force being used to push the assistive handle. The printing process of this part is achieved by creating a rear and front cover plate. When assembled, they are glued and bolted to the intersection of the handle and frame. Following printing, a visual effect of the layer orientation is observed that is not initially considered. As can be seen in the figure below, the rear strain gauge cover is slightly darker than the other. Though they are made from filament of the same color, a slight color discrepancy becomes observable when they are assembled due to the layers being perpendicular to one another when compared in their design orientations. This effect does not affect the performance of the part, though slightly lowers the industrial design of the part and the quality of its finish. For subsequent prototypes, care is made to print these two parts in the same orientation.



Figure 5.17: 3D Printed Strain gauge cover. The part on the right can be observed to be slightly darker than its right counterpart.

The rear component of the screen assembly is initially difficult to fabricate. Though its dimensional profile is supported by the 3D printer used, the large size causes difficulty in maintaining a consistent heat across the entire piece during the printing process. This causes some shrinkage deformation as one side of the printing bed cools down, causing one side of a layer to slightly change shape. When the nozzle returns to this location, the subsequent layer can be offset slightly, or not successfully joined to the previous. In order to address this, the part is split into two parts and joined post-print using glue. This is successful in preserving the function of the part, however creates a seam that can be visually observed on the rear of the screen. Therefore, for future builds, this part is redesigned to be fabricated from laser cut sheet metal.

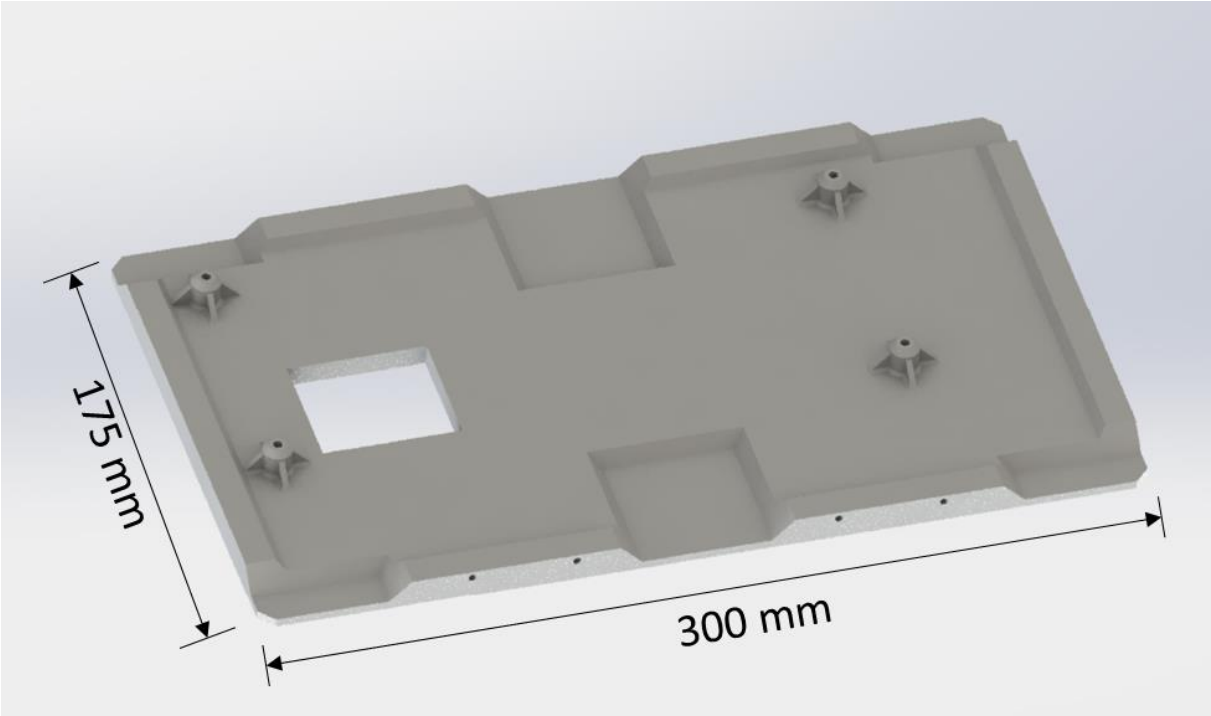


Figure 5.18: Initial 3D printed rear screen assembly component.



Figure 5.19: 3D printed screen components after redesign, printed successfully.

Mechatronic Module Assembly

The mechatronic module itself is successfully assembled according to the design component layout and has a total mass of 29.5 kg. The assembly of the module components confirms the compactness of the design which is a crucial parameter to adhere to in order to maximize the amount of existing equipment that can be retrofit.

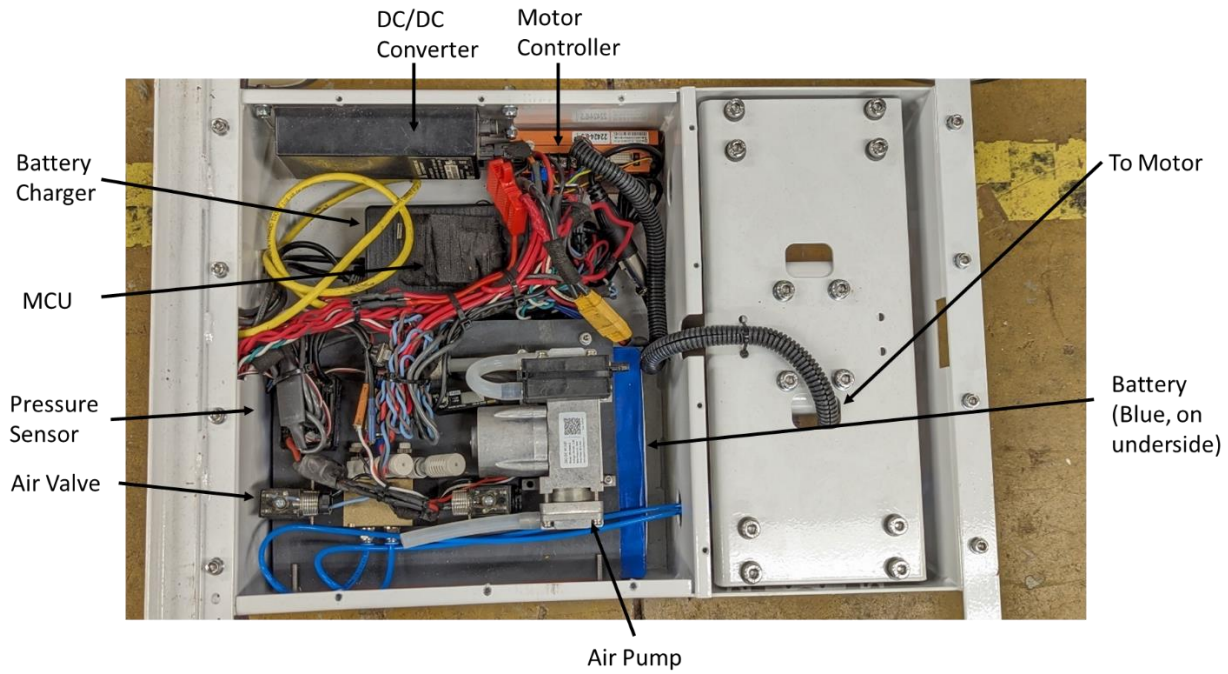


Figure 5.20: Assembled electromechanical system.

The completed assistive cart module and frame has a mass of 54.5 kg without the medicine cabinet mounted.



Figure 5.21: Completed assistive cart assembly



Figure 5.22: Completed assistive cart with sample cabinets.

Stainless Steel Food Cart

A second assistive cart prototype is fabricated, incorporating each of fabrication shortcomings of the first prototype. This design outfits a stainless steel cart designed and fabricated in the MVS lab with the module and handle technology designed for the assistive cart. Though this cart is designed with the intention use with the electromechanical module, the ability to secure the design to an alternate type of cart reinforces its adaptability for various different pieces of equipment that require movement. The total fabricated cart has a mass of 82.5 kg.

The 3D printed parts are adjusted to be uniform visually, the back of the screen assembly is laser cut and welded, and space is reserved in the module and frame design for cable management.



Figure 5.23: Stainless steel cart featuring revised design.

5.2.2 Assistive Cart Operation

The assistive carts both feature similar capabilities in that they are able to overcome the obstacle guidelines outlined during the design process similar to the bed. In addition to this, the stainless steel cart is used in Grand River Hospital for several days, and garnering positive feedback from workers using it throughout this time.

The functionalities of both assistive cart prototypes are successful and the electromechanical system allows allowed for control and software development to be performed using the platform. The main driving motor is sufficient for accelerating and decelerating to match the desired indoor movement speed of an operator. In addition to this, the cart performs similarly across concrete, tiled, and carpeted floors when the drive motor is engaged, not significantly altering the amount of force that the user must exert. This differs from the fully manual operation, where the force required to push equipment noticeably increases when rougher flooring or high carpet is present. The ability to traverse each of these indoor terrains without problems also confirms that the pneumatic system is sufficient in generating the necessary pressures in order to ensure adequate traction between the powered wheel and ground.

The powered carts are also able to maneuver over small obstacles such as wired, as well as drive into and out of elevators. The operator experience also does not significantly change when driving on ascending or descending slopes. Though this design does not have steering capabilities, the steering experience is more intuitive when compared to the assistive bed counterpart. When the motor is engaged, its contact point with the ground in the center of the underside of the cart becomes the pivot point, allowing for a tight turning radius. The sharpness of the turns is controlled similarly to existing manual carts, but creating a moment about the pivot point, though this becomes much easier while moving as the force required to move the cart forward or back is greatly reduced. This also makes pulling the cart a viable method of maneuvering, unlike with the bed, because the sensed strain value does not cause any unwanted steering. The ability to quickly lift the driving motor is also received positively by hospital and long-term care workers, as it allows for the cart to assume the driving experience of a 4-rotating caster cart. This offers the advantage of easily being able to perform fine movements to the cart without much effort, such as rotating it in place, or parking it adjacent to a wall.

The infrared sensors installed in the front of the cart are also successful in facilitating collision avoidance, however, it also caused operational annoyances when driving the cart through doorways and busy narrow hallways. This is addressed during the cart development process by allowing for the operator to approach an obstacle at an adequately slow speed, allowing for doors to be pushed open, but minimizing the chance

for walking-speed collisions. During testing with Grand River Hospital, a physical pushbutton is added to the stainless steel cart, which allows for an additional method for engaging the assistive cart for operation in busy and obstructed environments.

During operation at Grand-River Hospital, the cart is heavily used over a 1 to 2-hour period each day, with smaller maneuvers being performed occasionally between these times. The system is left powered through the majority of this trial, and is able to operate considerably well throughout.

The system required an occasional reboot to remedy slow or stalled software or an unresponsive screen. This is likely due to a combination of a relatively weak raspberry pi computer powering the platform, and the refrigeration-temperatures the assistive cart was stored within. This issue is not replicable when testing at room temperature in a controlled lab environment, suggesting that the frigid temperatures are the leading cause. LCD screens are known to be susceptible to ghosting and responsiveness issues in colder weather, and this is likely also affecting the assistive cart's screen when stored in near-freezing temperatures for extended periods of time.

5.2.3 Assistive Cart Test Results

Results involving the assistive cart's operation are collected by performing various maneuvering tests under a considerable load. The stainless steel assistive cart is loaded with about 122 kg of metal weights, which results in a total mass of about 205 kg. This is slightly under the maximum weight that is previously used to design the electromechanical module components, and simulates a load that is difficult to move manually.



Figure 5.24: Assistive Cart with a total mass of 205 kg.

The first series of tests are performed on concrete flooring, wherein the cart is pushed and pulled. In figures 5.25 and 5.26 below, it can be seen that the cart successfully accelerates and decelerates without issue.

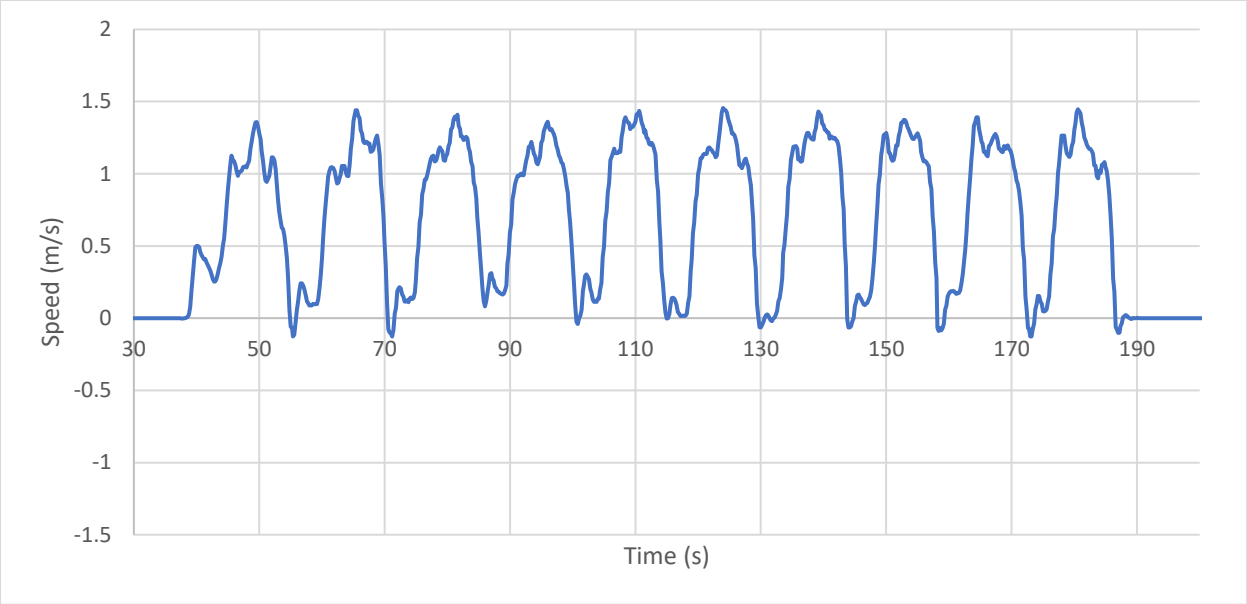


Figure 5.25: Speed of assistive cart, pushing.

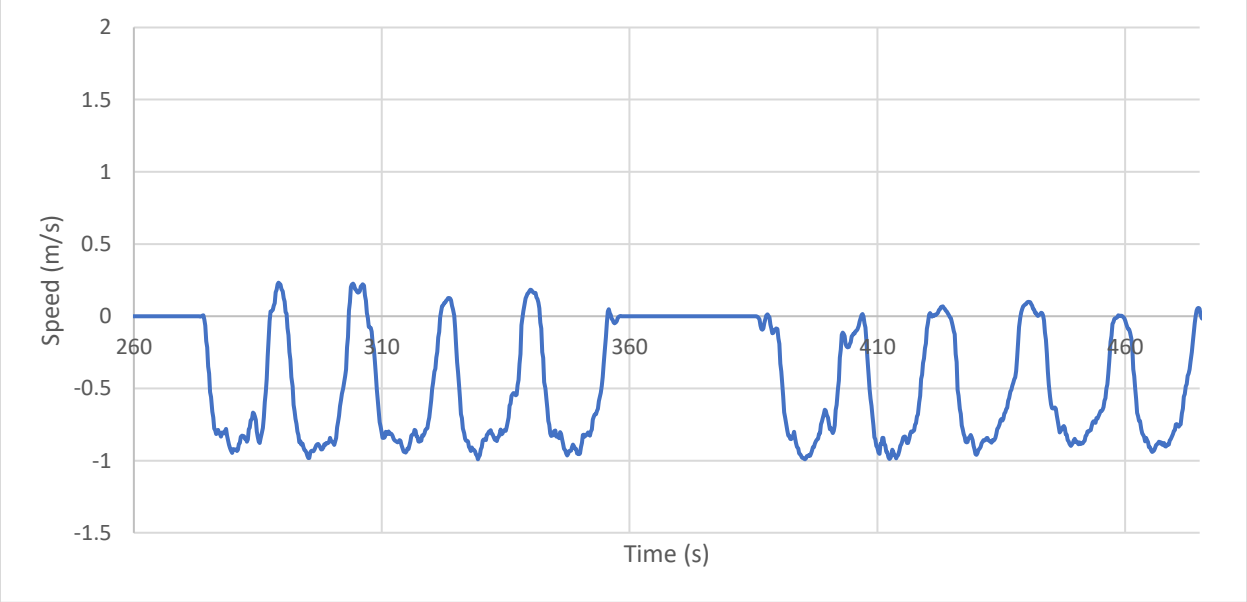


Figure 5.26: Speed of assistive cart, pulling.

Within these tests it is also observed that the assistive cart is able to reduce the forces that are required to accelerate to and brake from a comfortable walking speed. The maximum force magnitudes experienced by the handle typically occur when beginning to accelerate from a stopped position, or while attempting to stop suddenly. The control algorithm delays the motor's assistive torque slightly as a safety feature, in order to avoid movement when the strain gauges sense a brief bump into the handle. Following the initial accelerations, the assistive properties of the module regulate the speed and significantly reduce the amount of force that the operator must apply to move the system. This is depicted in figure 5.27.

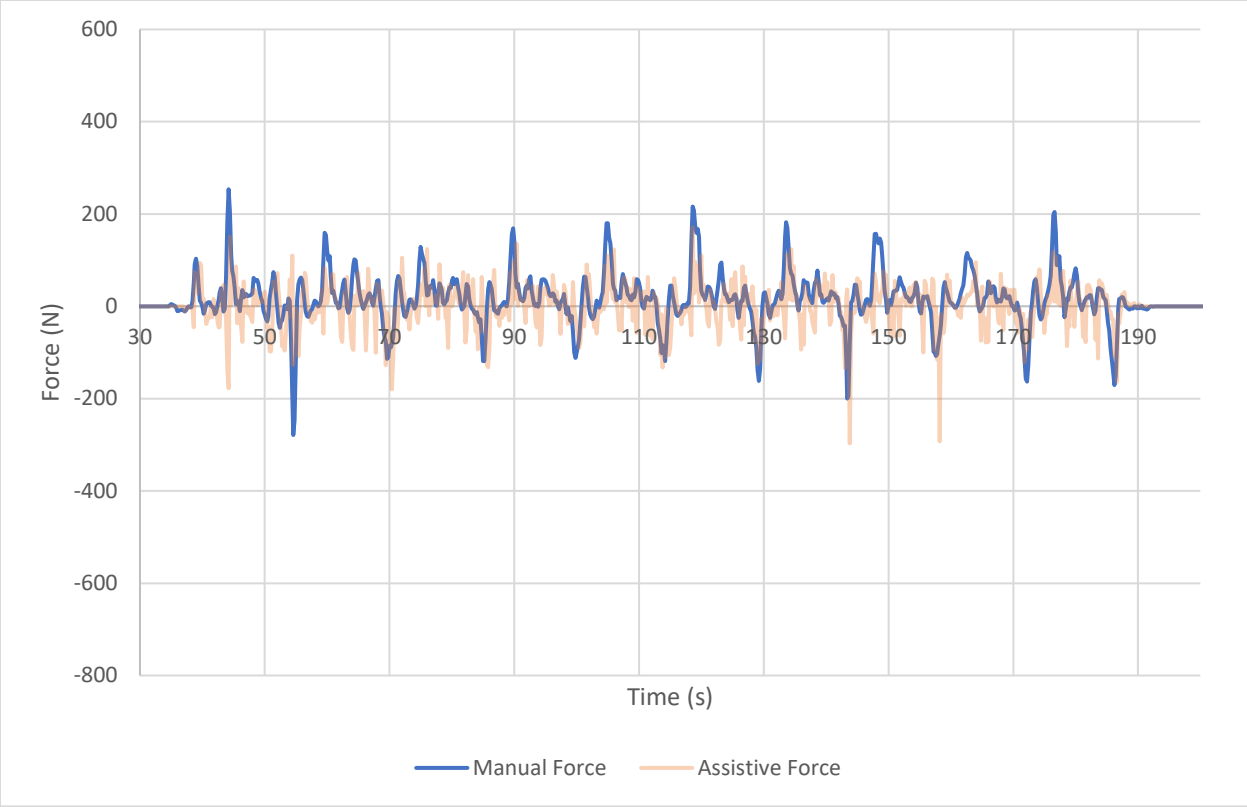


Figure 5.27: Handle and motor forces applied during driving.

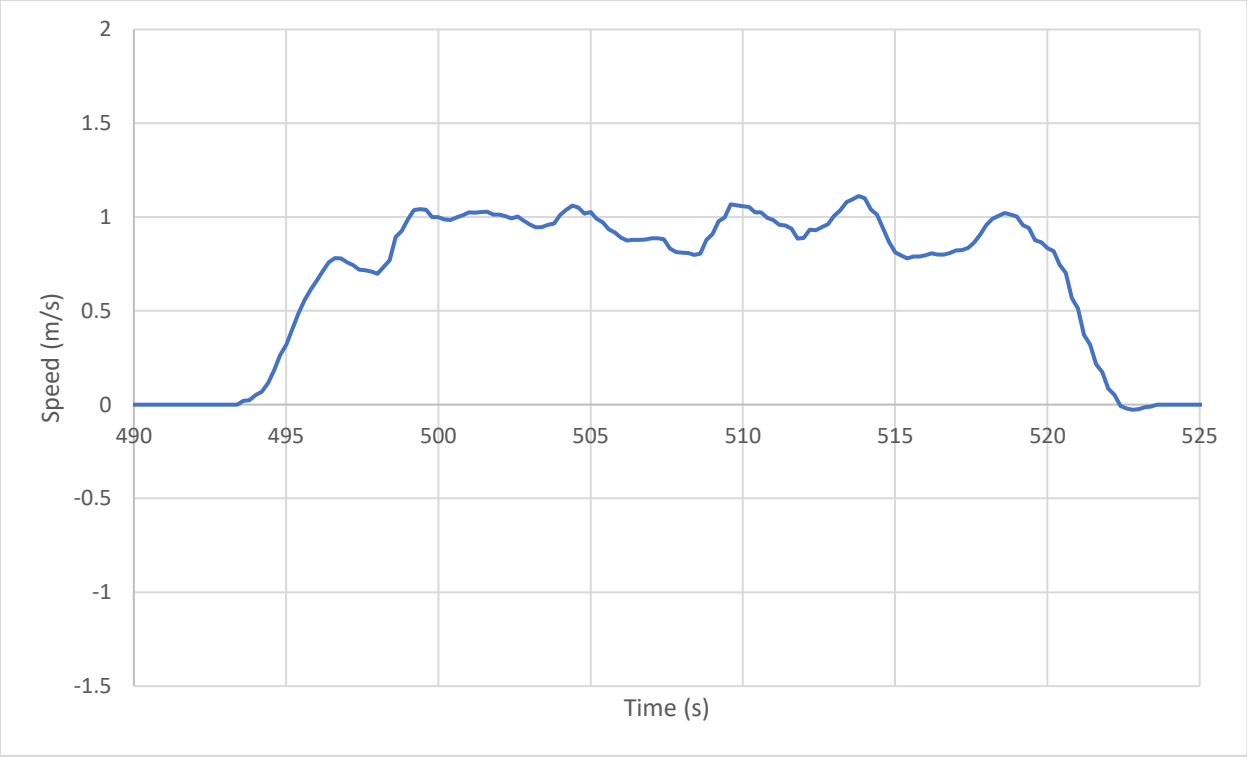


Figure 5.28: Speed of assistive cart driving on concrete for a single acceleration and brake.

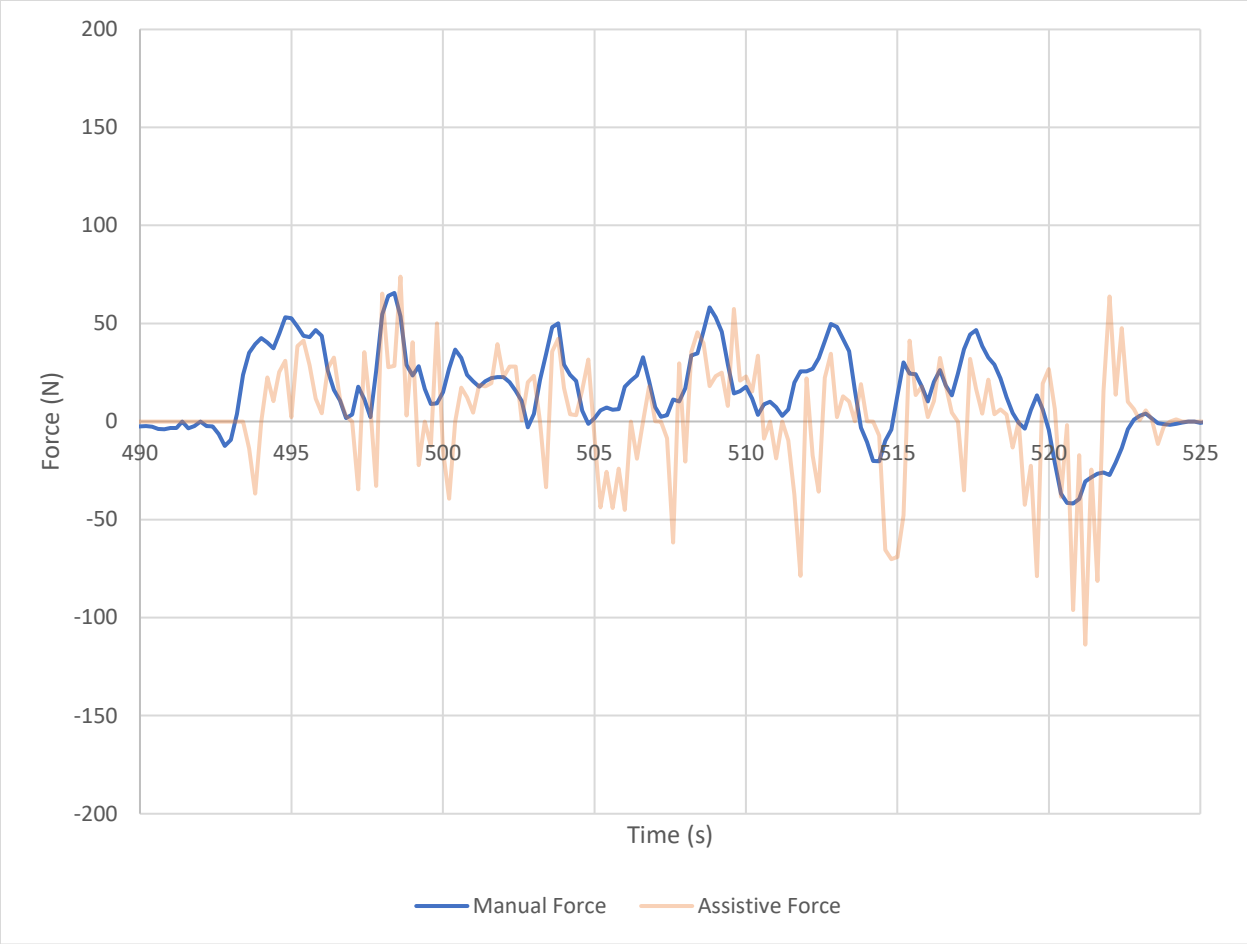


Figure 5.29: Manual and assistive forces applied during driving on concrete for a single acceleration and brake.

Manual operation on carpeted flooring typically requires a much larger amount of force to be exerted by the operator, however, similar force quantities are observed when the assistive motor is engaged on this terrain. Though the pushing force exerted briefly exceeds the recommended value of 250 N when the handle is pushed or pulled quickly, the majority of the peak forces while driving remain under 200 N, with about 50 N being required to maintain a desired speed.

Figure 5.31 shows a caster-wheeled cart loaded with a mass of 136.1 kg for comparison with figure 5.32 which shows the forces when operating that the assistive cart. While operating the manual cart, over 300 N is exerted to start and stop the movement of the cart, while 100 N to 200 N is used to keep the cart moving at a comfortable walking pace. Contrasting this, some of the initial acceleration forces are significant when moving a heavy load on carpeted floor with the stainless steel cart. The force, however, quickly declines as the motor begins to assist the user and remains low while maintaining a walking speed during operation.

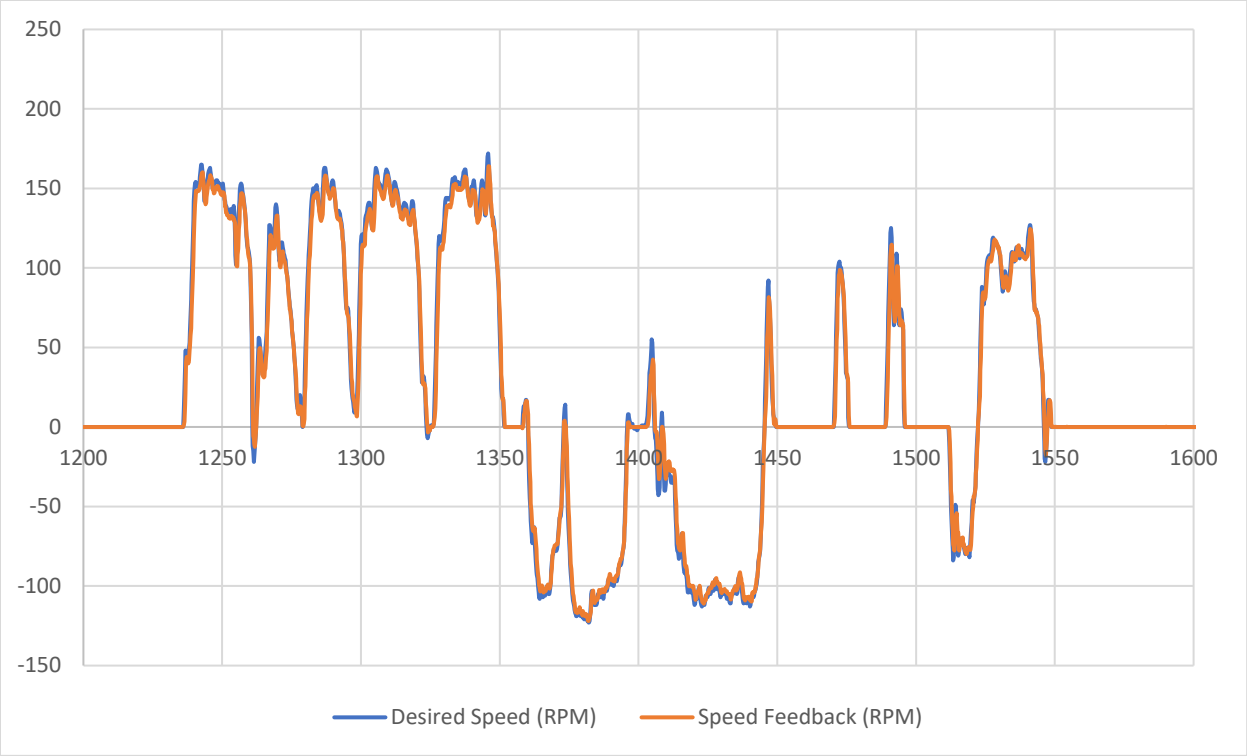


Figure 5.30: RPM speed feedback on a carpeted floor.

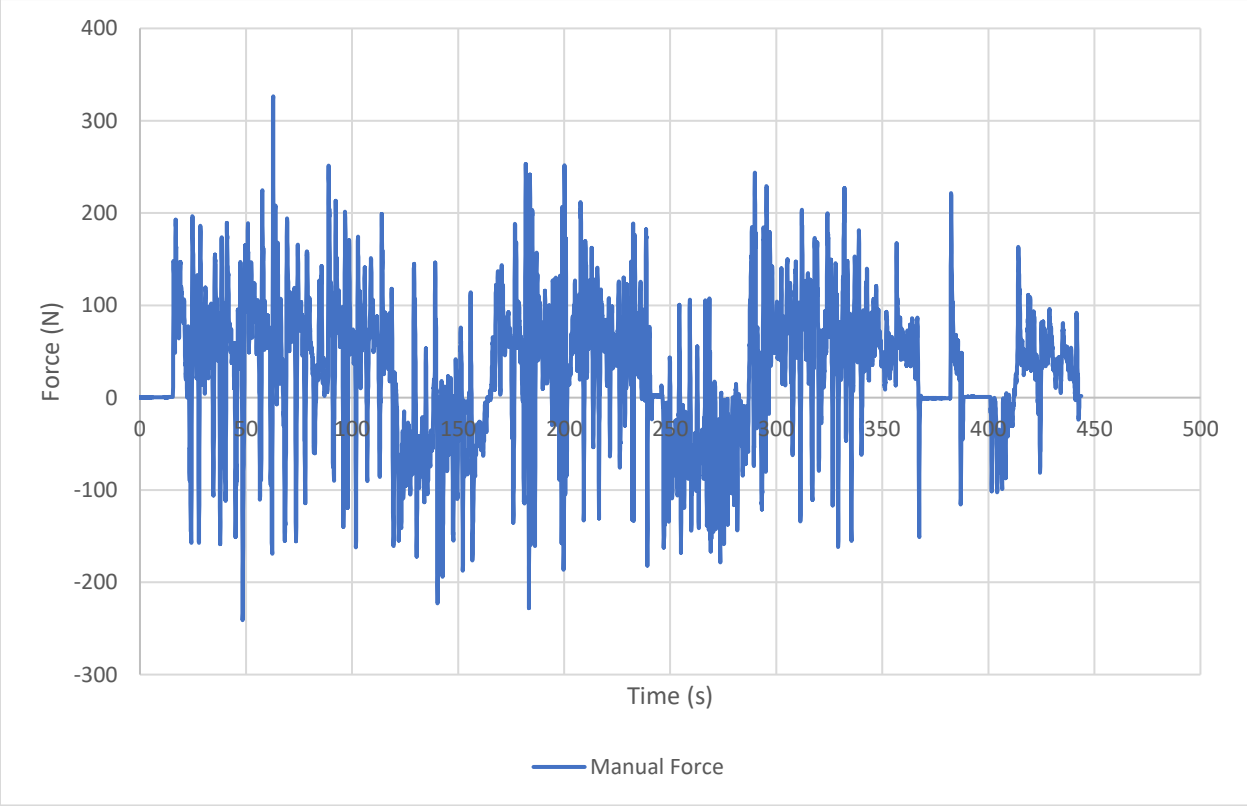


Figure 5.31: Fully manual pushing force of a cart loaded with a 136 kg load on a carpeted floor.

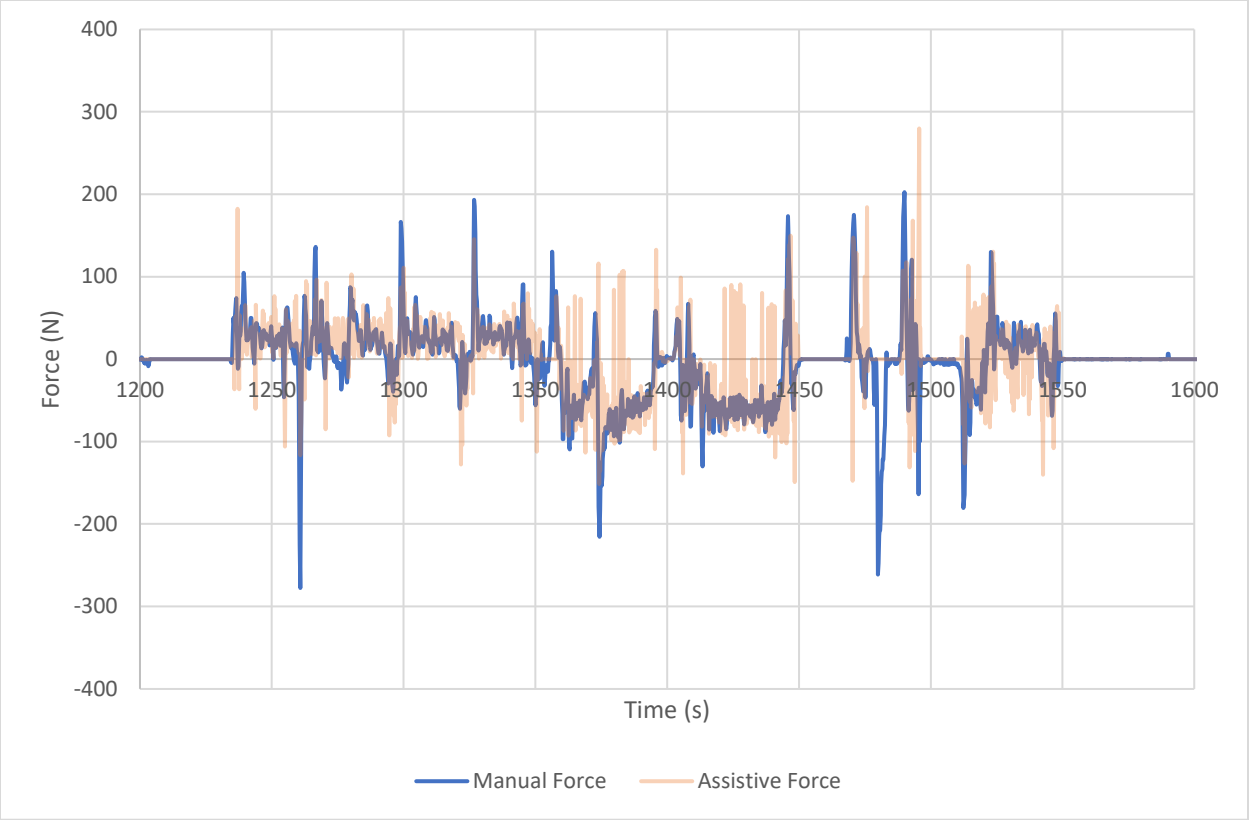


Figure 5.32: Manual and assistive pushing forces applied during driving on a carpeted floor.

Throughout the tests, the assistive motor is able to relieve the majority of the excessive forces required to drive the loaded cart. A final test that depicts the successful achievement of this goal is the operation of the assistive cart on a 6% indoor slope. In this test, a maximum acceleration of 1.4 m/s^2 and deceleration of -3.8 m/s^2 are achieved. Though these are both faster than what is designed for, the driving experience remained comfortable and the control of the cart is maintained by the operator. This is due to the contribution from the motor, which provided about 30 Nm and -52 Nm of torque to the system for brief periods of time when considering the acceleration and handle force contributions. Though this is slightly higher than the listed maximum torque specification of the driving motor, the short time that this torque is experienced allows for the quantity to not be of concern. The motor torque remains under the rated torque of 22 Nm during cruising and typically only surpasses this value for sudden starts and stops.

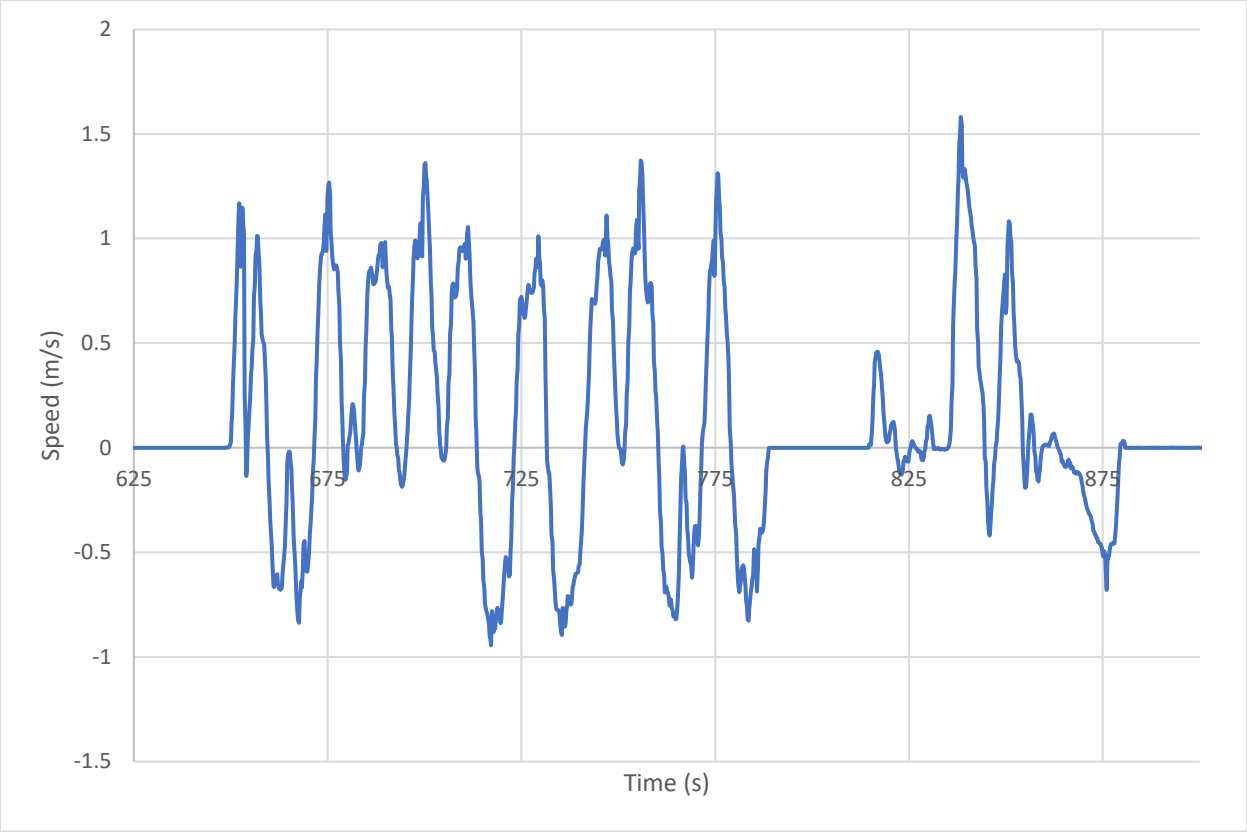


Figure 5.33: Speed of Assistive Cart Sloped Driving, Up and Down Slope

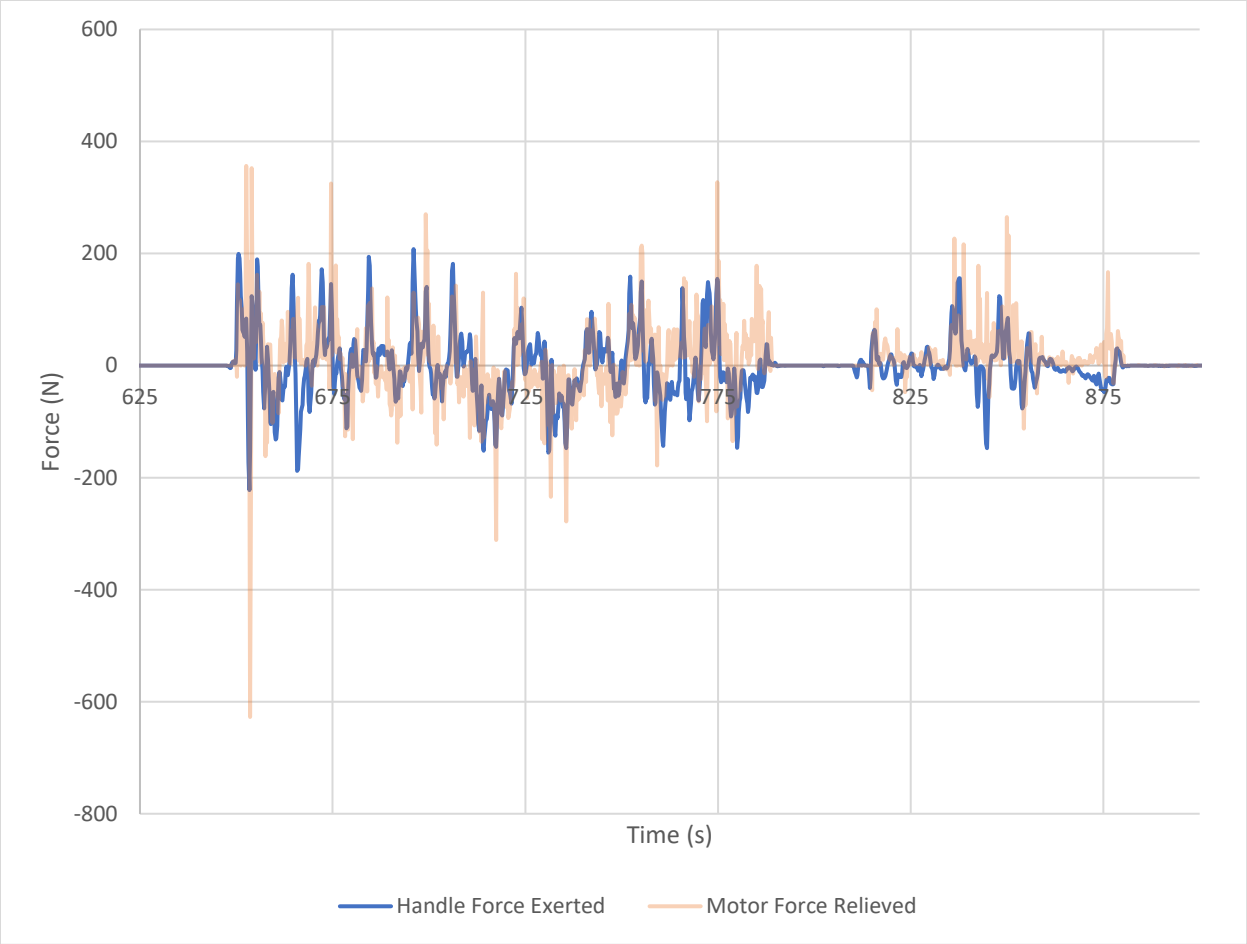


Figure 5.34: Handle and Motor Forces Applied During Driving, On Slope

In summary, the cart is successful throughout testing in limiting the operator's force on the handle to less than 250 N during operation. Though this threshold may be increased with sudden pushes or pulls of the handle, the value is quickly reduced by the contribution of the electric motor, resulting in a shorter overexertion period for the user. This conclusion is also anecdotally agreed upon by nurses at Grand River Hospital, reinforcing the effectiveness of the assistive cart for real-life workflows.

5.2.4 Cart Hauler Fabrication

The cart hauler design is also fabricated, and displayed in figure 5.35 below. The fabrication process of the cart hauler is largely shared with that of the general assistive cart. The handle shape is adjusted to accommodate the narrower bottom section, which connects directly to the module. This allows for a greater moment to be generated while applying force to the left and right beams. During manufacturing,

it is also decided to move the screen to the top of the module rather than in an assembly on the handle. This, both, prevents damage to the screen if the prototype is dropped during testing, while also reducing the complexity with routing cables through the hollow handle. As the module frame is used for force transfer in this design to a greater extent than that of the assistive cart, the sheet metal thickness is increased to 11-gauge (3.175”) in critical locations, such as the bottom plate, and plate connecting the hauler lifts to the module. The electronics are compact within the module enclosure, as intended with the design, leaving adequate space for wiring and placement.

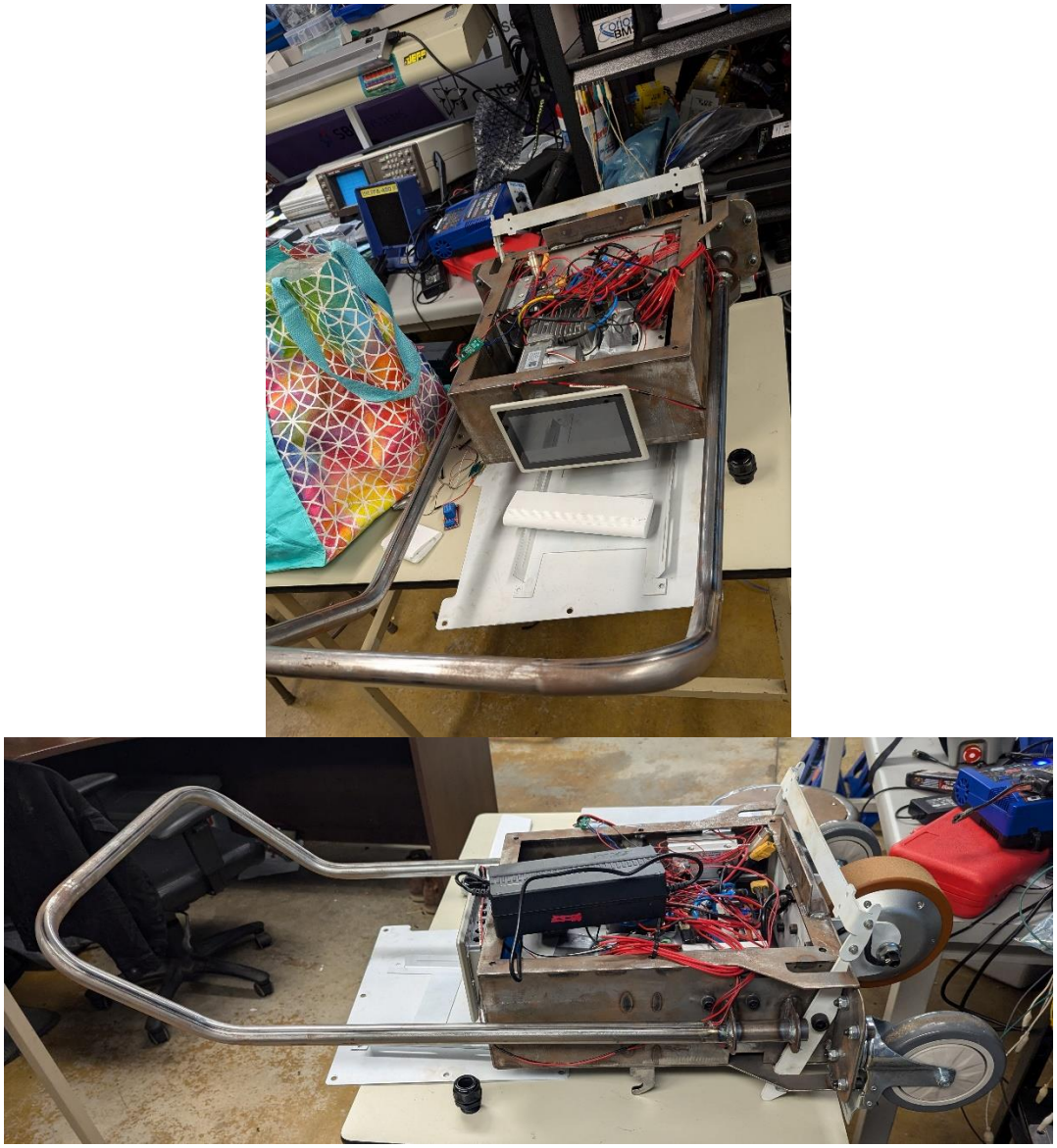


Figure 5.35: Cart Hauler during the assembly process.

CHAPTER 6
CONCLUSIONS AND FUTURE RECCOMENDATIONS

6.1 Conclusion

The primary research goal of developing designs to help health care and long-term care workers by reducing the forces needed to push equipment is successfully approached by targeting bed and cart applications. State of the art electromechanical modules are designed to be retrofit existing equipment to improve their function.

The Canadian aging population and the COVID-19 pandemic have both contributed to surfacing the fact that new innovations and technologies are imperative for the continued success of the health care industry. This thesis directly addresses this by contributing a solution to strain and overexertion of workers, one of the largest problems in health care.

Using combination of original designing, knowledge on the available market for health care mobility solution, and previous MVS prototypes, new assistive bed, assistive cart, and cart hauler modules are created. Each design shares technology and design foundations to allow for parallel development, though each targets a slightly different application.

The assistive bed design successfully created a mechatronic platform which can be used to transport patients and equipment with less manpower than a manual bed. A motorized wheel is retrofitted to an existing bed in a similar fashion to inspirational prototypes, however, with a much higher degree of reliability. The components are redesigned to allow for the bed to be able to navigate any typical indoor environment with a reasonable load, which includes ascending and descending ramps as well as driving over small obstructions. The assistive bed platform successfully achieves the goal of becoming robust enough for further testing for its dual steering bicycle control system and for implementation of different sensors for future autonomy.

The assistive cart design builds upon the design of the bed, but in a fashion that makes it easier to deploy in real health care environments for data collection about its usage from professionals. The cart module is scaled down to be compact and easy to outfit on carts of various different sizes. The component selections differ slightly to better match the intended applications, and the steering motor is removed. This significantly decreases the complexity of controlling the cart during operation, and allowed for strain gauges to be used to design a handle that drives the motor based on the force used to push. The cart is

successful in deployment, and is used for several weeks at Grand River Hospital successfully. In addition to this, the cart is observed to consistently limit the forced required by the operator to push a heavy load to 250 N during operation. Though an operator can naturally exert more than this while attempting to quickly accelerate or brake due to the similarity of the assistive handle's user interface with a manual handle, the amount required to move equipment is consistently kept to a comfortable level regardless of the terrain or obstacles encountered.

Additionally, a hauler cart is designed and manufactured. This design defers from the standard cart as it is removable in order to use one electromechanical assemble to move manual carts that are part of a fleet. The main advantage of this system is that it does not require every piece of equipment to be retrofitted vying to instead attached to each one when they require movement. This is very beneficial when the quantity of a cart design in large, though each individual cart sits idle for the majority of a working day. The hauler cart's effectiveness still requires testing to optimize its mechanical attachment mechanism and to receive feedback from industry partners, though is a solid proof of concept that can be used to justify expanded development in the future.

The scope initially set out to be investigated over the span of this thesis is successfully completed, and the mechanical design for the assistive mobility project is reliable enough to move forward parallel research.

6.2 Future Advancements

As designing and testing of the semi-autonomous and assistive solutions for mobility in health and long-term care facilities matures, several opportunities will arise. Software, hardware, and mechatronic improvements can be made to improve the ease of designing new solutions to better fit a breadth of applications for pushing various equipment. While significant progress has been made integrating the cart designs in workflows during this thesis, other products with more frequent loads can be implemented in the future.

An immediate source for future advancements would be continuing to test the designs in their intended use environments, as well as expanding to multiple carts or beds at a time. During the scope of this thesis, the assistive food cart is deployed in Grand River Hospital for several weeks for usage, and although it improved the overall workflow by lowering the amount of force required by workers, other optimization and testing opportunities arose. The food cart's durability was tested with prolonged use where the system was left on for several days at a time spent in refrigerator temperatures, which

occasionally caused small issues such as unresponsiveness in the screen. With the feedback and data from long-term use, issues like this should be removed from occurrence during operation. In addition to continued testing of the food cart, the hauler cart should be assessed in its intended environment as well.

The ease of installation of the bed module design should be explored as well, and should be integrated in a less-critical design. Due to the nature of the implications of adding a new bed design to a critical health care fixture, it is difficult to integrate this design for early testing. A solution to this would be to find an opportunity to install this module on a less critical piece of equipment to collect usage data until the technology is mature enough that it can confidently operate for extended periods of time without becoming a safety concern or hinderance. Additionally, partnering with body mechanics and health care experts can help further enhance the design for operation of future prototypes and products.

Alongside the design of solutions discussed in this thesis, the commencement of development involving further autonomy ensued. The person-following capabilities are currently being explored using a camera and tag system, which will require more research to develop a deployable solution. In addition to this, autonomous control is being tested wherein the cameras and lidar are part of an indoor sensor node design which can be mounted on the ceiling. A more 5g-capable computer is included in these sensor nodes that allows for communication between other nodes as well as autonomous equipment, which can be used to issue controls. Research in this area is crucial for pushing the future design towards autonomy that does not require constant supervision from an operator.



Figure 6.1: Indoor sensor nodes mounted in MVS lab.

The existing designs have served as a success for moving the overall project to a phase where some products can be deployed for testing in their intended environments, however, opportunities still exist for

improvement. Further design involving waterproofing and dustproofing can be integrated in future iterations to allow for the module to be able to withstand water jets, which are often used for cleaning at hospitals. In addition to this, opportunities exist to streamline the manufacturing process by farther simplifying parts to reduce space and power requirements. Repairability and upkeep can also be enhanced by creating documents that allow for fast repair and troubleshooting. With an expanding fleet, it is imperative that alternative designs are still explored as the software, hardware, or mechanical design may require changes to better suit various different applications in the future.

References

[1] S. Canada, "Population estimates on June 1, by age and gender (17-10-0005-01 (formerly CANSIM 051-0001))," 12 June 2024. [Online]. Available: https://www150.statcan.gc.ca/t1/tbl1/en/cv.action?pid=1710000501. [Accessed 12 June 2024].

[2] A. G. Ozkil, Z. Fan, S. Dawids, H. Aanes, J. K. Kristensen and K. H. Christensen, "Service robots for hospitals: A case study of transportation tasks in a hospital," *IEEE International Conference on Automation and Logistics*, pp. 289-294, 2009.

[3] VitalMobility Home Health Care, "Full Electric Hospital Beds," VitalMobility, 2024. [Online]. Available: https://www.vitalmobility.ca/electric-hospital-bed.php. [Accessed 5 May 2024].

[4] VitalMobility Home Health Care, "Vitalflex LTC Bed," Vital Mobility, 2024. [Online]. Available: https://www.vitalmobility.ca/media/wysiwyg/UserGuides/VitalFlex%20Standard%20LTC%20Bed%20-%20Spec%20Sheet.pdf. [Accessed 5 May 2024].

[5] VitalMobility Home Health Care, "Invacare Carroll CS Series CS7 Bed," VITAL MOBILITY MEDICAL SUPPLIES INC., 2024. [Online]. Available: https://www.vitalmobility.ca/invacare-continuing-care-cs-series-cs7-bed.php. [Accessed 6 May 2024].

[6] Rotec International Medical Beds, "VersaTech 1100 ULB Rotec Ultra Low Bed," 2024. [Online]. Available: https://www.vitalmobility.ca/media/wysiwyg/UserGuides/VersaTech1100ULB-EN.pdf. [Accessed 6 May 2024].

[7] HillRom, "HillRom® Century Series Bed," Hillrom Services, Inc., 2019. [Online]. Available: https://parts.hillrom.com/hillromUS/en/Products/Beds/CENTURY-BED/p/1592CB2B-DB15-4C4B-842C-880DC3F9AFA1. [Accessed 11 February 2024].

[8] C. Wang, A. V. Savkin, R. Clout, H. T. Nguyen and I. Senior Member, "An Intelligent Robotic Hospital Bed for Safe Transportation of Critical Neurosurgery Patients Along Crowded Hospital Corridors," *IEEE TRANSACTIONS ON NEURAL SYSTEMS AND REHABILITATION ENGINEERING*, vol. 23, no. 5, pp. 744-754, September 2015.

[9] Z. Guo, R. B. Yee, K.-R. Mun and A. P. b. Haoyong Yu (Dr., "Experimental Evaluation of a Novel Robotic Hospital Bed Mover with Omni-Directional Mobility," *Applied Ergonomics,* vol. 65, pp. 389-397, November 2017.

[10] SAE International, "Levels of Autonomy," 30 April 2021. [Online]. Available: https://www.sae.org/standards/content/j3016_202104/. [Accessed 24 May 2024].

[11] W. W. Tai, B. Ilias, S. A. Shukor, N. A. Rahim and M. Markom, "A Study of Ultrasonic Sensor Capability in Human Following," IOP Conf. Ser.: Mater. Sci. Eng, 2019.

[12] J. H. Choi, K. Samuel, K. Nam and S. Oh, "An Autonomous Human Following Caddie Robot with High-Level Driving Functions," *Electronics,* vol. 9, no. 9, 15 September 2020.

[13] S. R. Z. Q. H. J. M. E. C. H. M. V. d. L. Wesley P. Chan, "Autonomous person-specific following robot," *CoRR,* vol. 2010.08017, 11 November 2020.

[14] Mobile Material Handling Inc., "MOTORIZED PLATFORM CART," Mobile Material Handling Inc., 2019. [Online]. Available: https://www.mobilept.ca/product/motorized-platform-cart/. [Accessed 15 January 2023].

[15] Granite Industries, "Indoor/Outdoor Electric Utility Carts," Granite Industries, 2023. [Online]. Available: https://store.graniteind.com/category/power-carts/indoor-outdoor-electric-utility-carts/. [Accessed 2023 15 January].

[16] Granite Industries, "Overland Electric Powered 44″ Chassis," Granite Industries, 2023. [Online]. Available: https://store.graniteind.com/product/overland-electric-powered-44-chassis/. [Accessed 15 January 2023].

[17] Granite Industries, "Overland Electric Powered Appliance Hand Truck – With Turf Tires," Granite Industries, 2023. [Online]. Available: https://store.graniteind.com/product/overland-electric-powered-appliance-hand-truck-with-turf-tires/. [Accessed 15 January 2023].

[18] Y. Volkert, "Development of a Propulsion System for Autonomous Transport Applications in Health Care," 2023.

[19] D. M. E.-P. Brian J. Maguire, P. M. Katherine L. Hunting, M. M. Tee L. Guidotti and M. M. Gordon S. Smith, "Occupational Injuries among Emergency Medical Services Personnel," Prehospital Emergency Care, 2009.

[20] M. e. a. Brutting, "Muskel-Skelett-Belastungen beim Schieben und Ziehen von Krankenbetten und Rollstühlen," Zentralblatt für Arbeitsmedizin, Arbeitsschutz und Ergonomie 67.2, 2017.

[21] "Ergonomics - Pushing and Pulling - General," Canadian Centre for Occupational Health and Safety, 20 December 2022. [Online]. Available: https://www.ccohs.ca/oshanswers/ergonomics/push1.html. [Accessed 26 March 2023].

[22] "Overweight and obese adults, 2018," Statistics Canada, 25 June 2019. [Online]. Available: https://www150.statcan.gc.ca/n1/pub/82-625-x/2019001/article/00005-eng.htm. [Accessed 25 April 2023].

[23] T. KL, F. C and M. N, "Objective and subjective assessments of normal walking pace, in comparison with that recommended for moderate intensity physical activity," *Int J Exerc Sci,* vol. 3, no. 3, pp. 87-96, 15 July 2010.

[24] Canada Mortgage and Housing Corporation, "Accessible Housing by Design," 14 June 2016. [Online]. Available: https://publications.gc.ca/collections/collection_2017/schl-cmhc/NH18-24-63A-2016-eng.pdf. [Accessed 17 April 2023].

[25] D. Jiménez, S. Hernández, J. Fraile-Ardanuy, J. Serrano, R. Fernández and F. Álvarez, "Modelling the Effect of Driving Events on Electrical Vehicle Energy Consumption Using Inertial Sensors in Smartphones," *Energies 2018,* vol. 2, no. 412, 10 February 2018.

[26] Suzhou Micro Actuator Technology Co., Ltd., "RMD-X10-S2 1:35 V3," MyActuator, 2021. [Online]. Available: https://www.myactuator.com/product-page/rmd-x10-s2-1-35. [Accessed 18 December 2022].

[27] Shenzhen ZhongLing Technology Co., Ltd., "ZLLG80ASM800 V2.0," ZLTECH, 2023. [Online]. Available: http://www.zlrobotmotor.com/info/391.html. [Accessed 25 March 2023].

[28] B. C. Ltd, "Castor Wheels Roll Resistance," Bulldog Castors, 10 May 2016. [Online]. Available: https://www.bulldogcastors.co.uk/blog/castor-wheels-roll-resistance/. [Accessed 26 March 2023].

[29] W. H. Daniel W. Baker, "9.7 Rotating Discs," Engineering Statics: Open and Interactive, 30 March 2024. [Online]. Available: https://engineeringstatics.org/Chapter_09-disc-friction.html. [Accessed 12 April 2024].

[30] L. Ningbo Zhongda Leader Intelligent Transmission Co., "Z4BLD60 80 Series Brushless DC Motor," ZD Motor, 2019. [Online]. Available: https://en.zd-motor.com/product/Z4BLD60-149.html. [Accessed 15 May 2022].

[31] I. Teknic, "CPM-MCPV-2311S-RLS," Teknic, Inc., 2022. [Online]. Available: https://teknic.com/model-info/CPM-MCPV-2311S-RLS/. [Accessed 10 December 2022].

[32] Shenzhen Boden Technology Development Co., Ltd., "BD-08AB-D/BD-08VB-D Double head Small Air Compressor & High Flow Air Pump," BODENFLO, 2023. [Online]. Available: https://bodenpump.com/product/bd-08ab-d-bd-08vb-d-double-head-small-air-compressor-high-flow-air-pump/. [Accessed 14 June 2023].

[33] L. Ningbo Xinchao Automatization Component Co., "MGP Series Three-Shaft Cylinder," Alibaba, [Online]. Available: https://www.alibaba.com/product-detail/China-Supplier-MGP-Series-Three-Shaft_1600051119026.html?spm=a2700.shop_plgr.41413.43.9e5472e9gOIl7C. [Accessed 9 July 2023].

[34] J. K. Nisbeth and R. G. Budynas, Shigley's Mechanical Engineering Design, McGraw-Hill, 2011.

[35] SKF, "51109 Single direction thrust ball bearing," SKF UK, 2023. [Online]. Available: https://www.skf.com/uk/products/rolling-bearings/ball-bearings/thrust-ball-bearings/productid-51109. [Accessed 25 May 2023].

[36] SKF, "51106 Single direction thrust ball bearing," AKF UK, 2023. [Online]. Available: https://www.skf.com/uk/products/rolling-bearings/ball-bearings/thrust-ball-bearings/productid-51106. [Accessed 27 May 2023].

[37] SKF, "6004 Deep groove ball bearing," SKF UK, 2023. [Online]. Available: https://www.skf.com/uk/products/rolling-bearings/ball-bearings/deep-groove-ball-bearings/productid-6004. [Accessed 25 May 2023].

[38] SKF, "16004 Deep groove ball bearing," SKF UK, 2023. [Online]. Available: https://www.skf.com/uk/products/rolling-bearings/ball-bearings/deep-groove-ball-bearings/productid-16004. [Accessed 27 May 2023].

[39] Audesse, "Audesse FlexCase," Audesse, 2022. [Online]. Available: https://www.audesseinc.com/products/flexcase/. [Accessed 21 December 2022].

[40] EPFamilyDirect, "EPAuto Tire Inflator Digital 12V DC Portable Air Compressor Tire Pump, Blue," Amazon.ca, 2022. [Online]. Available: https://www.amazon.ca/EPAuto-Portable-Compressor-Digital-Inflator/dp/B01L9WSTEG/ref=asc_df_B01L9WSTEG/?tag=googleshopc0c-20&linkCode=df0&hvadid=292895474807&hvpos=&hvnetw=g&hvrand=7070818439216248843&hvpone=&hvptwo=&hvqmt=&hvdev=c&hvdvcmdl=&hvlocint=&hvlo. [Accessed 20 December 2022].

[41] CANCARD, "Vintage Encore Series Treatment Cart," 2021. [Online]. Available: https://cancard.com/product/vintage-encore-series-treatment-cart. [Accessed 2023 July 2023].

[42] "Ergonomics - Pushing and Pulling - Handcarts," Canadian Centre for Occupational Health and Safety, 01 March 2018. [Online]. Available: https://www.ccohs.ca/oshanswers/ergonomics/push2.html. [Accessed 26 March 2023].

[43] Agilent Technologies Inc, "PRACTICAL STRAIN GAGE," Agilent Technologies Inc, 1999. [Online]. Available: https://www.omega.co.uk/techref/pdf/straingage_measurement.pdf. [Accessed 5 June 2023].

[44] R. C. Juvinall and K. M. Marshtek, Fundamentals of Machine Component Design, Wiley, 2017.

[45] ShenZhen ZhongLing Technology Co., Ltd, "ZLLG 64ASM500 Motor," ZLTech, 2019. [Online]. Available: http://www.zlrobotmotor.com/info/385.html. [Accessed 5 July 2023].